



**US Army Corps  
of Engineers®**  
Engineer Research and  
Development Center



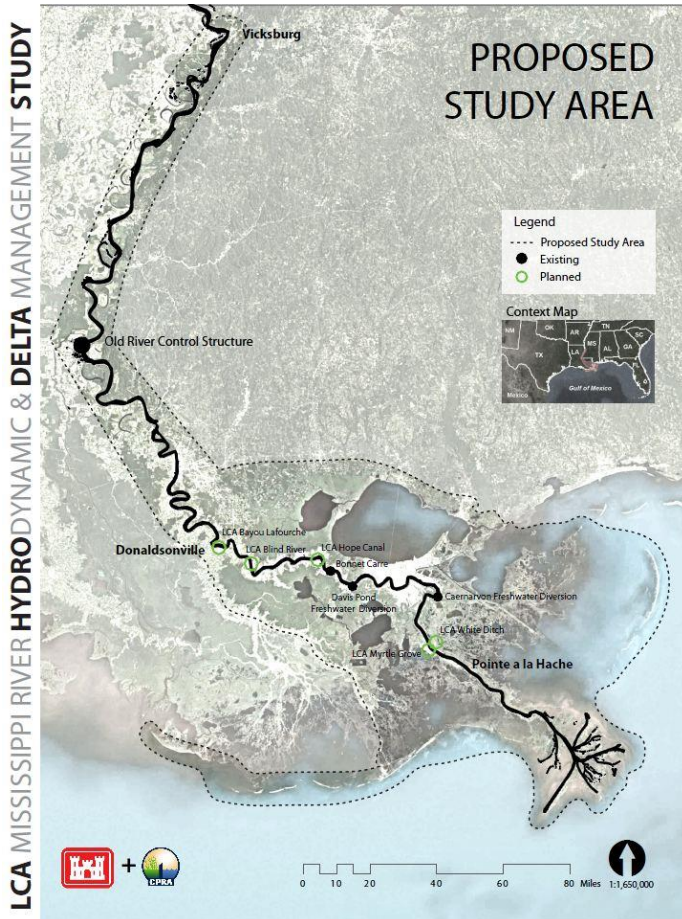
*Louisiana Coastal Area Program-Mississippi River Hydrodynamic and Delta  
Management Study*

# Multidimensional Modeling

Local Applications of Delft-3D Model

Ehab A. Meselhe and Kazi M. Sadid

March 2015



Approved for public release; distribution is unlimited.

## **Acknowledgements**

This report was prepared by Ehab Meselhe and Kazi Sadid of the Water Institute of the Gulf (the Institute). The report was reviewed by the numerical modeling teams of the Mississippi River Hydrodynamic and Delta Management Study (MRHDMS). The report was also reviewed by the Independent External Peer Review Panel of MRHDMS. Finally, this report was reviewed by Denise Reed (Chief Scientist) and edited by Kathleen Hastings and Taylor Kimball of the Institute.

# **Multidimensional Modeling**

Local Application of the Delft-3D Model

Ehab A. Meselhe and Kazi M. Sadid

The Water Institute of the Gulf  
301 N. Main Street, Suite 2000  
Baton Rouge, LA 70825

Final report

Approved for public release; distribution is unlimited.

Coastal Protection and Restoration Authority (CPRA) of Louisiana  
LCA Mississippi River Hydrodynamic and Delta Management Study (MRHDMS)

## Abstract

This report describes the development of near-field Delft-3D models for proposed sediment diversions for the Lower Mississippi River. It is part of the multidimensional modeling effort of the Mississippi River Hydrodynamic and Delta Management Study (MRHDMS). The modeling domains include the proposed diversions at Upper Breton Sound, White Ditch and Myrtle Grove, and the existing Bonnet Carré Spillway. Models were validated against field observations. Once validated, the models were used to perform detailed analysis of each diversion site and provide insights on the ability of diversions to capture sediment efficiently, and on the response of the river to such extraction of water and sediment.

The models were used to analyze individual diversions as well as the interaction between two adjacent diversions. Key findings of this study include: (1) diversions located on sand bars capture sediment efficiently if they are of sufficiently large size (> 5% of the river water discharge); (2) the invert elevation of the diversion intake has to be sufficiently deep to adequately capture the coarse (sand) material, (3) reduction in river stream power due to extraction of water results in sediment aggradation downstream of the diversion, (4) the larger the diversion size the more significant the sediment deposition downstream of the diversion intake (regardless of how efficient a diversion is in capturing sediment), and (5) Neighboring diversions do not necessarily diminish their respective sediment capture efficiency.

# Contents

<b>Acknowledgements</b> .....	<b>i</b>
<b>Abstract</b> .....	<b>iii</b>
<b>Illustrations</b> .....	<b>v</b>
<b>Preface</b> .....	<b>ix</b>
<b>Unit Conversion Factors</b> .....	<b>x</b>
<b>1 Overview and Objectives</b> .....	<b>1</b>
<b>2 Delft-3D Modeling – Bonnet Carré Spillway</b> .....	<b>3</b>
2.1 Calibration and Validation of Hydrodynamics, Sediment Transport, and Morphology .....	3
<i>Model Calibration for the 2011 flood</i> .....	5
2.2 Model Application .....	18
<b>3 Delft-3D Modeling – Myrtle Grove and White Ditch</b> .....	<b>25</b>
3.1 Calibration and Validation Hydrodynamics and Sediment Transport .....	25
3.2 Model Application .....	38
<i>Sediment-Water Ratio</i> .....	49
<b>4 Delft-3D Modeling – Upper Breton Sound</b> .....	<b>52</b>
4.1 Calibration and Validation of Hydrodynamics and Sediment Transport .....	52
4.2 Model Application .....	65
<b>5 Conclusions and Closing Remarks</b> .....	<b>77</b>
<b>6 References</b> .....	<b>79</b>

# Illustrations

## Figures

Figure 1. Near-Field Applications of Delft-3D to Bonnet Carré, Upper Breton Sound, and Myrtle Grove and White Ditch.....	2
Figure 2. Model domain and location of the polygons - BC Model. ....	4
Figure 3. Location for velocity measurement.....	6
Figure 4. Velocity at RM 128 on May 21, 2011.....	7
Figure 5. Velocity at RM 126.9 on June 25, 2011. ....	7
Figure 6. Water-level calibration during May 1- June 25, 2011.....	8
Figure 7. Discharge calibration at Airline Hwy during May 1- June 25, 2011.....	9
Figure 8. Calibration of suspended sand concentration between model and observations at the US of BC (RM 136) and DS of BC (RM 126.9) on May 21, 2011 when the structure was open with peak diversion discharge.....	11
Figure 9. Calibration of suspended sand concentration between model and observations at the US of BC (RM 136) and DS of BC (RM 126.9) on June 22, 2011 in post-flood condition when the structure was closed. ....	12
Figure 10. Model calibration for the suspended and bed load: (a) suspended sand loads, (b) fine sediment loads, and (c) bed loads, at the US of BC (RM 136) and DS of BC (RM 126.9). ....	13
Figure 11. Model calibration for the suspended load at Airline Hwy: (a) suspended sand loads, and (b) fine sediment loads.....	13
Figure 12. Erosion and accretion volume (a) May-June 2011; and (b) June 2011-June 2012. ....	15
Figure 13. Erosion and accretion pattern during the pulse (May-June 2011): Observation polygons A to I.....	16
Figure 14. Erosion and accretion pattern in the main channel from June 2011 to June 2012. ....	16
Figure 15. BC Model validation for the 1997 flood. ....	17
Figure 16. BC Model validation for 2008 flood.....	18
Figure 17. Calculated erosion and accretion volume during the 2011, 2008, and 1997 flood. ....	19
Figure 18. Erosion and accretion pattern during the 1997 flood.....	19
Figure 19. Erosion and accretion pattern during the 2008. ....	19
Figure 20. Sediment budget for sand load during the 2011 flood for BC model. ....	21
Figure 21. Sediment budget for fine sediment during the 2011 flood for BC model.....	21
Figure 22. Cumulative SWR of Bonnet Carré spillway during the flood events: (a) 2011; (b) 2008, and (c) 1997. ....	23
Figure 23. Longitudinal water surface profile on May 6 and May 21, 2011. ....	24
Figure 24. Main Stem Model Domain, Boundaries and initial bathymetry for MG-WD. ....	26
Figure 25. Stage calibration for MG-WD. ....	27
Figure 26. Stage validation for MG-WD.....	28
Figure 27. Depth averaged velocity transect calibration for MG-WD model. ....	28
Figure 28. Vertical velocity profile calibration for MG-WD model. ....	29
Figure 29. Suspended fine load rating curve – Belle Chasse (2008-2012). ....	30

Figure 30. Suspended sand load rating curve – Belle Chasse (2008-2012).	31
Figure 31. Suspended fine sediment calibration for MG-WD.	32
Figure 32. Suspended fine sediment validation for MG-WD.	32
Figure 33. Suspended sand load calibration for MG-WD.	34
Figure 34. Suspended sand load validation for MG-WD.	34
Figure 35. Total load calibration for MG-WD.	36
Figure 36. Total load validation for MG-WD.	36
Figure 37. Bed load calibration for MG-WD.	37
Figure 38. Bed load validation for MG-WD.	38
Figure 39. Simulated discharge in the Mississippi River and WD diversion in 2008 – 2010.	39
Figure 40. Simulated discharge in the Mississippi River and MG diversion in 2008 – 2010.	39
Figure 41. River segments considered to quantify morphologic changes for MG-WD.	<b>Error! Bookmark not defined.</b>
Figure 42. Erosion and accretion volume change in response to MG-WD diversions during 2008 – 2010.	41
Figure 43. Sand Instantaneous and Cumulative SWR for WD.	50
Figure 44. Mud Instantaneous and Cumulative SWR for WD.	50
Figure 45. Sand Instantaneous and Cumulative SWR for MG.	51
Figure 46. Mud Instantaneous and Cumulative SWR for MG.	51
Figure 47. Model domain, grid, and boundaries for UBS.	53
Figure 48. Stage Calibration for UBS.	54
Figure 49. Stage Validation for UBS.	55
Figure 50. Depth averaged velocity transect calibration for UBS.	56
Figure 51. Velocity vertical profiles for UBS.	56
Figure 52. Suspended fine load calibration for UBS.	<b>Error! Bookmark not defined.</b>
Figure 53. Suspended fine load validation for UBS.	60
Figure 54. Suspended sand load calibration for UBS.	<b>Error! Bookmark not defined.</b>
Figure 55. Suspended sand load validation for UBS.	62
Figure 56. Total suspended load calibration for UBS.	63
Figure 57. Total suspended load validation for UBS.	63
Figure 58. Simulated discharge in the Mississippi River and UBS diversion at RM 77 in 2008 – 2010.	66
Figure 59. Simulated discharge in the Mississippi River and UBS diversion at RM 81.5 in 2008 – 2010.	66
Figure 60. River segments considered to quantify morphologic changes for UBS model.	67
Figure 61. Erosion and accretion volume change in response to UBS diversion for the 2011 flood.	68
Figure 62. Erosion and accretion volume change in response to UBS diversion in 2008 - 2010.	68
Figure 63. Erosion and accretion volume change in response to UBS diversion at RM 77 and RM 81.5.	69

Figure 64. Erosion and accretion volume change in 1.5 and 3 years due to the UBS diversion at RM 81.5. ....	69
Figure 65. Cumulative SWR comparison for different sizes of diversion at RM 77 in 2008 – 2010. ....	76
Figure 66. Cumulative SWR comparison for different locations at capacity 250k cfs in 2008 – 2010. ....	76

## Tables

Table 1. Statistical analysis for velocity calibration for BC model. ....	7
Table 2. Statistical analysis for water-level calibration for BC model. ....	8
Table 3. Statistical analysis for Discharge calibration at Airline Hwy for BC model. ....	8
Table 4. Statistical analysis for suspended sand concentration profiles for BC model. ....	12
Table 5. Sediment loads calibration at Airline Hwy statistical analysis for BC model. ....	14
Table 6. BC Model performance in the 1997 flood event. ....	17
Table 7. BC Model performance in the 2008 flood event. ....	18
Table 8. Sediment budget for sand load during the 2011 flood for BC model. ....	20
Table 9. Sediment budget for fine sediment during the 2011 flood for BC model. ....	21
Table 10. Sediment budget for total sediment load during the 2011 flood for BC model. ....	22
Table 11. Stage calibration and validation statistical analysis for MG-WD. ....	28
Table 12. Velocity calibration statistical analysis for MG-Wd model. ....	29
Table 13. Suspended fine load calibration and validation statistical analysis for MG-WD. ....	33
Table 14. Suspended sand load calibration and validation statistical analysis for MG-WD. ....	35
Table 15. Total Suspended Load Calibration and Validation Statistical Analysis for MG-WD. ....	37
Table 16. Sediment budget for sand load for PR 1: MG-WD. ....	44
Table 17. Sediment budget for fine sediment for PR 1: MG-WD. ....	44
Table 18. Sediment budget for total sediment load for PR 1: MG-WD. ....	45
Table 19. Sediment budget for sand load for PR 2: MG-WD. ....	46
Table 20. Sediment budget for fine sediment for PR 2: MG-WD. ....	47
Table 21. Sediment budget for total sediment load for PR 2: MG-WD. ....	47
Table 22. Sediment budget for sand load for PR 3: MG-WD. ....	48
Table 23. Sediment budget for fine sediment for PR 3: MG-WD. ....	48
Table 24. Sediment budget for total sediment load for PR 3: MG-WD. ....	48
Table 25. Stage Calibration and Validation Statistical Analysis for UBS. ....	55
Table 26. Velocity calibration statistical analysis for UBS. ....	58
Table 27. Suspended fine load calibration and validation statistical analysis for UBS. ....	61
Table 28. Suspended sand load calibration and validation statistical analysis for UBS. ....	62
Table 29. Total suspended load calibration and validation statistical analysis for UBS. ....	64
Table 30. Description of production runs for UBS model. ....	65
Table 31. Sediment budget for sand load for PR 1: UBS model. ....	70
Table 32. Sediment budget for fine sediment for PR 1: UBS model. ....	71



---

Table 33. Sediment budget for total sediment load for PR 1: UBS model.....	71
Table 34. Sediment budget for sand load for PR 2: UBS model. ....	71
Table 35. Sediment budget for fine sediment for PR 2: UBS model.....	72
Table 36. Sediment budget for total sediment load for PR 2: UBS model.....	72
Table 37. Sediment budget for sand load for PR 3: UBS model. ....	72
Table 38. Sediment budget for fine sediment for PR 3: UBS model.....	73
Table 39. Sediment budget for total sediment load for PR 3: UBS model.....	73
Table 40. Sediment budget for sand load for PR 4: UBS model. ....	73
Table 41. Sediment budget for fine sediment for PR 4: UBS model.....	74
Table 42. Sediment budget for total sediment load for PR 4: UBS model.....	74
Table 43. Sediment budget for sand load for PR 5: UBS model. ....	74
Table 44. Sediment budget for fine sediment for PR 5: UBS model. ....	75
Table 45. Sediment budget for total sediment load for PR 5: UBS model.....	75

## **Preface**

This study was conducted for the U.S. Army Corps of Engineers (USACE) New Orleans District and CPRA of Louisiana as part of MRHDMS. The project managers for USACE were Bill Hicks and Daimia Jackson, and the Plan Formulator was Cherie Price. The project managers for CPRA were Carol Parsons Richards, Austin Feldbaum, Elizabeth Jarrell, and Wes LeBlanc. Ehab Meselhe from the Institute and Barb Kleiss from USACE Mississippi Valley Division were the Technical Leads.

Ehab Meselhe and Kazi Sadid conducted this study under CPRA Task Orders 5 and 7.

## Unit Conversion Factors

Multiply	By	To Obtain
acres	4,046.873	square meters
acre-feet	1,233.5	cubic meters
angstroms	0.1	nanometers
cubic feet	0.02831685	cubic meters
cubic inches	1.6387064 E-05	cubic meters
cubic yards	0.7645549	cubic meters
feet	0.3048	meters
foot-pounds force	1.355818	joules
gallons (US liquid)	3.785412 E-03	cubic meters
hectares	1.0 E+04	square meters
inches	0.0254	meters
inch-pounds (force)	0.1129848	newton meters
microns	1.0 E-06	meters
miles (US statute)	1,609.347	meters
miles per hour	0.44704	meters per second
mils	0.0254	millimeters
pounds (mass)	0.45359237	kilograms
pounds (mass) per cubic foot	16.01846	kilograms per cubic meter
pounds (mass) per cubic inch	2.757990 E+04	kilograms per cubic meter
pounds (mass) per square foot	4.882428	kilograms per square meter
pounds (mass) per square yard	0.542492	kilograms per square meter
square feet	0.09290304	square meters
square inches	6.4516 E-04	square meters
square miles	2.589998 E+06	square meters
square yards	0.8361274	square meters
tons (force)	8,896.443	newtons
tons (long) per cubic yard	1,328.939	kilograms per cubic meter
yards	0.9144	meters

# 1 Overview and Objectives

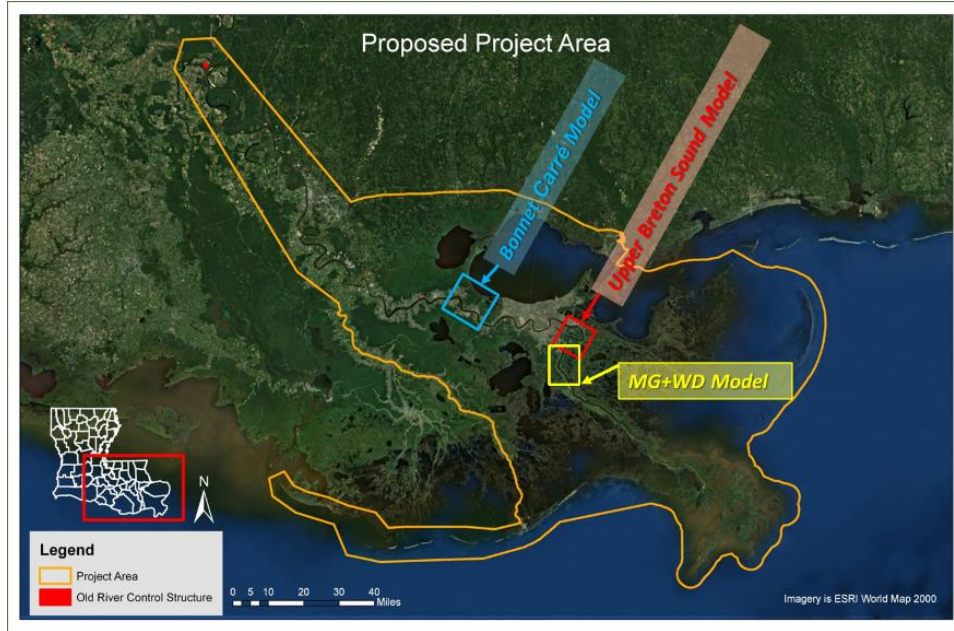
This report summarizes the multidimensional numerical modeling effort performed by the modeling team of the Water Institute of the Gulf as part of MRHDMS. This modeling effort focuses on near-field or local applications of Delft-3D model near areas of interest, specifically Bonnet Carré, Upper Breton Sound, LCA-White Ditch, and LCA-Myrtle Grove. The local reaches modeled by Delft-3D are shown in Figure 1. These domains have sufficient resolution to capture the flow dynamics in the vicinity of the diversion intake, as well as the upstream and downstream reaches of the diversion. The specific tasks include model development, calibration, validation, and model applications, and are intended to address the following:

- Investigate the short-term (< 5 years) geomorphic responses of the river channel to a sediment diversion;
- Investigate the sediment capture efficiency calculated by the numerical model during periods in which the diversions are in operation;
- Estimate the mass quantities and spatial pattern of erosion and accretion in the river channel;
- Assess the potential morphologic impact of the diversion on the river channel for different design capacities and locations of the diversion;
- Quantify a sediment budget at each diversion site;
- Investigate the interaction between the Myrtle Grove and White Ditch Diversions and the potential impact on their individual sediment capture efficiency.

As this modeling effort focuses entirely on the near-field for a shorter time period and the domain is limited to the main stem of the river and the outfall channel, the results should not be used to:

- Infer the morphologic alteration of the river channel for long-term (decadal) periods. Larger domain models should be used for such purpose;
- Infer the overall efficiency of a sediment diversion for long-term (decadal) periods.

Figure 1. Near-Field Applications of Delft-3D to Bonnet Carré, Upper Breton Sound, and Myrtle Grove and White Ditch.



## 2 Delft-3D Modeling – Bonnet Carré Spillway

This chapter provides an overview of the Delft-3D Modeling for the Bonnet Carré Spillway. The opening of the Bonnet Carré spillway during the flood event of May-June 2011 presents an opportunity to observe the hydro and morphodynamics in the vicinity of a large diversion and how sediment is captured and delivered through an outfall channel of pathway to the receiving area. A Delft3D model was setup and calibrated using an extensive field surveys performed before, during, and after the 2011 flood. The model was also applied to the flood events of 2008 and 1997 to gain further insights into the response of the river to such large diversions (~ 250,000 to 300,000 CFS).

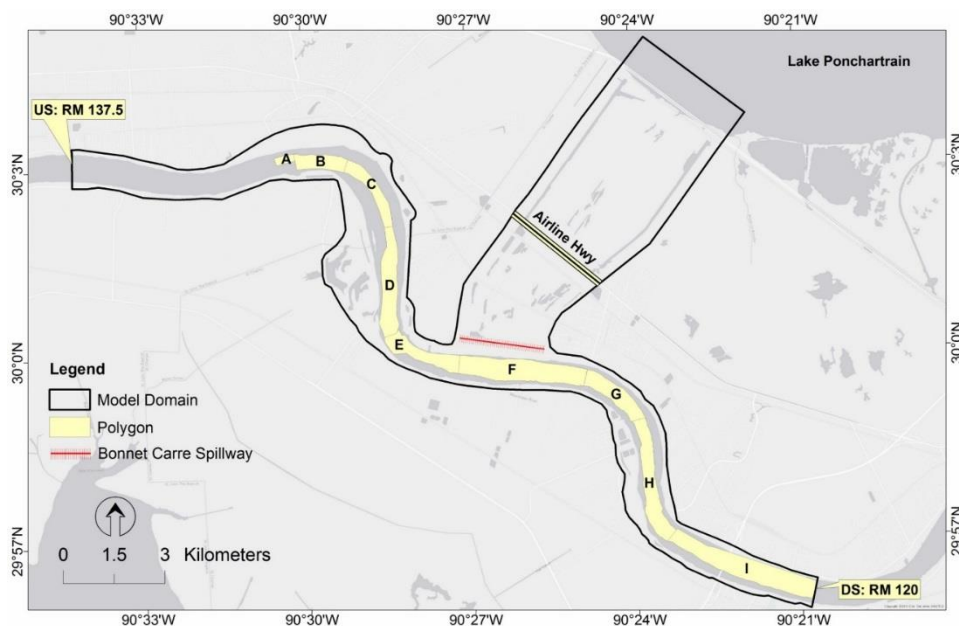
### 2.1 Calibration and Validation of Hydrodynamics, Sediment Transport, and Morphology

The Bonnet Carré spillway (BC) model includes an 18-mile reach of the lower Mississippi River (RM 137 through 119, measured from the river mouth known as the Head of Passes) immediately upriver of New Orleans, Louisiana. This river reach includes the Bonnet Carré Spillway, the floodway, and a small portion of Lake Pontchartrain (Figure 2). The model setup includes the following:

- A 2011 multibeam bathymetry for the main river (Allison et. al., 2013)
- A 2010 Light detection and ranging (LIDAR) survey data used for overbank areas;

The model was setup in a three-dimensional format with 10 vertical sigma layers. The model used the Van Rijn (1984) formulations for sand and the Partheniades-Krone formulations for fine sediment transport. The main calibration parameters were bed roughness (Manning's  $n$ ), suspended load and bed load factors, settling velocity and reference height, critical shear stress for fine material, and erosion parameter.

Figure 2. Model domain and location of the polygons - BC Model.



The Bonnet Carré (BC) model is calibrated for hydrodynamics, sediment transport, and morphological responses of the river during the flood event of 2011. During this event, the spillway was open for approximately 56 days during the period of May-June 2011. Boat-based field observations were collected on May 9-11, 2011; May 20-22, 2011 (peak flow); and June 23-25, 2011. Multibeam bathymetry, flow velocities, suspended sediment load, and bed sediment load data were collected. Data collection also included grain size distribution of the suspended sediment material as well as bed grab samples (Allison et al., 2013).

The model was validated from 26<sup>th</sup> June, 2011, after the closing of the spillway, to 15<sup>th</sup> June, 2012, for an entire year. Another boat-based survey was conducted on June 12-14, 2012, when only the multibeam bathymetry was collected. Therefore, the model was validated based on the sediment quantities deposited and eroded within the river channel during the one year period. The model was further validated for historical flood events based on the U.S. Geological Survey (USGS) measurements at the Airline Highway, namely the flood of 2008 and 1997. In summary, the model was calibrated and validated as follows:

- Calibration: May 1st to June 25th, 2011;
- Validation: June 2011 to June 2012, March 8th, 1997 to April 18th, 1997 (the 1997 flood) and April 1st, 2008 to May 11th, 2008 (the 2008 flood).

The main stem model has a grid resolution ranging from 30 m by 30 m to 30 m by 90 m. A time-step of 0.10 min (6 s) was used in all calibration and validation simulations.

The model was first calibrated and validated for hydrodynamics only. The following boundary conditions were used:

- Upstream (US) Boundary: Flow at Baton Rouge (U.S. Geological Survey [USGS]) station ID: 07374000 and USACE station ID: 01160 at RM 228.4;
- Downstream (DS) Boundary: Water-level interpolated between gauges DS of Bonnet Carré Spillway (RM 126.9) and at Carrollton (RM 102.8) by USACE (vertical datum NAVD88);
- Lake Pontchartrain Boundary: Water-level at the gauge at the west end of the Lake by USACE (vertical datum NAVD88).

### **Model Calibration for the 2011 flood**

The hydrodynamic component of the model was compared against flow velocity profiles, water-level, and discharge measurements collected from the Mississippi channel in May-June 2011. Spatially varying Manning's roughness coefficients were used as calibration parameters for hydrodynamic simulations. In the main channel, the Manning's  $n$  is  $0.024 \text{ s/m}^{1/3}$ ; on the flood plain it is  $0.05 \text{ s/m}^{1/3}$ ; and in the outfall of the spillway  $n$  is  $0.06 \text{ s/m}^{1/3}$  due to dense vegetation. The Manning's  $n$  is also as high as  $0.08 \text{ s/m}^{1/3}$  at Airline Highway and the Railway Bridge section within the floodway.

Field velocity profiles obtained from boat-based Acoustic Doppler Current Profiler (ADCP) measurements (Figure 3) were compared to model-derived velocity profiles. Not all locations where measurements were taken during the peak of the event were repeated in the surveys collected May 9-11, 2011 and June 23-25, 2011. Model results were compared with the field velocity profiles for all locations where measurements were available.



Figure 3. Location for velocity measurement.

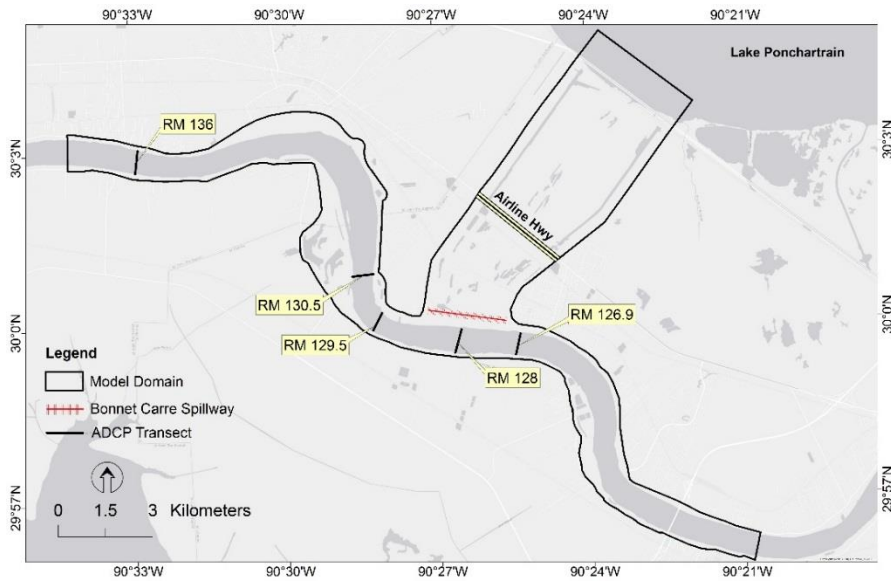


Figure 4 shows calibration for a depth averaged horizontal velocity profile and a vertical velocity profile extracted in the vicinity of the river thalweg at RM 128, respectively, which were collected on May 21, 2011. The model reproduced the measured velocities within the range of observed velocity fluctuations. Similar performance is shown in Figure 5, with a horizontal and vertical profile at RM 126.9 on June 25, 2011 after the closure of the structure. The statistical analysis for the velocity is presented in Table 1. The statistics for depth average velocity profiles match the desired target limit. For vertical velocity profiles, the statistics are lower than the desired target, but are close to the acceptable target presented in Meselhe and Rodrigue (2013). The statistics for vertical velocity profiles were estimated based on the mean of the observed velocities in each vertical layer. The observed velocity in verticals were collected by boat based ADCP in a span of 15-20 minutes for each location. Figure 4 and 5 show that the observed velocities fluctuated around 4 ft/sec during the measurement. As seen in the figures, the model was able to predict the velocity verticals within the variation observed in the field.

Figure 4. Velocity at RM 128 on May 21, 2011.

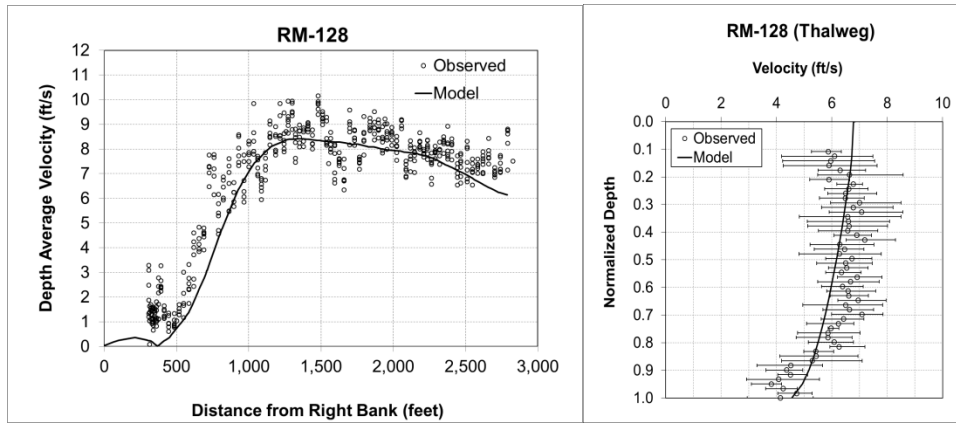


Figure 5. Velocity at RM 126.9 on June 25, 2011.

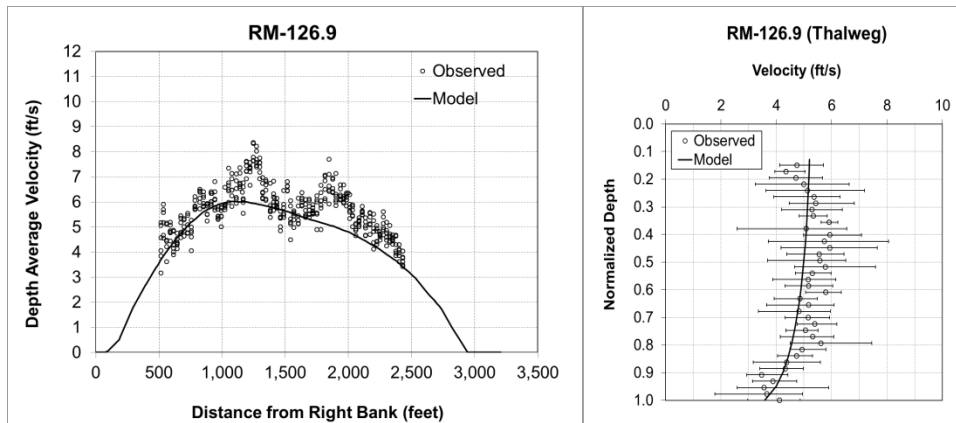


Table 1. Statistical analysis for velocity calibration for BC model.

Calibration period: May-June 2011	Bias % of Range	RMSE%	Corr. Coef.
Velocity (transverse profile)	-4.6%	18.87%	0.91
Velocity (Vertical Profile)	-19.5	21.5%	0.81
Meselhe and Rodrigue (2013) Report	Bias % of Range	RMSE%	Corr. Coef.
Target Desired	< 15% for all stations	< 20% for all stations	> 0.75 for all stations
Target Acceptable	< 15% for 50% of stations	< 30% for 50% of stations	> 0.75 for 50% of stations

The 56 days of flooding between May 1 and June 25, 2011 during the opening of the Bonnet Carré Spillway, was used to calibrate the model for water-level and discharge. The simulated water-level at upstream (US) and downstream (DS) of the Bonnet Carré Spillway (RM 129.5 and RM 126.9, respectively) was compared against the gauge data provided by U.S. Army Corp. of Engineers (USACE). The water-level calibration is shown in Figure 6. Figure 7 presents the calibration of water discharge passing through at Airline Highway against USGS observations during the spillway opening. For the

model performance assessment, a statistical analysis was performed based Meselhe and Rodrigue (2013), and presented in Table 2 and Table 3. The statistical results show that the model predicted water-levels and discharges through the spillway both compare well and conform to the desired target limit presented in Meselhe and Rodrigue (2013).

**Table 2. Statistical analysis for water-level calibration for BC model.**

Modeled Period	Bias % of Range	RMSE%	Corr. Coef.
May 21 <sup>st</sup> – June 25 <sup>th</sup> , 2011	-1.5%	0.9%	1.0
Meselhe and Rodrigue (2013) Report	Bias % of Range	RMSE%	Corr. Coef.
Target Desired	< 10% for all stations	< 15% for all stations	> 0.9 for all stations
Target Acceptable	< 10% for 80% of stations	< 15% for 80% of stations	> 0.9 for 80% of stations

**Table 3. Statistical analysis for Discharge calibration at Airline Hwy for BC model.**

Modeled Period	Bias % of Range	RMSE%	Corr. Coef.
May 21 <sup>st</sup> – June 25 <sup>th</sup> , 2011	3%	11%	0.95
Meselhe and Rodrigue (2013) Report	Bias % of Range	RMSE%	Corr. Coef.
Target Desired	< 15% for all stations	< 20% for all stations	> 0.8 for all stations
Target Acceptable	< 15% for 50% of stations	< 20% for 50% of stations	> 0.7 for 50% of stations

**Figure 6. Water-level calibration during May 1- June 25, 2011.**

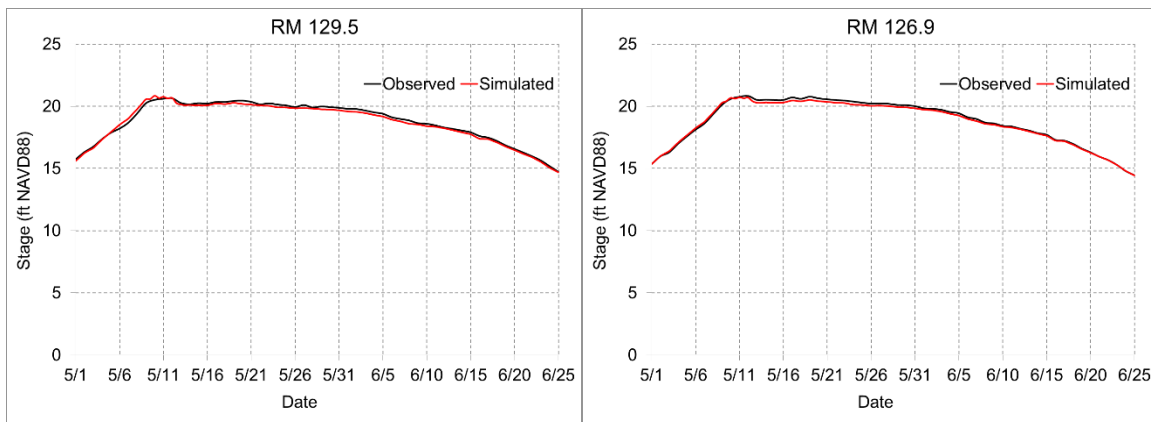
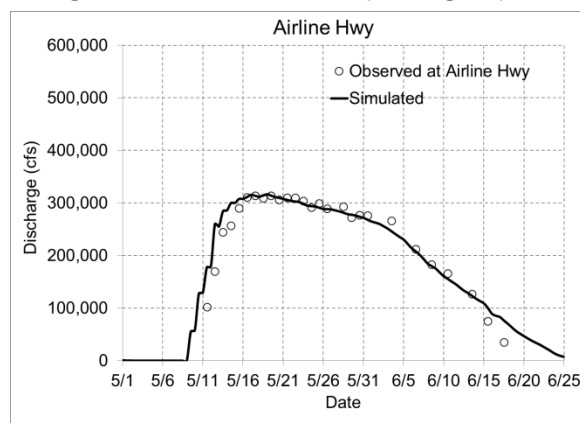


Figure 7. Discharge calibration at Airline Hwy during May 1- June 25, 2011.



The calibration of sediment transport followed the hydrodynamic calibration. The prescribed boundary conditions were:

- US boundary: Suspended sediment concentrations for the following size-classes:
- Non-cohesive sediment: very fine sand ( $D_{50} = 83 \mu\text{m}$ ), fine sand ( $D_{50} = 167 \mu\text{m}$ ) and medium sand ( $D_{50} = 333 \mu\text{m}$ );
- Cohesive sediment: clay ( $D < 2 \mu\text{m}$ ) and silt ( $2 \mu\text{m} < D < 63 \mu\text{m}$ ).

It should be noted that only  $D_{50}$  is provided based on the grain size distribution of the suspended sediment material as well as bed grab samples, collected from the field during the calibration period (Allison et al., 2013). The numerical model then generates a distribution curve internally. The suspended sediment concentrations were estimated daily to be prescribed as inputs to the Delft-3D model based on rating curves at Baton Rouge (Allison et. al., 2012).

Sediment calibration was performed with the field measurements available at upstream (RM 136) and downstream (RM 126.9) of Bonnet Carré Spillway during the peak of the flood (May 21) and during the recession period (June 22) of 2011. Delft-3D has two separate scalar multiplication factors (Sus and Bed, as named in the model input) to calibrate the non-cohesive suspended load and bed load transport rate (Deltares, 2011). Different values of the calibration parameters were tested. Finally, the suspended load and bed load multiplication factors were selected as 0.5 and 6, respectively. The reference height ( $a$ , as named in the model input) is an essential parameter for sediment transport calibration in Delft-3D. The reference height is the roughness height or the bed load layer thickness and a user defined input parameter of the Van Rijn (1984) transport formula. According to a previous study by El Kheishy (2007) the bed form height in the study area under consideration should be around 2.25 m. The model was tested with different reference height numbers from 1-4 m. At the end, a 2-meter reference height was selected which agreed with observations at most locations. Figure 8

and Figure 9 show the model predicted suspended sand concentration profile at RM 136 and RM 126.9 on May 21 and June 22, 2011 from three different scenarios, where Case 1:  $a=4\text{m}$ ,  $Sus=1$ ; Case 2:  $a=2\text{m}$ ,  $Sus=1$ ; and Case 3:  $a=2\text{m}$ ,  $Sus=0.5$ . It can be clearly seen from Figures 8 and 9 that the model has a very good ability to reproduce sand concentrations for the May-June 2011 flow. The surface concentrations of sand are predicted fairly well (except for the left bank cast at RM 136 on June 22), while the bottom concentrations are often in slight disagreement with the observations. Therefore, Case 3 was selected ( $a=2\text{m}$ ,  $Sus=0.5$ ), which agreed with observations at most locations. The statistics for concentrations were calculated and presented in Table 4. The comparison conforms to the desired target limit, as described in Meselhe and Rodrigue (2013).

The suspended and bed load fluxes were measured at RM 136 and RM 126.9 on May 21 and June 22, 2011. There were several observations available as suspended sand and fine sediment loads within the floodway at Airline Hwy, measured by USGS during the 2011 flood. Figure 10 and Figure 11 show the model calibration both for sand and fine sediment loads. Following Meselhe and Rodrigue (2013), the statistical analysis for the sediment load calibration is presented in Table 5. There were only two observations available at RM 136 and RM 126.9 during the calibration period, so the sample size was not sufficient for calculating statistics. As such, statistics were only calculated for USGS observations at Airline Hwy.

Figure 8. Calibration of suspended sand concentration between model and observations at the US of BC (RM 136) and DS of BC (RM 126.9) on May 21, 2011 when the structure was open with peak diversion discharge.

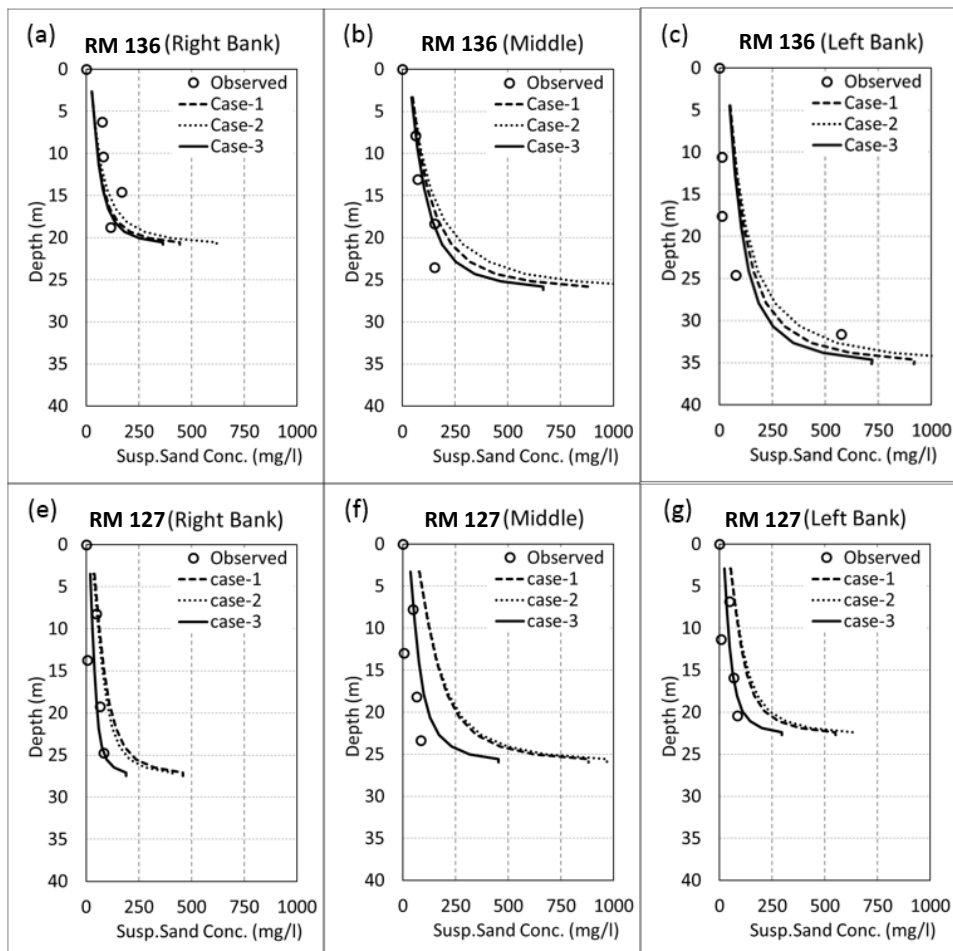


Figure 9. Calibration of suspended sand concentration between model and observations at the US of BC (RM 136) and DS of BC (RM 126.9) on June 22, 2011 in post-flood condition when the structure was closed.

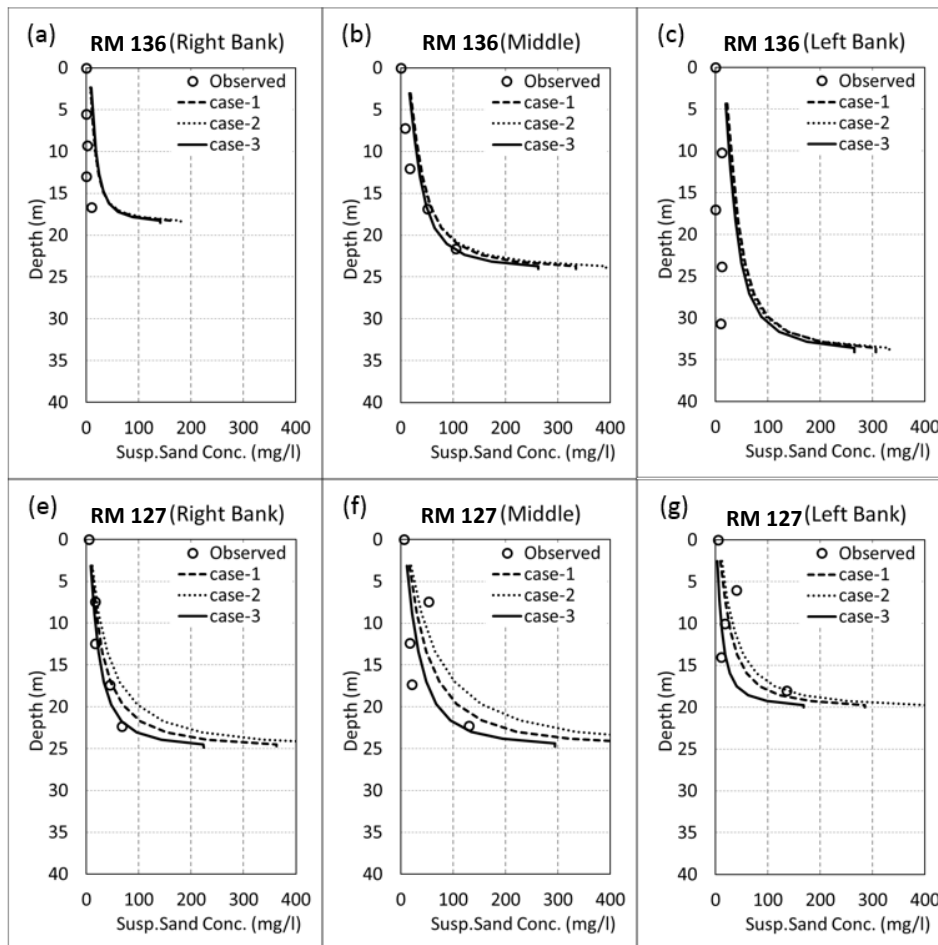


Table 4. Statistical analysis for suspended sand concentration profiles for BC model.

Calibration Period	Bias (%)	RMSE%	Corr. Coef.
May 21 <sup>st</sup> – June 25 <sup>th</sup> , 2011	-5%	21%	1.0
Meslehe and Rodrigue (2013) Report	Bias (%)	RMSE%	Corr. Coef.
Target Desired	< 20% for all stations	< 33% for all stations	> 0.5 for all stations
Target Acceptable	< 20% for 50% of stations	< 50% for 50% of the stations	> 0.5 for 50% of stations

Figure 10. Model calibration for the suspended and bed load: (a) suspended sand loads, (b) fine sediment loads, and (c) bed loads, at the US of BC (RM 136) and DS of BC (RM 126.9).

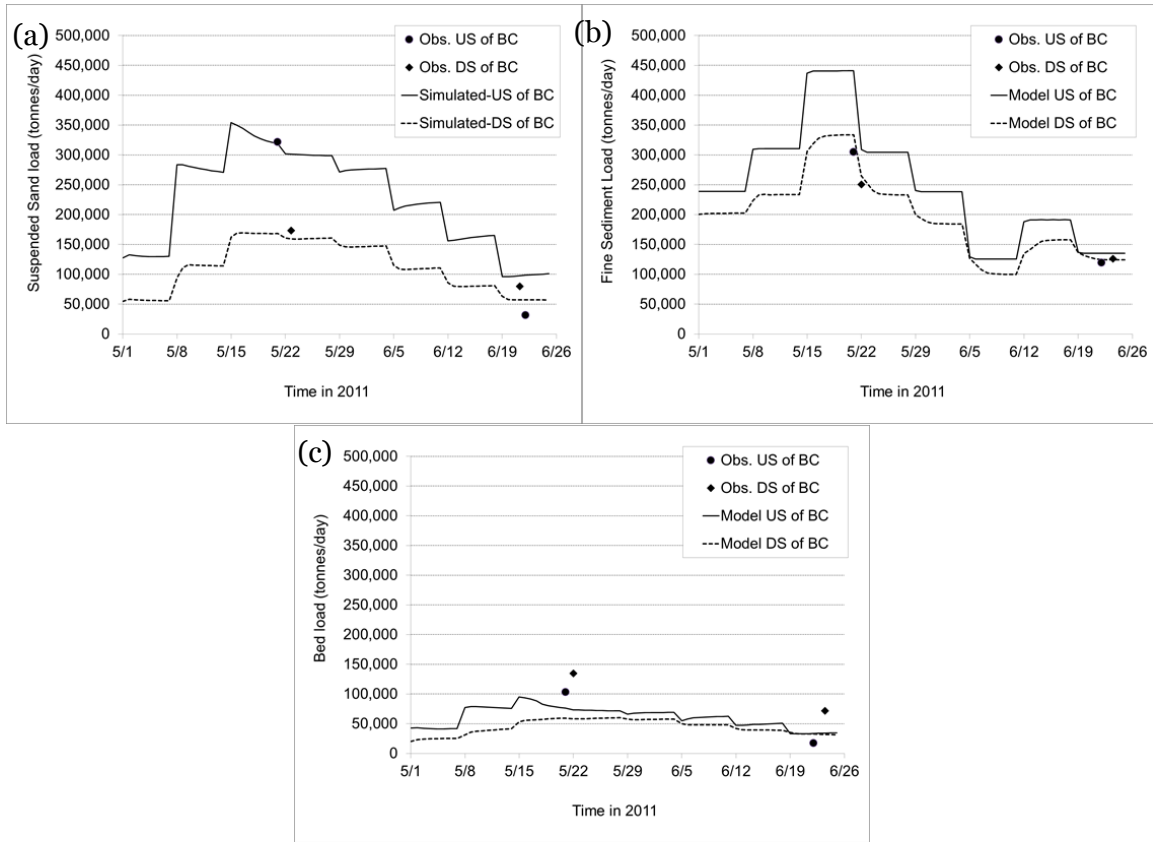


Figure 11. Model calibration for the suspended load at Airline Hwy: (a) suspended sand loads, and (b) fine sediment loads.

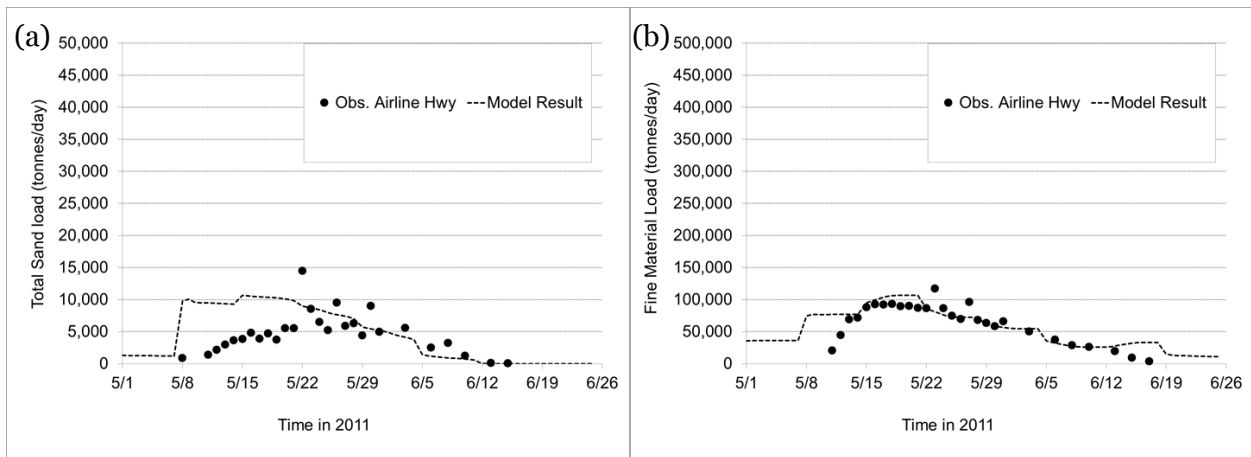




Table 5. Sediment loads calibration at Airline Hwy statistical analysis for BC model.

	Bias (%)	RMSE%	Corr. Coef.
Sand	22%		0.91
Fine sediment	13%	32%	0.81
<b>Meselhe and Rodrigue (2013) Report</b>	<b>Bias (%)</b>	<b>RMSE%</b>	<b>Corr. Coef.</b>
Target Desired	< 20% for all stations	< 33% for all stations	> 0.5 for all stations
Target Acceptable	< 20% for 50% of stations	< 50% for 50% of the stations	> 0.5 for 50% of stations

### Morphologic Calibration:

A multilayer bed composition model consisting of all the sediment fractions has been defined based on the collected bed grab samples. The field observations (Allison et al, 2013) indicate that there are areas of exposed relict material highly resistant to erosion in the river bottom. An examination of the geometry of these relict areas in the field data allowed for the assumption that bed elevation below -35 m NAVD88 is considered to be bedrock (Allison et al., 2012). The remaining areas of the river bottom have variable sediment thickness with maximum availability between the thalweg and the bar. The sediment layer thickness gradually reduces from the bar to the banks of the river. This design has been prepared based on professional experiences and using the multibeam surface of the river bottom which shows relative changes in bed forms between the crossing and the bend.

The BC model was calibrated for morphologic changes in the river in response to the 56-day diversion pulse during the 2011 flood by the aggradation and erosion volumes. These volumes were also estimated from multi-beam surveys (Figure 12). As shown in Figure 2, the multi-beam measurements in polygons A, B, and C did not cover the full river width (Allison et al., 2013), and as such, the field observations were not sufficient to provide information within these polygons. However, the overall calculated and measured deposition/erosion patterns are consistent. The uncertainty band around the field observations shown in Figure 12 corresponds to a random error (representing the measurement uncertainty) of approximately +/- 20cm at each coordinate of the multi-beam survey. Figure 12 shows significant deposition occurring in front of the spillway in polygon-F.

A full-year analysis (June 2011- June 2012) was performed following the 2011 flood event for model validation. Detailed mapping of the river bottom in June 2012 was undertaken to quantify the morphologic changes after a full-flood year (Allison et al., 2013). Figure 12(b) shows that most of the deposited material during the pulse (polygon F) was eroded and migrated downstream (polygons G and H). The model captured the

most prominent morphological changes that occurred during the flood and in the following year. Figure 13 and Figure 14 show the full pattern of aggradation and erosion that occurred during the pulse (May-June 2011) and between June 2011-June 2012, respectively.

Figure 12. Erosion and accretion volume (a) May-June 2011; and (b) June 2011-June 2012.

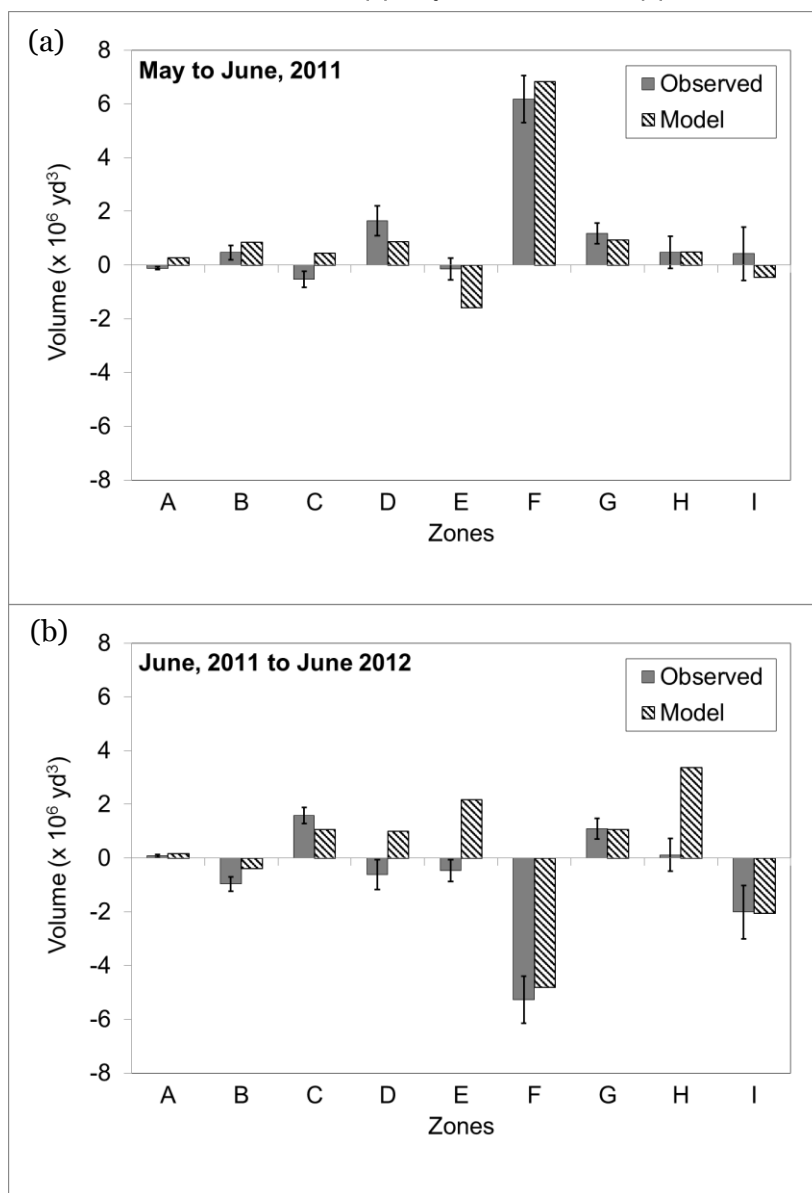


Figure 13. Erosion and accretion pattern during the pulse (May-June 2011): Observation polygons A to I.

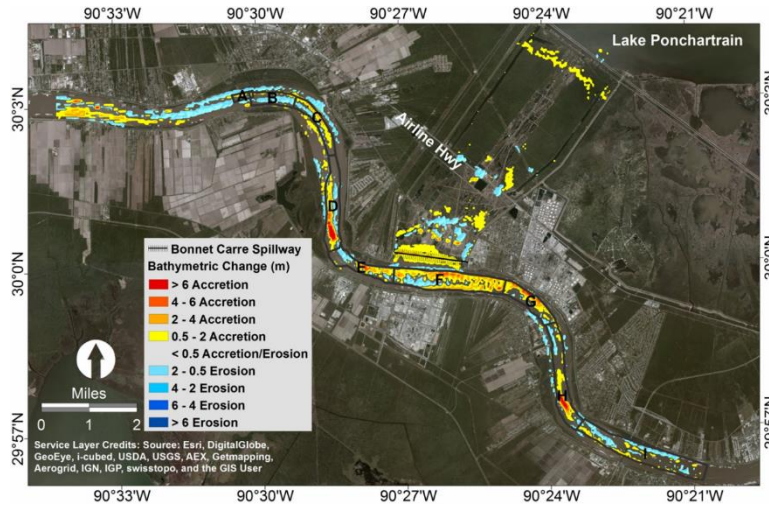
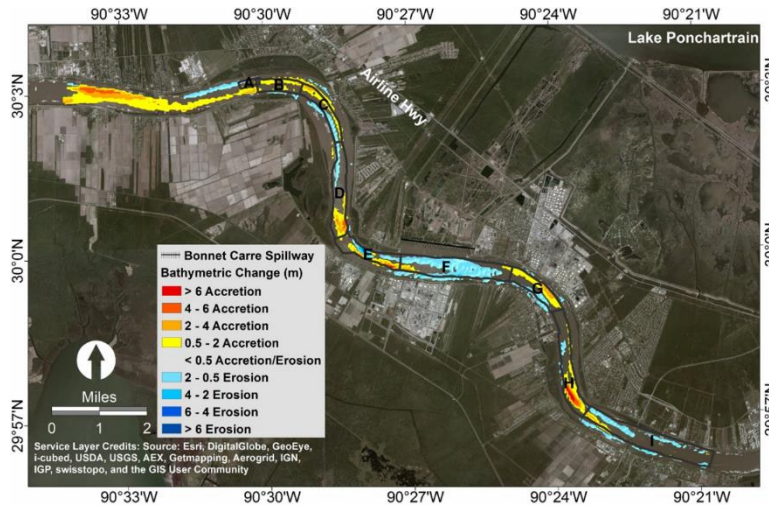


Figure 14. Erosion and accretion pattern in the main channel from June 2011 to June 2012.



Model Validation for the 1997 flood:

The validation of Bonnet Carré Spillway model for the 1997 flood was performed for water and sediment volume. The water volume was measured only at Airline Hwy. But the sediment volume was measured at the fore bay, at Airline Hwy and at I-10. Figure 15 shows the validation performed at three different locations. The performance of the model is summarized through the statistical analysis provided in Table 6.

Figure 15. BC Model validation for the 1997 flood.

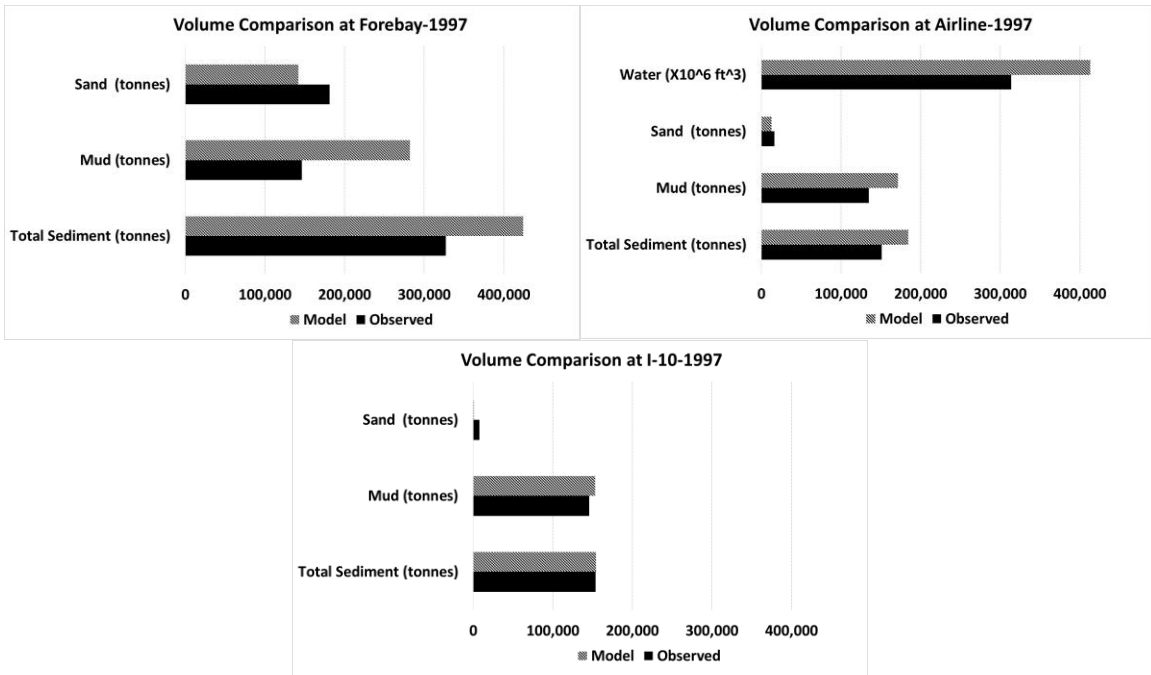


Table 6. BC Model performance in the 1997 flood event.

AIRLINE HWY.			
	Observed	Model	Bias%
Total Sediment (tonnes)	151,286	184,613	18
Mud (tonnes)	135,087	171,761	21
Sand (tonnes)	16,199	12,852	-26
Water (X10 <sup>6</sup> ft <sup>3</sup> )	313,874	413,346	24
I-10			
	Observed	Model	Bias%
Total Sediment (tonnes)	153,559	154,281	0
Mud (tonnes)	145,907	153,423	5
Sand (tonnes)	7,652	858	-792
FOREBAY			
	Observed	Model	Bias%
Total Sediment (tonnes)	327,381	424,457	23
Mud (tonnes)	146,176	282,265	48
Sand (tonnes)	181,205	142,192	-27

Model Validation for the 2008 flood:

The Bonnet Carré Spillway model is further validated for the 2008 flood event. The model validation was performed for the water and sediment volumes. The field observations were available only at the Airline Hwy for the 2008 flood. Figure 16 and Table 7 show the model validation at Airline Hwy and the statistical analysis for model performance respectively.

Figure 16. BC Model validation for 2008 flood.

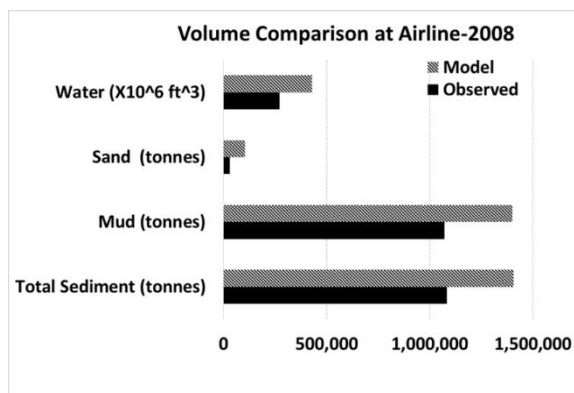


Table 7. BC Model performance in the 2008 flood event.

	Observed	Model	Bias%
Total Sediment (tonnes)	1,084,141	1,406,169	23
Mud (tonnes)	1,070,979	1,400,649	24
Sand (tonnes)	30,560	105,352	71
Water ( $\times 10^6 \text{ ft}^3$ )	271,931	428,634	37

## 2.2 Model Application

Morphologic Response in the River Channel:

The validated BC model was applied to quantify the morphologic response of the river during the spillway opening in the 1997 and 2008 flood events. The aggradation and erosion volumes were calculated after both events. Similar to the 2011 flood, significant aggradation occurred in both 1997 and 2008 floods. The comparison among erosion and deposition volumes near the spillway indicates that nearly the same volume, i.e.  $4 \text{ yd}^3$  of materials deposited in front of the spillway in polygon F for all three events (Figure 17). Figure 18 and 19 show the full pattern of aggradation and erosion during the pulses of 1997 and 2008.

Figure 17. Calculated erosion and accretion volume during the 2011, 2008, and 1997 flood.

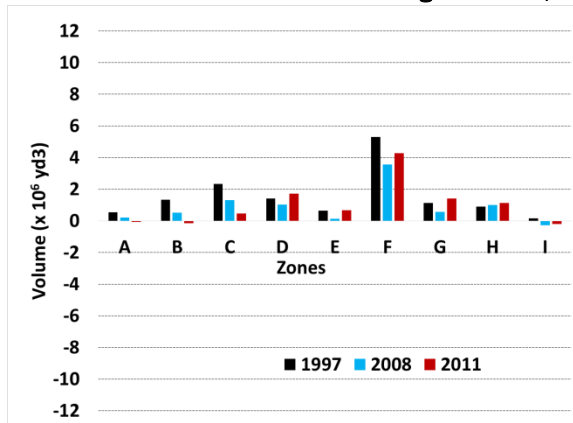


Figure 18. Erosion and accretion pattern during the 1997 flood.

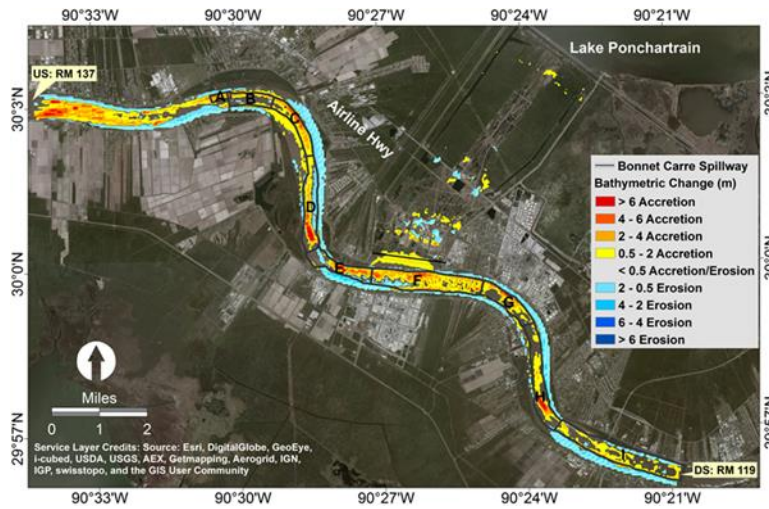
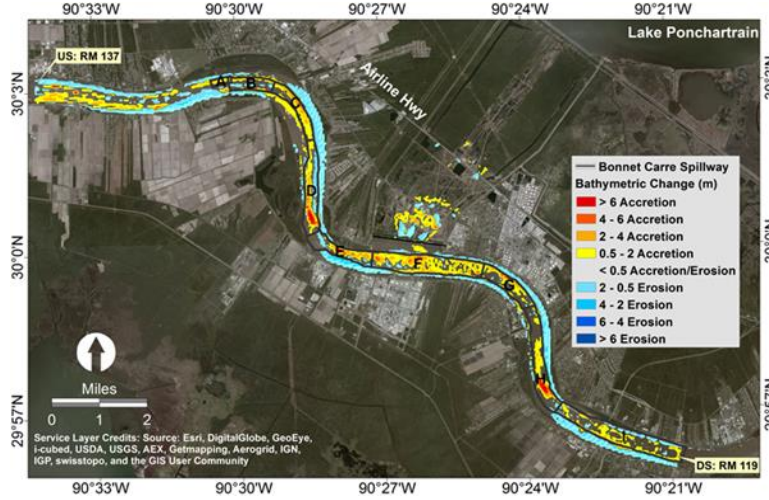


Figure 19. Erosion and accretion pattern during the 2008



**Sediment Budgets:**

In order to provide additional insights into the morphologic response of the river to the operation of Bonnet Carré spillway in the 2011 flood, a sediment budget was developed. The budget shows the cumulative sediment mass and bulk volume based on a dry density of 1,600 kg/m<sup>3</sup>: (a) entering/leaving the river segment studied here, (b) passing through the diversion structure, and (c) eroding or depositing within the river channel. The sand budget showed that 29% of the inflowing sand load, which was about 5.1 million tonnes, was deposited on the riverbed and 44% exited through the downstream section (Table 8). The fine sediment budget (clay and silt) indicates that 4% of the entering fine sediment load was deposited and 87% exited the system (Table 9). These estimates of the two budgets are fully supported by field observations. The model-based sand budget shows that 17% of the inflowing sand load was deposited in the forebay, 8% was deposited between the spillway opening and Airline Hwy. The remaining 2% of the inflowing sand load was deposited in between Airline Hwy and I-10. No sand load passed beyond the I-10 Bridge. The model also showed that 2 million tonnes of fine materials were entrained from the forebay area by the flood flow diverting through the spillway, none of which deposited in the floodway. Nearly 3.5 million tonnes of silt and clay washed away into Lake Pontchartrain during the spillway opening. Table 10 shows the budget for total load, i.e. the summation of the sand and fine sediment. Figure 20 and Figure 21 are presented to help visual interpretation of the sediment budget for sand and fine sediment load.

Table 8. Sediment budget for sand load during the 2011 flood for BC model.

	Inflow at the U/S	Outflow at DS of the river	Deposited in the river	Deposited in the fore bay	Deposited between spillway and Airline Hwy	Deposited between Airline Hwy and I-10	Outflow at I-10
Total Mass (10 <sup>6</sup> tonnes)	17.3	7.5	5.1	2.9	1.4	0.4	0.0
Total Volume (10 <sup>6</sup> yd <sup>3</sup> )	19.6	8.5	5.7	3.3	1.6	0.5	0.0
% of U/S Inflow		44%	29%	17%	8%	2%	0%

Figure 20. Sediment budget for sand load during the 2011 flood for BC model.

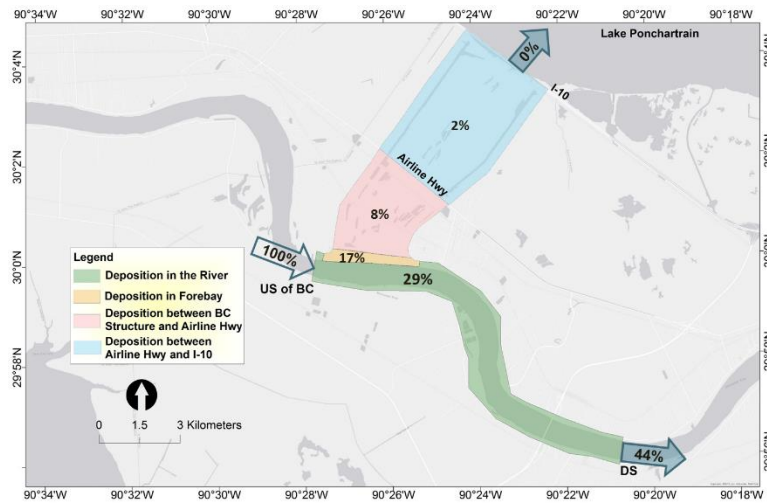


Table 9. Sediment budget for fine sediment during the 2011 flood for BC model.

	Inflow at the U/S	Outflow at DS of the river	Deposited in the river	Deposited in the forebay	Deposited between spillway and Airline Hwy	Deposited between Airline Hwy and I-10	Outflow at I-10
Total Mass (10 <sup>6</sup> tonnes)	15.4	13.4	0.6	-1.9	-0.1	0.0	3.4
Total Volume (10 <sup>6</sup> yd <sup>3</sup> )	17.3	15.1	0.7	-2.1	-0.1	0.0	3.8
% of U/S Inflow		87%	4%	-12%	0%	0%	22%

Figure 21. Sediment budget for fine sediment during the 2011 flood for BC model.

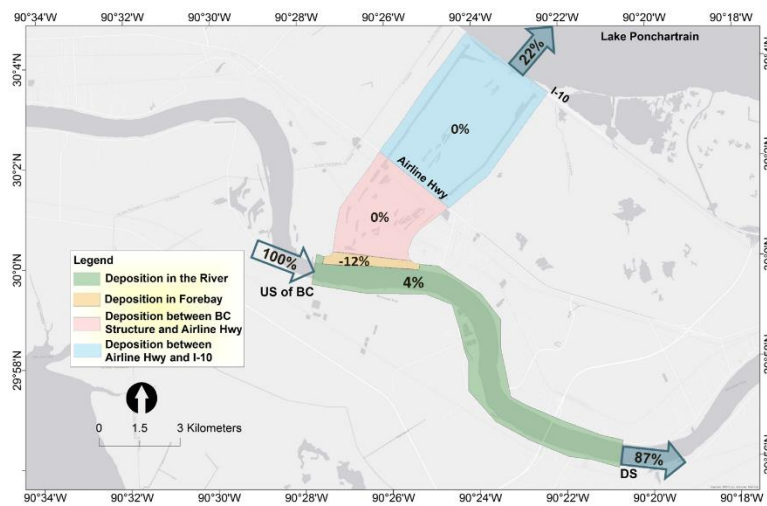




Table 10. Sediment budget for total sediment load during the 2011 flood for BC model.

	Inflow at the U/S	Outflow at DS of the river	Deposited in the river	Deposited in the fore bay	Deposited between spillway and Airline Hwy	Deposited between Airline Hwy and I-10	Outflow at I-10
Total Mass (10 <sup>6</sup> tonnes)	32.7	20.9	5.6	1.0	1.4	0.4	3.4
Total Volume (10 <sup>6</sup> yd <sup>3</sup> )	36.9	23.6	6.4	1.1	1.5	0.4	3.8
% of U/S Inflow		64%	17%	3%	4%	1%	10%

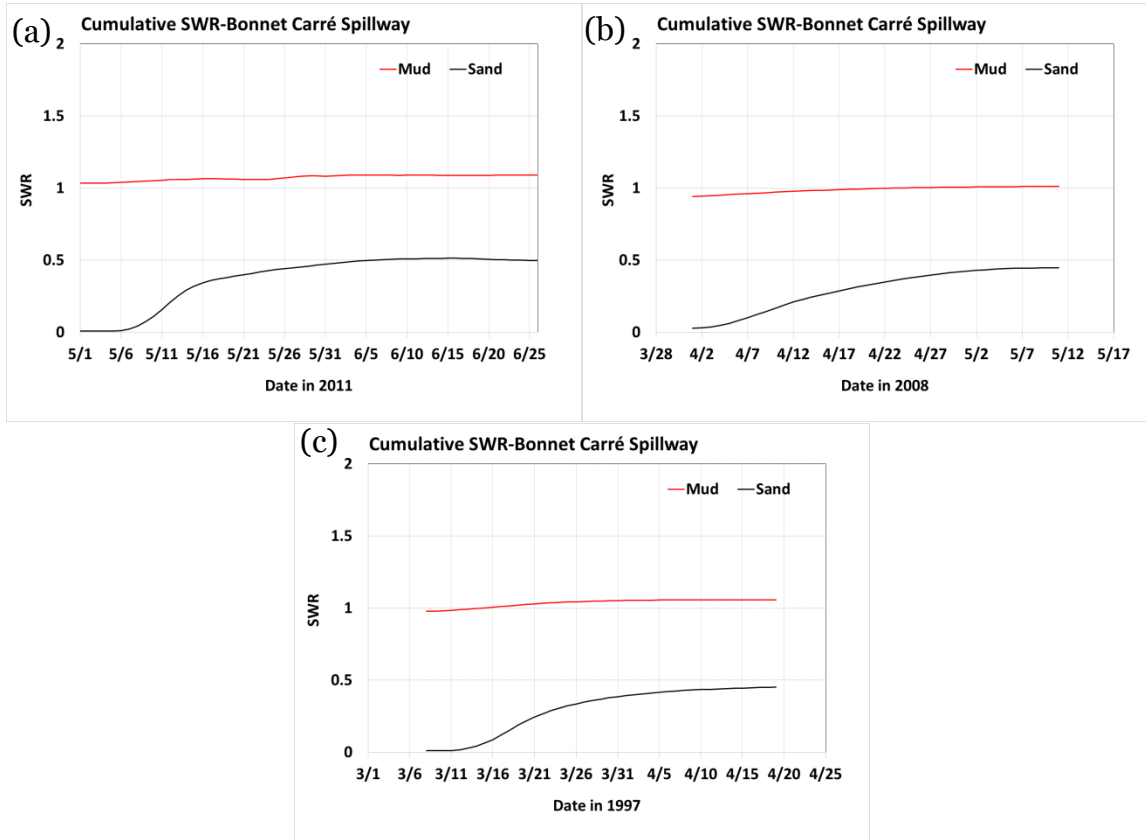
#### Sediment Water Ratio:

A sediment-water ratio (SWR) was used to quantify the sediment capture efficiency of a river diversion. This ratio is defined as follows:

$$SWR = \frac{\text{Sediment Load Diverted/Sediment Load in the River}}{\text{Water Discharged/Water Discharged in the River}}$$

A higher SWR value indicates a higher capture efficiency of a diversion, thereby lowering the potential for undesirable deposition in the river. The SWR for the spillway was calculated during the pulse in the 2011, 2008, and 1997 flood events. The cumulative SWR for fine sediment was approximately ~1. This is expected due to the low settling velocity of fine material. However, the ratio for sand was approximately 0.5 during all three events. This low SWR partially explains the large amount of sand deposition immediately downstream of the diversion intake.

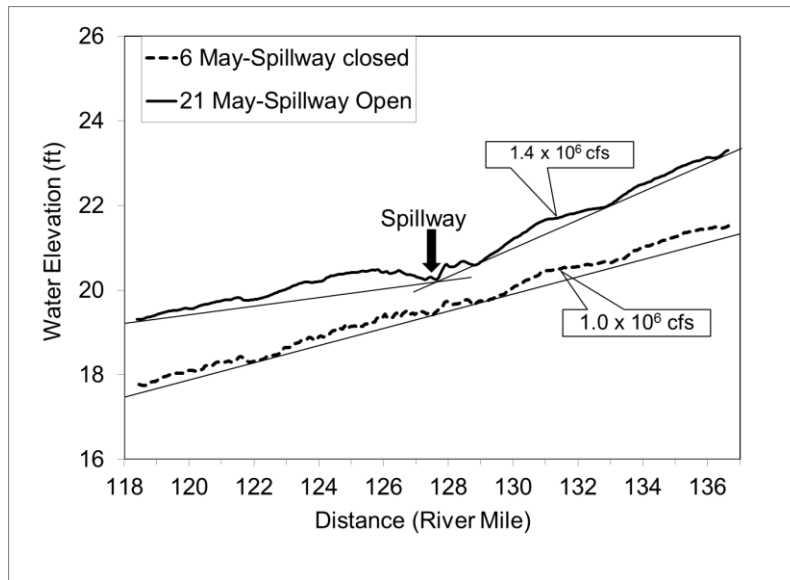
Figure 22. Cumulative SWR of Bonnet Carré spillway during the flood events: (a) 2011; (b) 2008, and (c) 1997.



**Stream Power:**

Stream power is the rate of energy dissipation along a river per unit length and is defined as:  $\rho QS$ , where  $\rho$  is water density,  $Q$  is total discharge, and  $S$  is the energy slope (Bagnold, 1966; Yang 1971). To avoid excessive riverine deposition, a reduction in the stream power should be accompanied by a proportional reduction in the sediment load. Figure 13 shows two water surface profiles during the 2011 flood; one at a river discharge of 1 million cfs when the diversion was closed, and a second at a river discharge of 1.4 million cfs with a peak diversion discharge of approximately 300,000 cfs. There is a clear decline in the water surface slope downstream of the diversion when it is operational. A one-dimensional model was used to adequately estimate the energy surface slope upstream and downstream of the diversion. A reach of approximately 80 miles was used to estimate the slope upstream of the diversion and a 40-mile reach was used to estimate the downstream slope. The reduction of discharge and slope due to the diversion resulted in an approximate 47% loss of stream power. Clearly, the reduction in the stream power accompanied by a minimum removal of sand load (SWR < 0.5) resulted in the rapid aggradation downstream of the diversion.

Figure 23. Longitudinal water surface profile on May 6 and May 21, 2011.



### **3 Delft-3D Modeling – Myrtle Grove and White Ditch**

This chapter provides an overview of the Delft-3D modeling for the proposed diversions at White Ditch (WD) and Myrtle Grove (MG) located near river mile (RM) 67 and 61, respectively. The Delft-3D model for the Myrtle Grove diversion has already been developed at the Institute for other studies. The model domain has been extended to include a river reach between RM 76 and RM 56 to include White Ditch diversion. The combined Myrtle Grove-White Ditch (MG-WD) model has been refined by adding fine sediment (silt and clay) to the sediment model and was recalibrated based on newly available field observations. The list below summarizes the specific tasks performed in this effort.

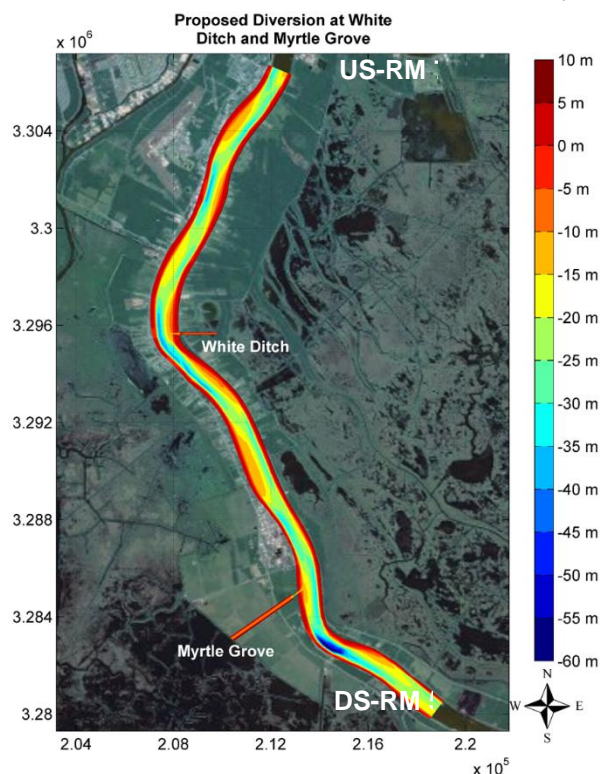
- Calibration and validation of the main river stem hydrodynamics and sediment transport;
- Production runs including the diversions (main stem + outfall channel).

#### **3.1 Calibration and Validation Hydrodynamics and Sediment Transport**

Below is a summary of how the model (as shown in Figure 22) has been setup:

- 2003 single beam bathymetry provided by USACE for the main river;
- Multibeam bathymetry for the intake area of WD and MG diversions provided by Arcadis US and HDR, respectively;
- Setup in a three-dimensional format with 10 vertical sigma layers;
- The main calibration parameters were:
  - Hydrodynamics – bed roughness (Chézy coefficient);
  - Non-cohesive sediment – Transport formula (van Rijn, 1984), suspended load and bed load factors, settling velocity and reference height;
  - Fine Sediment (Clay and Silt) – Critical Shear Stress, erosion parameter, and settling velocity.

Figure 24. Main Stem Model Domain, Boundaries and initial bathymetry for MG-WD.



Based on available hydrodynamic and sediment data, the following periods were selected for calibration and validation:

- Calibration: October 2008 to April 2010
- Validation: May 2010 to December 2011

The main stem model has a grid resolution ranging from 20m x 40m, to 40m x 80m. A time-step of 0.10 min (6s) was used in all calibration and validation simulations. The model was first calibrated and validated for hydrodynamics only. The following boundary conditions were used:

- Upstream (US) Boundary: Flow at Belle Chasse USGS station ID: 07374525) near RM 76 (gap for October 2008 filled with Baton Rouge USGS data);
- DS Boundary: Stage at RM 56 from a Mississippi River Regional Model (covering RM 138 to the Gulf) developed by the Institute.

Calibration and validation were performed for stage, depth-averaged transect velocities, and vertical velocity profiles. For the model calibration and validation, stage data were available at the USACE station at Alliance at RM 62, and flow and velocity data were collected by Dr. Mead Allison and his team as part of the CPRA-funded, LCA Myrtle Grove study. These data are presented in Ramirez and Allison (2013).

Figure 25 and Figure 26 display the stage calibration and validation performed at Alliance (RM 62). The statistical analysis based on the metrics provided in Meselhe and

Rodrigue (2013) indicates that the model is able to reproduce the measured stages. For the performance assessment, a statistical analysis was performed for the water depth, following the report Meselhe and Rodrigue (2013), and presented in Table 11. The model predicted water depths show a good match and meet the desired target of the statistical metrics for bias and correlation coefficient. However, the root mean square error was slightly higher than the acceptable limit during both the calibration and validation period.

As mentioned earlier, the MG-WD model is an extension to an existing MG model that covered a reach from RM 62.7 to RM 56. The original model was developed for other studies (Meselhe et. al., 2014; Meselhe, 2012). For the original MG model, velocity measurements from the April 2009 and March 2011 events were used for calibration, while the April and May 2011 measurements were used for validation. The velocity calibration of the extended MG-WD model was repeated for April 2009 measurements. The MG-WD model successfully reproduced the measured velocities within the range of observed velocity fluctuations. Figure 27 and Figure 28 present examples of velocity calibration for the April 2009 event. There is good agreement between the model results and the measurements. Following Meselhe and Rodrigue (2013), the statistical analysis for the depth average velocity calibration is presented in Table 12.

Figure 25. Stage calibration for MG-WD.

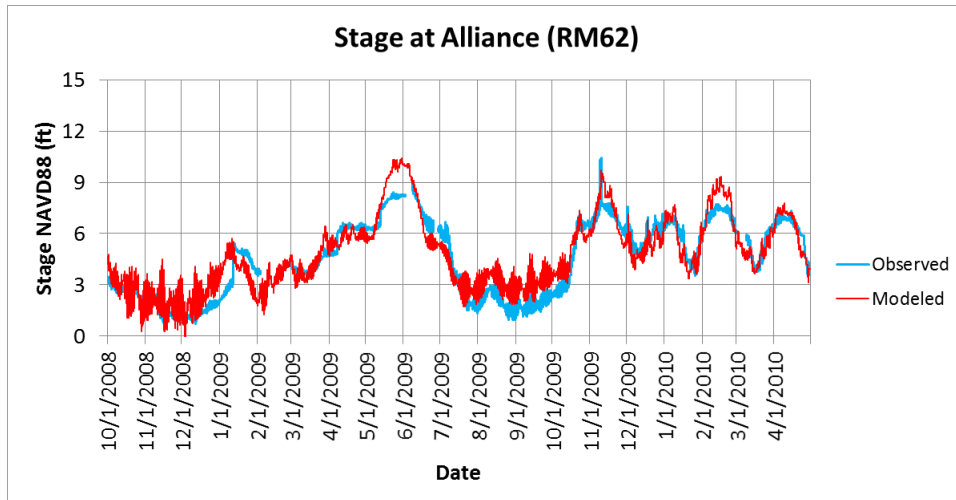


Figure 26. Stage validation for MG-WD.

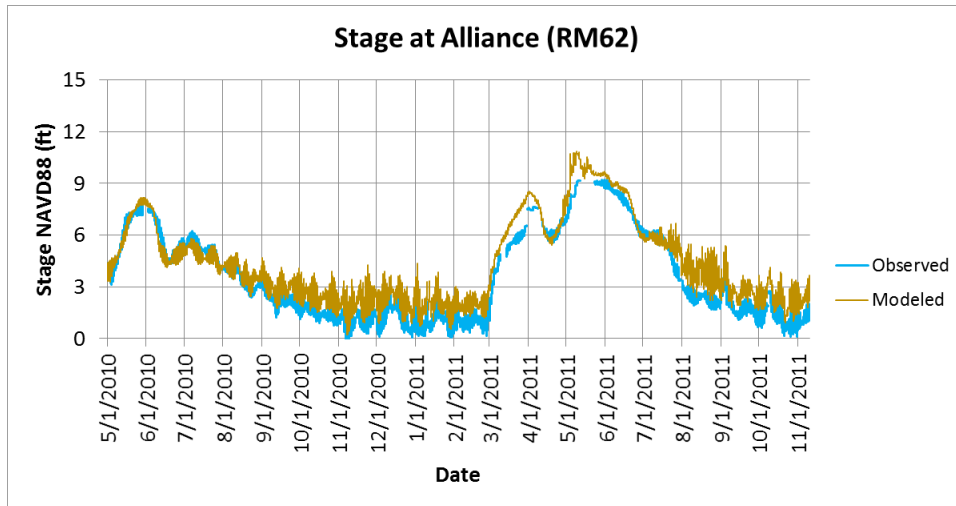


Table 11. Stage calibration and validation statistical analysis for MG-WD.

Modeled Period	Bias % of Range	RMSE%	Corr. Coef.
Calibration October 2008 to April 2010	3%	22%	0.90
Validation May 2010 to December 2012	7%	30%	0.94
<b>Meselhe and Rodrigue (2013) Report</b>	<b>Bias % of Range</b>	<b>RMSE%</b>	<b>Corr. Coef.</b>
Target Desired	< 10% for all stations	< 15% for all stations	> 0.9 for all stations
Target Acceptable	< 10% for 80% of stations	< 15% for 80% of stations	> 0.9 for 80% of stations

Figure 27. Depth averaged velocity transect calibration for MG-WD model.

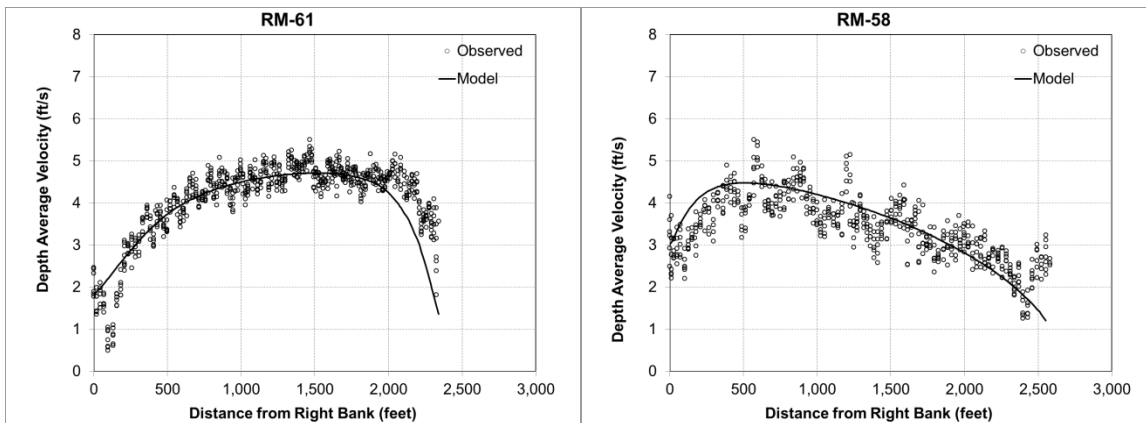


Figure 28. Vertical velocity profile calibration for MG-WD model.

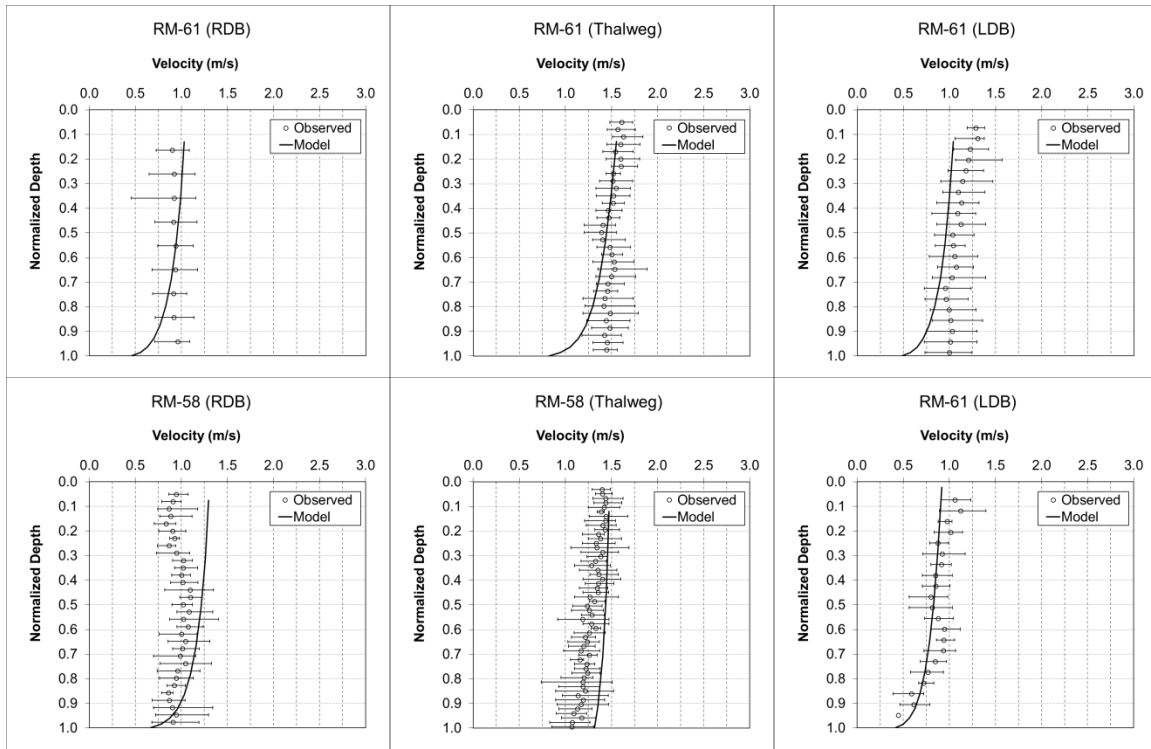


Table 12. Velocity calibration statistical analysis for MG-Wd model.

Modeled Period	RMSE%	Corr. Coef.
October 2008 to April 2010 Measurements: April 2009	22%	0.80
<b>Meselhe and Rodrigue (2013) Report</b>	<b>RMSE%</b>	<b>Corr. Coef.</b>
Target Desired	< 20% for all stations	> 0.75 for all stations
Target Acceptable	< 30% for 50% of stations	> 0.75 for 50% of stations

The calibration and validation of sediment transport followed the hydrodynamics validation. The boundary conditions prescribed were:

- US boundary: Suspended sediment concentrations for the following size-classes:
- Noncohesive sediment: very fine sand ( $D_{50} = 83 \mu\text{m}$ ), fine sand ( $D_{50} = 167 \mu\text{m}$ ) and medium sand ( $D_{50} = 333 \mu\text{m}$ )
- Cohesive sediment: clay ( $D < 2 \mu\text{m}$ ) and silt ( $2 \mu\text{m} < D < 63 \mu\text{m}$ )

The suspended sediment concentrations were estimated daily and prescribed as inputs to the Delft 3D model based on rating curves developed by the Institute using USGS measurements at Belle Chasse (RM 74) for the period 2008- 2012. Separate rating curves were used for Sand and for Fines transport. The plots of the rating curves are presented in Figure 29 and Figure 30. The equations of the rating curves are:



Suspended sand load (metric tons/day) =  $a*[1-\exp(-b*Q_w)]+c*[1-\exp(-d*Q_w)]$   
 $a = 7.716E+7$ ;  $b = 2.485E-7$ ;  $c = -5.748E+5$ ;  $d = 4.122E-5$

Suspended fine load (metric tons/day) =  $A*Q_w^B$   
 $A = 0.0020$ ;  $B = 1.8589$   
 Where,  $Q_w$  is the main stem water discharge ( $m^3/s$ ).

Calibration and validation of sediment transport was performed for suspended load and bed load. The sediment data were collected as part of the LCA Myrtle Grove study. The multilayer bed composition and substrates thickness were defined following the same procedure described in the Bonnet Carré model setup.

Figure 29. Suspended fine load rating curve – Belle Chasse (2008-2012).

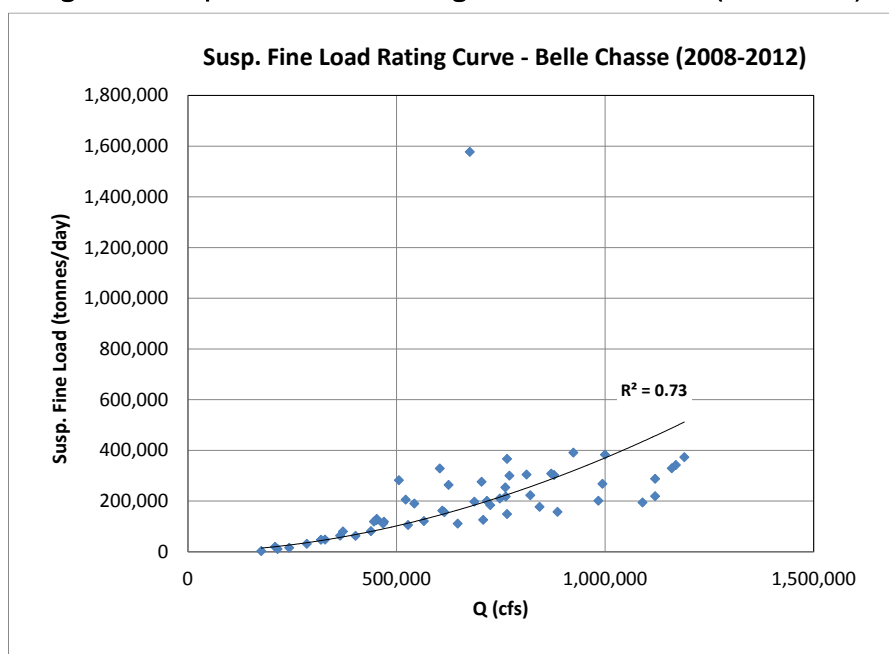


Figure 30. Suspended sand load rating curve – Belle Chasse (2008-2012).

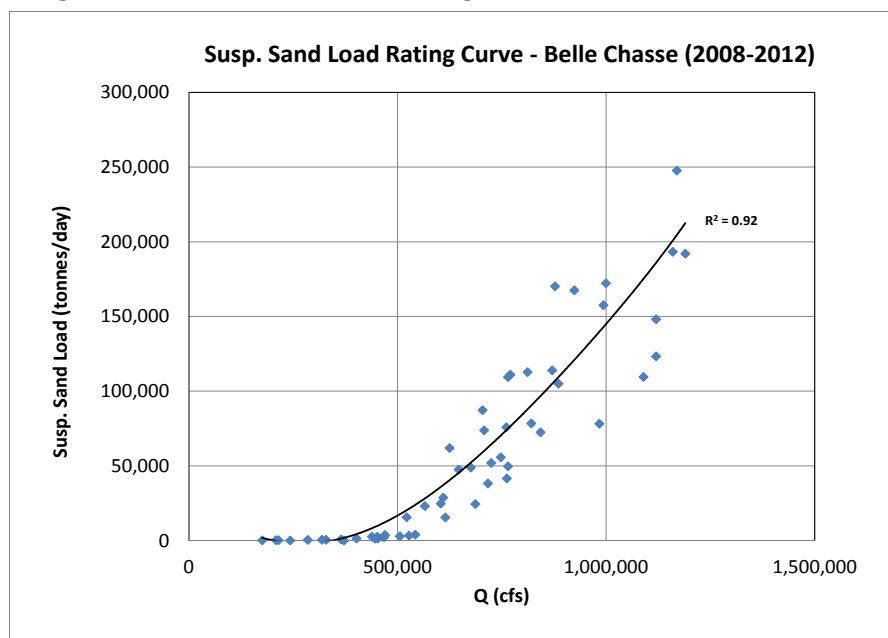


Figure 31 and Figure 32 show the suspended fine load calibration and validation. The calibration was performed for two different transects where data were available: Myrtle Grove Up (RM 61.6) and Myrtle Grove Down (RM 58.0). For the validation period, data were only available for Myrtle Grove Up (RM 61.6). For visual comparison, the USGS measurements at Belle Chasse are also presented on the calibration plots. The purpose of including such data in the plots is to examine the consistency of the boat-based measurements conducted by Dr. Allison and the USGS data. The outcome of this analysis indicates that the model is capable of capturing the order of magnitude and the temporal pattern of fluctuation of the suspended fine sediment transport. The statistical analysis results are presented in Table 13. The number of field observations was not sufficient to calculate RMSE and correlation coefficient. The model performance is acceptable based on the metrics provided in Meselhe and Rodrigue (2013). The calibration and validation of suspended sand load is shown in Figure 33 and Figure 34.

Figure 35 and Figure 36 display the calibration and validation of total suspended load (suspended sand + suspended fines). The statistical analysis is presented in Figure 37 and Figure 38. There are a smaller number of bed load measurements than there are for suspended load measurements. Thus, no statistical analysis was performed for bed load. The model approximates the magnitude of the bed load transport well, compared to the field observations. Overall, the model performance is acceptable for velocities and sediment transport based on the metrics provided in Meselhe and Rodrigue (2013).

Figure 31. Suspended fine sediment calibration for MG-WD.

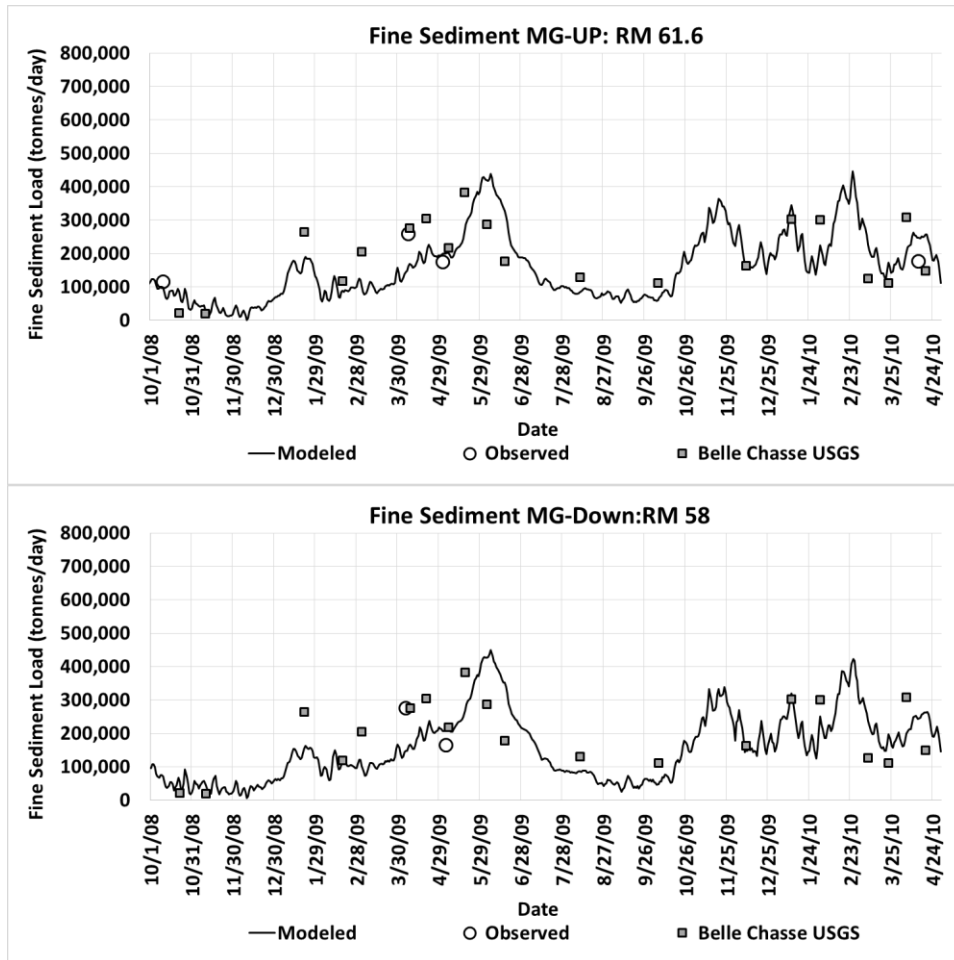


Figure 32. Suspended fine sediment validation for MG-WD.

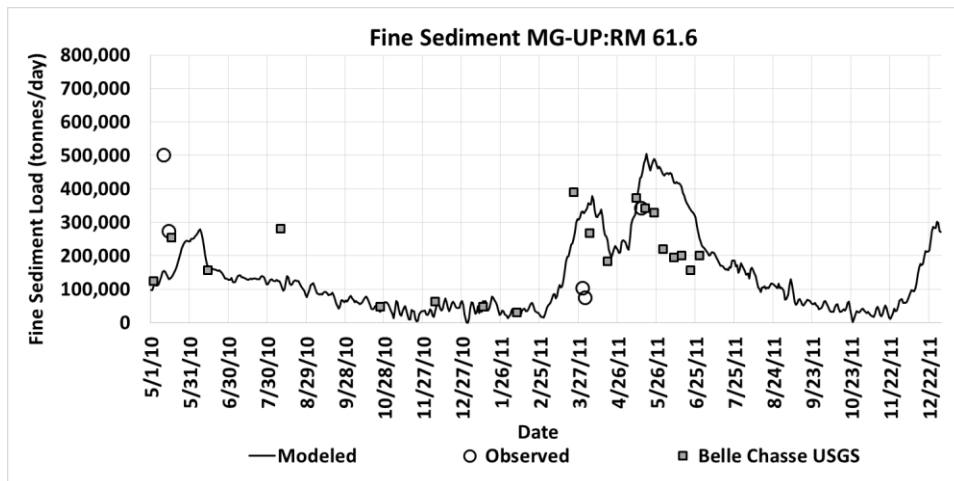


Table 13. Suspended fine load calibration and validation statistical analysis for MG-WD.

Modeled Period	Average Measured (tonnes/d)	Average Modeled (tonnes/d)	Average Bias (tonnes/d)	Bias (%)	RMSE%	Corr. Coef.
Calibration October 08 to April 10	194,825	177,055	-17,770	-9%	N/A	N/A
Validation May 10 to December 12	308,581	282,605	-25,976	-8%	N/A	N/A
Meselhe and Rodrigue (2013) Report	Average Measured (tonnes/d)	Average Modeled (tonnes/d)	Average Bias (tonnes/d)	Bias (%)	RMSE%	Corr. Coef.
Target Desired	-	-	-	< 20% for all stations	< 33% for all stations	> 0.5 for all stations
Target Acceptable	-	-	-	< 20% for 50% of stations	< 50% for 50% of the stations	> 0.5 for 50% of stations

Figure 33. Suspended sand load calibration for MG-WD.

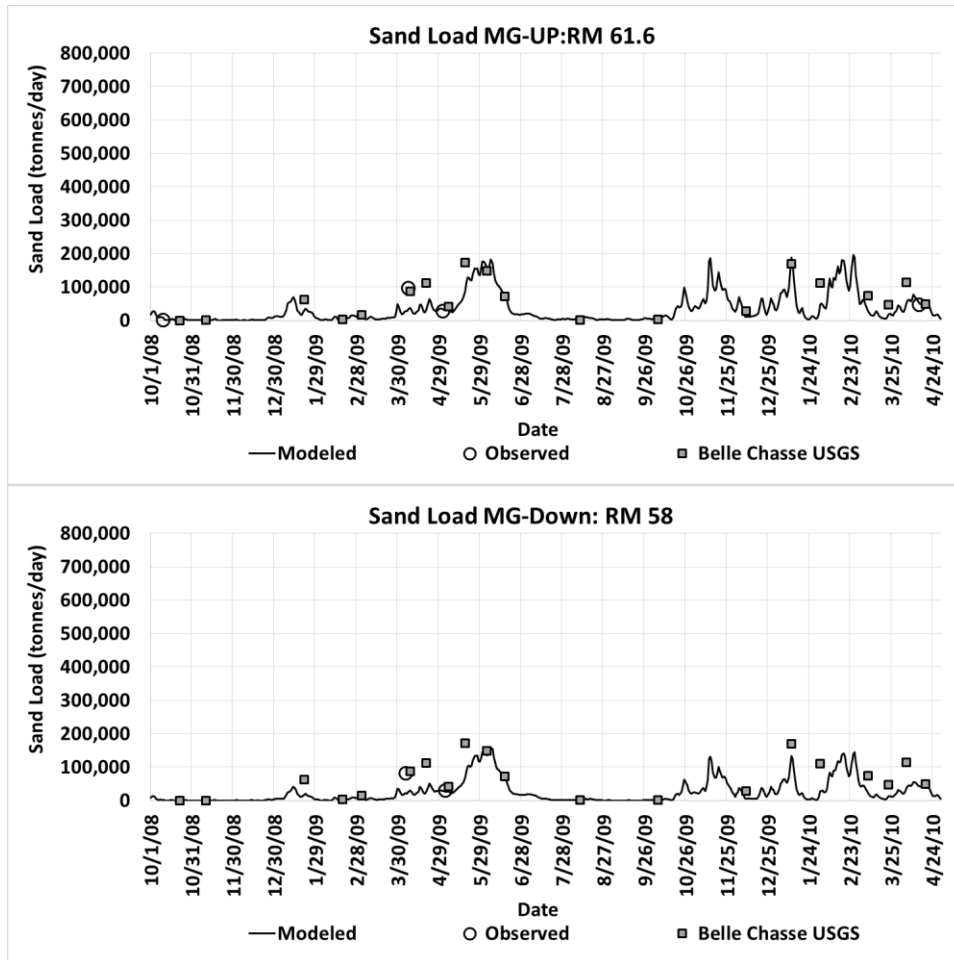


Figure 34. Suspended sand load validation for MG-WD.

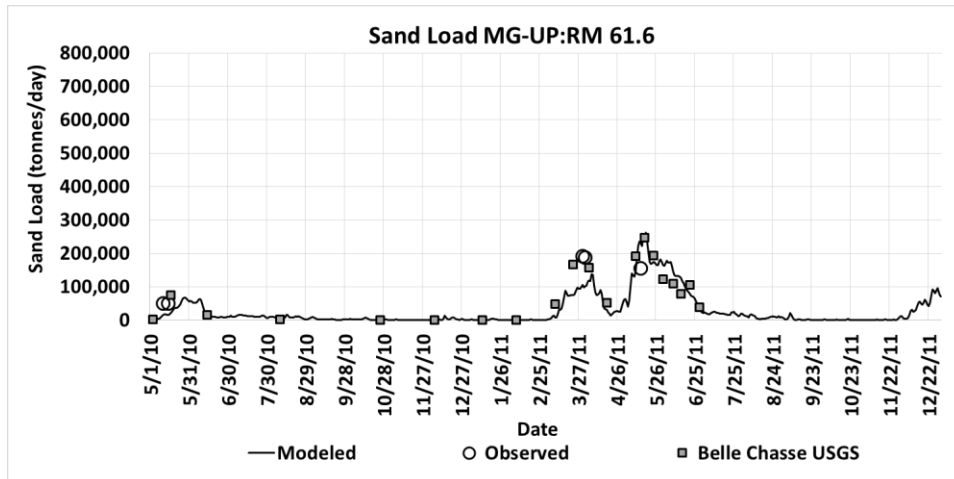


Table 14. Suspended sand load calibration and validation statistical analysis for MG-WD.

Modeled Period	Average Measured (tonnes/d)	Average Modeled (tonnes/d)	Average Bias (tonnes/d)	Bias (%)	RMSE%	Corr. Coef.
Calibration October 8 to April 10	47,433	29,674	-17,768	-37%	N/A	N/A
Validation May 10 to December 12	111,362	92,331	-19,031	-17%	N/A	N/A
<b>Meselhe and Rodrigue (2013) Report</b>	<b>Average Measured (tonnes/d)</b>	<b>Average Modeled (tonnes/d)</b>	<b>Average Bias (tonnes/d)</b>	<b>Bias (%)</b>	<b>RMSE%</b>	<b>Corr. Coef.</b>
Target Desired	-	-	-	< 20% for All stations	< 33% for all stations	> 0.5 for all stations
Target Acceptable	-	-	-	< 20% for 50% of stations	< 50% for 50% of the stations	> 0.5 for 50% of stations

Figure 35. Total load calibration for MG-WD.

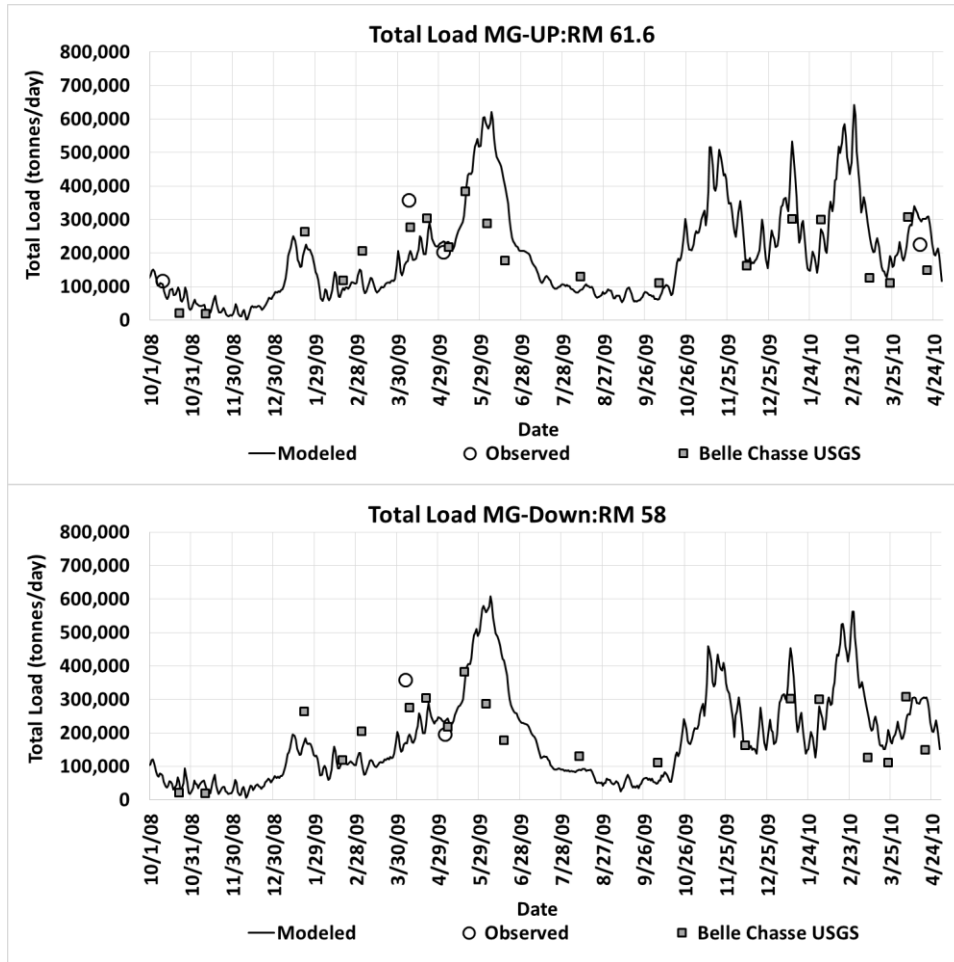


Figure 36. Total load validation for MG-WD.

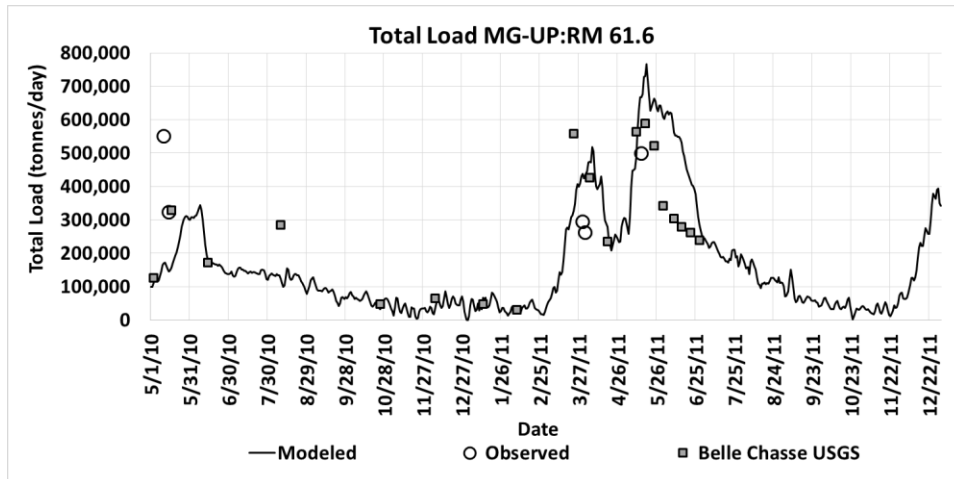


Table 15. Total Suspended Load Calibration and Validation Statistical Analysis for MG-WD.

Modeled Period	Average Measured (tonnes/d)	Average Modeled (tonnes/d)	Average Bias (tonnes/d)	Bias (%)	RMSE%	Corr. Coef.
Calibration October 08 to April 10	242,268	206,730	-35,538	-15%	N/A	N/A
Validation May 10 to December 12	411,117	406,271	-4,845	-1%	N/A	N/A
Meselhe and Rodrigue (2013) Report	Average Measured (tonnes/d)	Average Modeled (tonnes/d)	Average Bias (tonnes/d)	Bias (%)	RMSE%	Corr. Coef.
Target Desired	-	-	-	< 20% for all stations	< 33% for all stations	> 0.5 for all stations
Target Acceptable	-	-	-	< 20% for 50% of stations	< 50% for 50% of the stations	> 0.5 for 50% of stations

Figure 37. Bed load calibration for MG-WD.

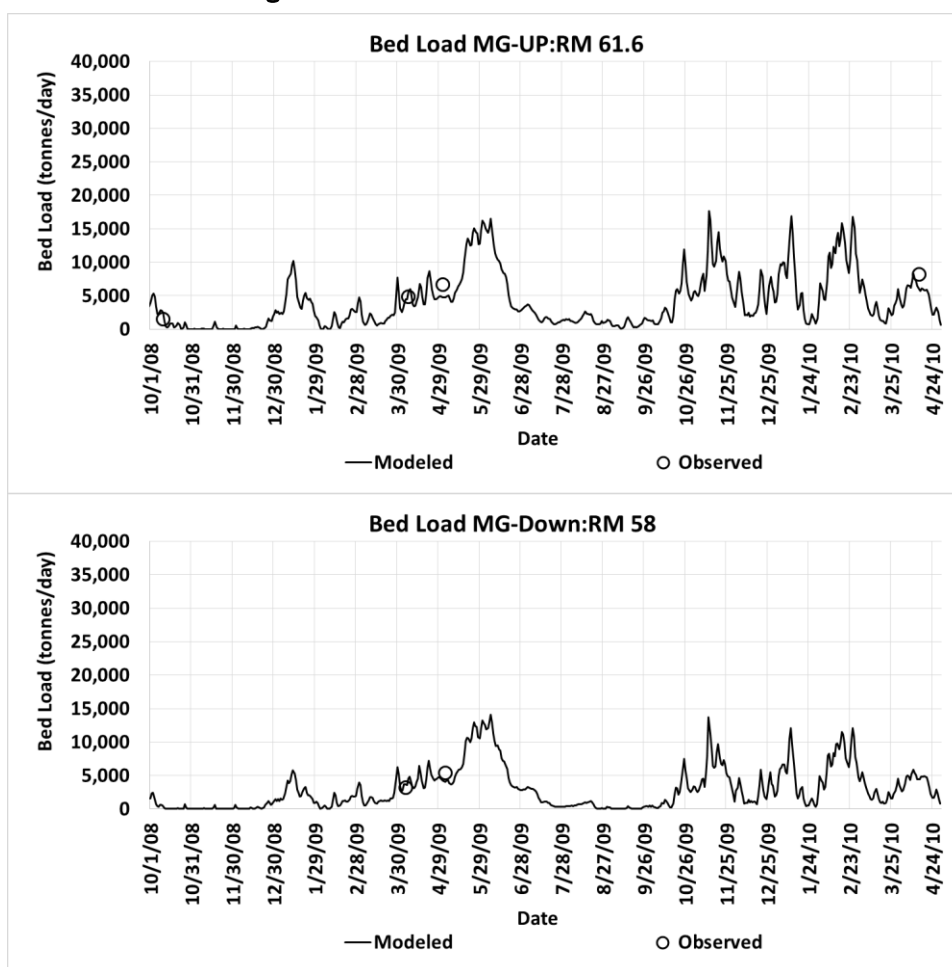
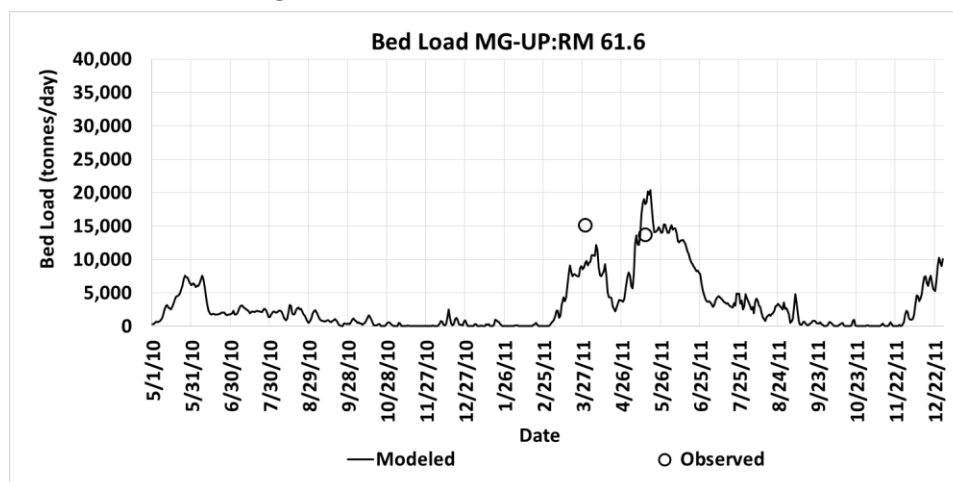




Figure 38. Bed load validation for MG-WD.



### 3.2 Model Application

The MG-WD validated model was used to provide quantitative information about the morphologic responses of the river and diversion sediment capture efficiency for a 3-year period from 2008- 2010. The following three production runs (PR) were accomplished using the MG-WD model:

- PR 1: Only WD diversion open (diversion size: 35,000 cfs with maintenance flow);
- PR 2: Only MG diversion open (diversion size: 75,000 cfs with maintenance flow);
- PR 3: Both WD and MG diversions open (diversion size: 35,000 cfs and 75,000 cfs, respectively with maintenance flow).

The model setup includes the following:

- The design diversion channel for MG provided by HDR;
- The design diversion channel for WD provided by Arcadis;
- Boundary Conditions:
  - U/S Boundary - Flow at Belle Chasse (RM 76), USGS; gap for October 2008 filled with Baton Rouge USGS data;
  - D/S Boundary - Stage at RM 56 from a Mississippi River Regional Model (RM 138 to the Gulf) developed by the Institute;
  - Outfall Boundary – WD-Stage averaged between CRMS stations 0114 and 0115;
  - Outfall Boundary – MG-Stage averaged between CRMS stations 0261 and 4103;
- Five sediment sizes were prescribed in the model as described during the calibration and validation

The simulated discharge at the intake of WD and MG is shown in Figure 39 and Figure 40. Data show that the flow passed through the diversions (about 75,000 cfs for MG and

35,000 cfs for WD for a river flow of 1,000,000 cfs) matches well to the design capacity of the intake and outfall channel.

Figure 39. Simulated discharge in the Mississippi River and WD diversion in 2008 – 2010.

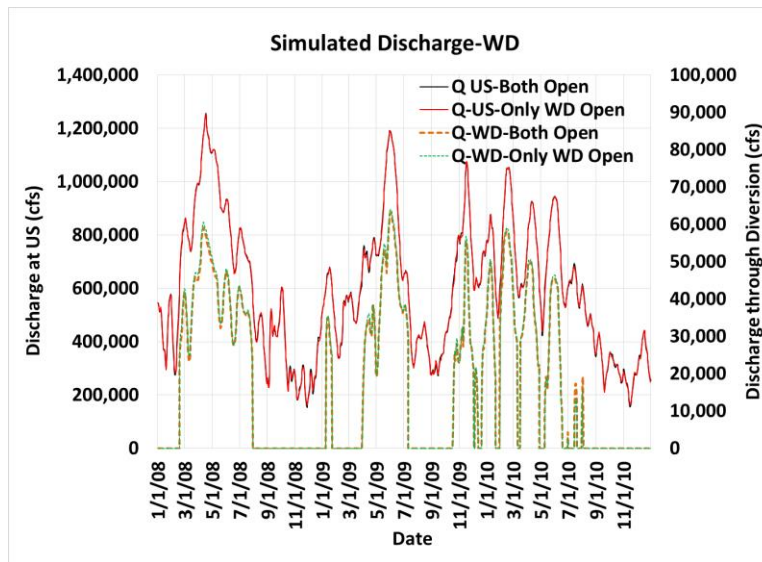
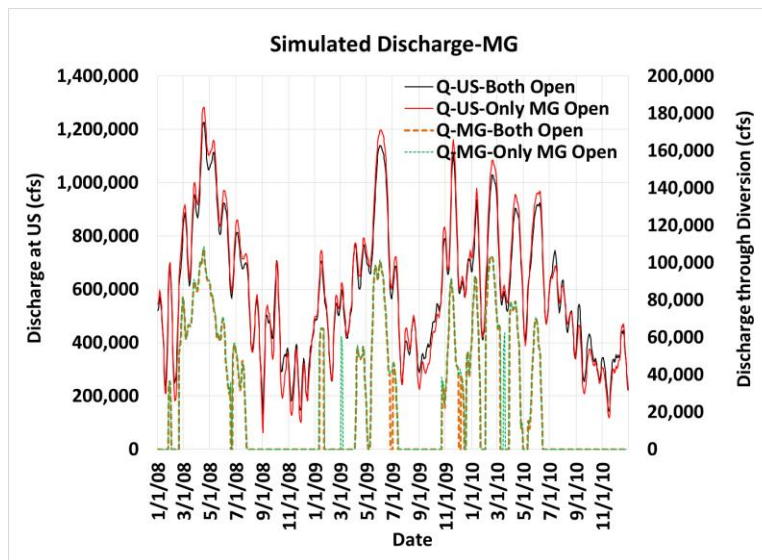


Figure 40. Simulated discharge in the Mississippi River and MG diversion in 2008 – 2010.



Morphologic Response in the River Channel:

The morphological response of the river to the operation of these two sediment diversions (individually and cumulatively) is assessed through a 3-year simulations by investigating the erosion and accretion volumes. These calculations were also performed for the same time period without the diversion in place to establish a reference. The quantities presented in the tables below represent the difference between the “with” and “without” project. The river channel was divided into nine segments (polygons) to

quantify the volume of the predicted accretion and erosion. The segments are labeled in **Error! Reference source not found.** and Figure 42 shows the erosion and accretion occurring in the river segments. The model results showed that accretion occurred adjacent to, and downstream of, the diversion. In general, there were little to no changes upstream of the diversion. This suggests that the diversion does not alter the morphology of the upstream sand bar, at least not during the short term (i.e., three years) analysis provided by this modeling effort. The operation of WD diversion reduced the accretion volume adjacent to, and at the downstream of the MG diversion when both the diversions were in operation.

Figure 41. River segments considered to quantify morphologic changes for MG-WD.

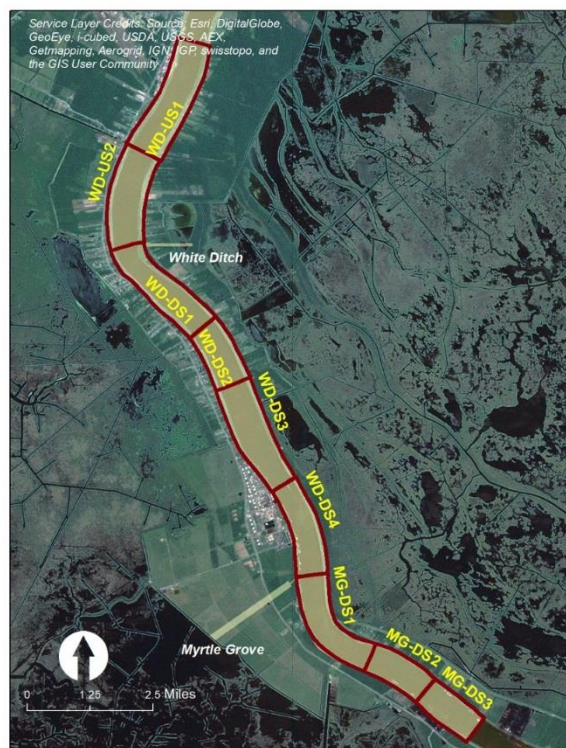
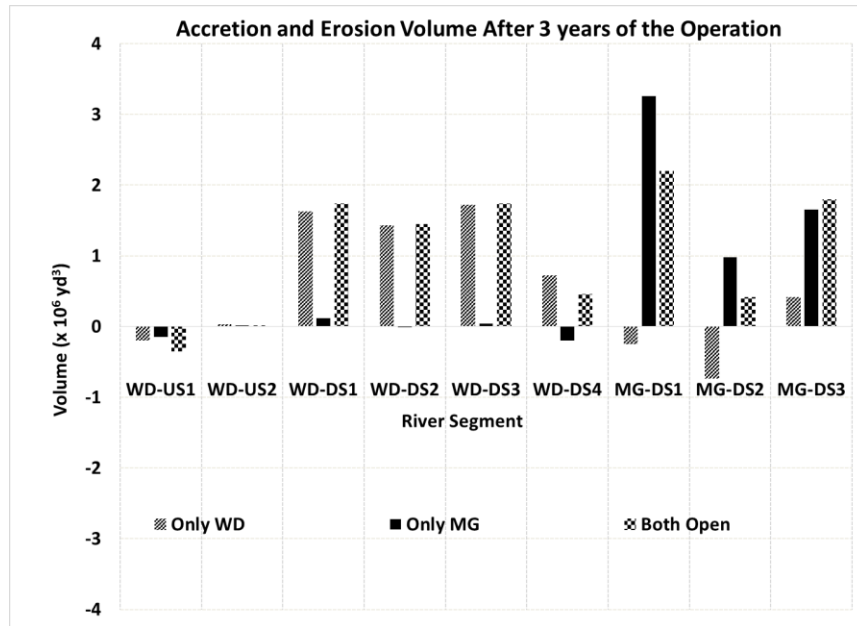


Figure 42. Erosion and accretion volume change in response to MG-WD diversions during 2008 – 2010.



**Sediment Budget:**

A sediment budget was developed to provide additional insights into the morphologic response of the river to the diversions. The budget shows the cumulative sediment mass and volume: (a) entering/leaving the river segments mentioned above, (b) passing through the diversion structure, and (c) eroding or depositing within the river channel. The budget was computed during 2008- 2010 both for sand and fine (silt and clay) material sediment separately.

**Sediment Budget for Production Run 1 (Only WD diversion open):**

The sand budget for WD diversion (

Table 16) shows that 14% of the inflowing sand load, which was about 6 million tonnes, has deposited in the river between WD and MG diversion, 4% was diverted through WD and only 1% eroded between MG and DS section. The remaining, i.e. 83% of the US sand load, exited through the downstream end of that river reach. The fine sediment budget (clay and silt) indicates that 3% of the entering fine sediment load was diverted and 97% exited the system (through the downstream end) and no accretion/erosion occurring on the riverbed (Table 17).

Table 18 shows the budget for total load, i.e. the summation of the sand and fine sediment. For reference, the total volume of water extracted through the WD diversion during the same 3-year period was 3% of the total water volume entering at the upstream end.

Table 16. Sediment budget for sand load for PR 1: MG-WD.

	Inflow at the U/S of WD	Deposited between WD and MG	Deposited in the WD Outfall	Diverted to the WD Basin	Deposited between MG and DS	Deposited in the MG Outfall	Diverted to the MG Basin	Outflow at DS of the river
Total Mass (10 <sup>6</sup> tonnes)	41.2	5.8	0.0	1.6	-0.4	0.0	0.0	34.2
Total Volume (10 <sup>6</sup> yd <sup>3</sup> )	46.5	6.5	0.0	1.8	-0.5	0.0	0.0	38.6
% of U/S Inflow		14%	0%	4%	-1%	0%	0%	83%

Table 17. Sediment budget for fine sediment for PR 1: MG-WD.

	Inflow at the U/S of WD	Deposited between WD and MG	Deposited in the WD Outfall	Diverted to the WD Basin	Deposited between MG and DS	Deposited in the MG Outfall	Diverted to the MG Basin	Outflow at DS of the river
Total Mass (10 <sup>6</sup> tonnes)	184.2	-0.1	0.0	6.2	0.2	0.0	0.0	177.9
Total Volume (10 <sup>6</sup> yd <sup>3</sup> )	207.9	-0.1	0.0	7.0	0.2	0.0	0.0	200.8
% of U/S Inflow		0%	0%	3%	~0%	0%	0%	97%

Table 18. Sediment budget for total sediment load for PR 1: MG-WD.

	Inflow at the U/S of WD	Deposited Between WD	Deposited In the WD Outfall	Diverted to the WD Basin	Deposited between MG and DS	Deposited in the MG Outfall	Diverted to the MG Basin	Outflow at DS of the river
Total Mass (10 <sup>6</sup> tonnes)	225.4	5.7	0.0	7.8	-0.2	0.0	0.0	212.1
Total Volume (10 <sup>6</sup> yd <sup>3</sup> )	254.4	6.4	0.0	8.8	-0.3	0.0	0.0	239.4
% of U/S Inflow		3%	0%	3%	~0%	0%	0%	94%

Sediment Budget for Production Run 2 (Only MG diversion open):

The sand budget for MG diversion (Table 19) shows that 14% of the inflowing sand load was deposited on the riverbed downstream of the diversion and 79% exited through the downstream section. The model also shows that 6% of the inflowing sand load was diverted. The sediment budget for fine sediment indicates that 5% of the entering fine sediment load was diverted and 95% exited the system (



Table 20). Table 21 shows the budget for total load. For reference, the total volume of water extracted through the MG diversion during the same 3-year period was 4.5% of the total water volume entering at the upstream end.

Table 19. Sediment budget for sand load for PR 2: MG-WD.

	Inflow at the U/S of WD	Deposited between WD and MG	Deposited in the WD Outfall	Diverted to the WD Basin	Deposited between MG and DS	Deposited in the MG Outfall	Diverted to the MG Basin	Out-flow at DS of the river
<b>Total Mass (10<sup>6</sup> tonnes)</b>	41.2	0.2	0.0	0.0	5.9	0.1	2.3	32.6
<b>Total Volume (10<sup>6</sup> yd<sup>3</sup>)</b>	46.5	0.2	0.0	0.0	6.7	0.1	2.6	36.8
<b>% of U/S Inflow</b>		~0%	0%	0%	14%	~0%	6%	79%

Table 20. Sediment budget for fine sediment for PR 2: MG-WD.

	Inflow at the U/S of WD	Deposited between WD and MG	Deposited in the WD Outfall	Diverted to the WD Basin	Deposited between MG and DS	Deposited in the MG Outfall	Diverted to the MG Basin	Out-flow at DS of the river
Total Mass (10 <sup>6</sup> tonnes)	184.2	0.0	0.0	0.0	-0.3	-0.3	9.9	174.9
Total Volume (10 <sup>6</sup> yd <sup>3</sup> )	207.9	0.0	0.0	0.0	-0.3	-0.4	11.2	197.4
% of U/S Inflow		0%	0%	0%	0%	~0%	5%	95%

Table 21. Sediment budget for total sediment load for PR 2: MG-WD.

	Inflow at the U/S of WD	Deposited between WD and MG	Deposited in the WD Outfall	Diverted to the WD Basin	Deposited between MG and DS	Deposited in the MG Outfall	Diverted to the MG Basin	Out-flow at DS of the river
Total Mass (10 <sup>6</sup> tonnes)	225.4	0.2	0.0	0.0	5.6	-0.3	12.2	207.5
Total Volume (10 <sup>6</sup> yd <sup>3</sup> )	254.4	0.2	0.0	0.0	6.3	-0.3	13.8	234.2
% of U/S Inflow		~0%	0%	0%	2%	~0%	5%	92%

Sediment Budget for Production Run 3 (Both WD and MG diversions open):

The sediment budget for sand when both the diversions were operating together (Table 22) shows that 14% of the US sand load was deposited in the river between the WD and MG diversion, 11% was deposited between MG and DS section, and 66% exited through the DS section. The model also shows that 4% and 5% of the entering sand load was diverted through WD and MG, respectively. The fine sediment budget indicates that total 8% of the entering fine sediment load passed through the diversions (WD: 3% and MG: 5%) and the rest exited the system (Table 23). Table 24 shows the total load budget. For reference, the combined volume of water extracted through the WD and MG diversions during the same 3-year period was 7% of the total water volume entering at the upstream end.

Table 22. Sediment budget for sand load for PR 3: MG-WD.

	Inflow at the U/S of WD	Deposited Between WD and MG	Deposited in the WD Outfall	Diverted to the WD Basin	Deposited Between MG and DS	Deposited in the MG Outfall	Diverted to the MG Basin	Outflow at DS of the river
Total Mass (10 <sup>6</sup> tonnes)	41.2	6.0	0.0	1.5	4.5	0.0	2.0	27.5
Total Volume (10 <sup>6</sup> yd <sup>3</sup> )	46.5	6.7	0.0	1.7	5.1	0.1	2.3	31.0
% of U/S Inflow		14%	0%	4%	11%	~0%	5%	66%

Table 23. Sediment budget for fine sediment for PR 3: MG-WD.

	Inflow at the U/S of WD	Deposited between WD and MG	Deposited in the WD Outfall	Diverted to the WD Basin	Deposited between MG and DS	Deposited in the MG Out-fall	Diverted to the MG Basin	Outflow at DS of the river
Total Mass (10 <sup>6</sup> tonnes)	184.2	-0.1	0.0	6.2	-0.1	-0.3	9.7	168.8
Total Volume (10 <sup>6</sup> yd <sup>3</sup> )	207.9	-0.1	0.0	7.0	-0.1	-0.4	10.9	190.6
% of U/S Inflow		0%	0%	3%	0%	0%	5%	92%

Table 24. Sediment budget for total sediment load for PR 3: MG-WD.

	Inflow at the U/S of WD	Deposited Between WD and MG	Deposited in the WD Outfall	Diverted to the WD Basin	Deposited between MG and DS	Deposited in the MG Outfall	Diverted to the MG Basin	Outflow at DS of the river
Total Mass (10 <sup>6</sup> tonnes)	225.4	5.9	0.0	7.7	4.4	-0.3	11.7	196.3
Total Volume (10 <sup>6</sup> yd <sup>3</sup> )	254.4	6.6	-0.1	8.7	5.0	-0.3	13.2	221.6
% of U/S Inflow		3%	0%	3%	2%	0%	5%	87%

In general, the sediment budget for fine sediment (clay and silt) indicates that there was no accretion of fine sediment occurring on the river bed. Both the MG and WD diversions caused similar amounts of depositions at the downstream although the WD diversion is less than half the size of the MG diversion. The WD diversion is located at a sharper bend than the MG diversion. The sharper the bend, the stronger is the

secondary motion. The secondary motion helps entraining sediments from the bed and bring them into suspension. The entrainment of bed materials definitely helps diverting the sediment through the diversion, but causes more sediment depositions in the river channel at the downstream of the diversion as well. This perhaps explains the reason why the WD diversion deposits the same amount of sediment in the river channel, although it is half the size of the MG diversion. Another finding shows that the riverbed accretion at the downstream of the MG diversion was less when both diversions were operated simultaneously. A back water effect is caused by the operation of the WD diversion. This back water effect creates the water surface slope between the WD and MG diversion steeper. Therefore, the velocity increases adjacent to the MG diversion. The increased velocity diverts more sediments through the intake, which results in less deposition in the river channel downstream of the diversion intake. Furthermore, the sediment budget also shows that the diversions have minor impact at the upstream reach of the diversion and the two diversions do not influence each other's performance especially in a short-term period (<5 years).

### **Sediment-Water Ratio**

The SWR was calculated for the MG and WD diversions to quantify the efficiency of these diversions to capture sediment from the river. The ratio is calculated here for flood events identified by a flow discharge larger than 600,000 cfs (Meselhe et al., 2012). This threshold has been determined based on numerous field observations identifying this discharge as the impetus for entraining coarse material into suspension (Allison et al., 2013). As such, the SWR analysis presented in this study was limited to these events only.

The instantaneous and cumulative SWR of sand and mud for WD and MG are presented in Figure 43 to Figure 46. The instantaneous SWR of sand for WD fluctuates between 2 and 0.75, based on the flow magnitude. The cumulative SWR was ~1.25 during the entire simulation period from 2008- 2010, indicating a good capture efficiency for this diversion. The operation of the MG diversion showed no impact on the WD diversion in capturing sediment from the river. The cumulative sand SWR for MG was also around 1.25 throughout the simulation period and thus confirmed the diversion efficiency for at least for the analysis period of 3 years. The concurrent operation of the WD diversion in fact enhances the efficiency of the MG diversion. The deposition occurred downstream of WD became available for entrainment from the riverbed during the rising phase of the flood events in 2010 and diverted toward the MG diversion. This explains the higher cumulative SWR and the spikes in the instantaneous SWR of sand for the MG diversion when both diversions were operated simultaneously (Figure 45). The SWR of mud was

consistently  $\sim 1.0$  for all the cases which explains why there was no accretion of fine sediment occurring on the river bed in the sediment budget.

Figure 43. Sand Instantaneous and Cumulative SWR for WD.

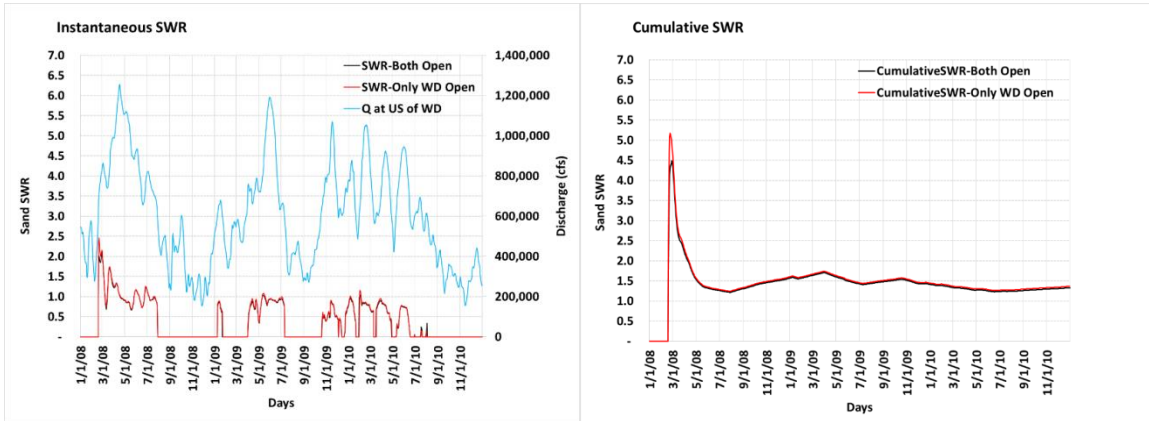


Figure 44. Mud Instantaneous and Cumulative SWR for WD.

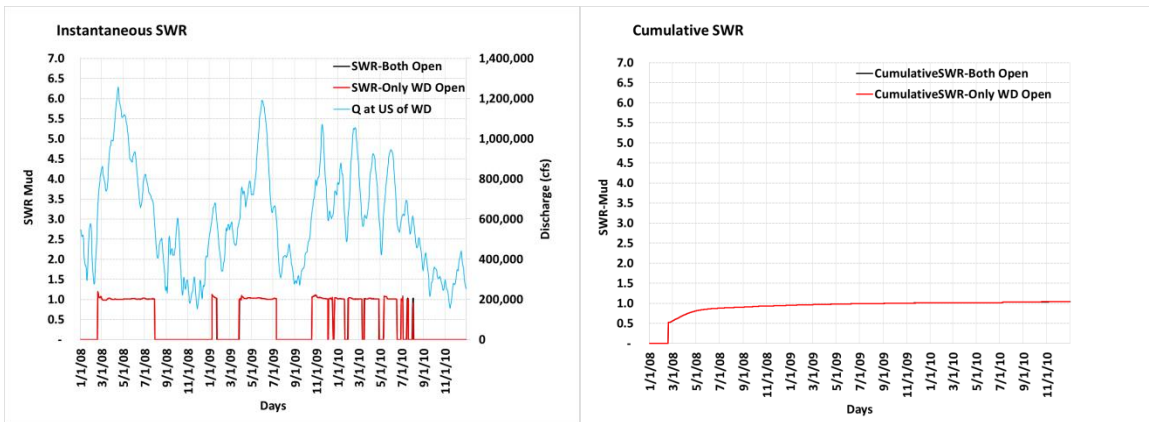


Figure 45. Sand Instantaneous and Cumulative SWR for MG.

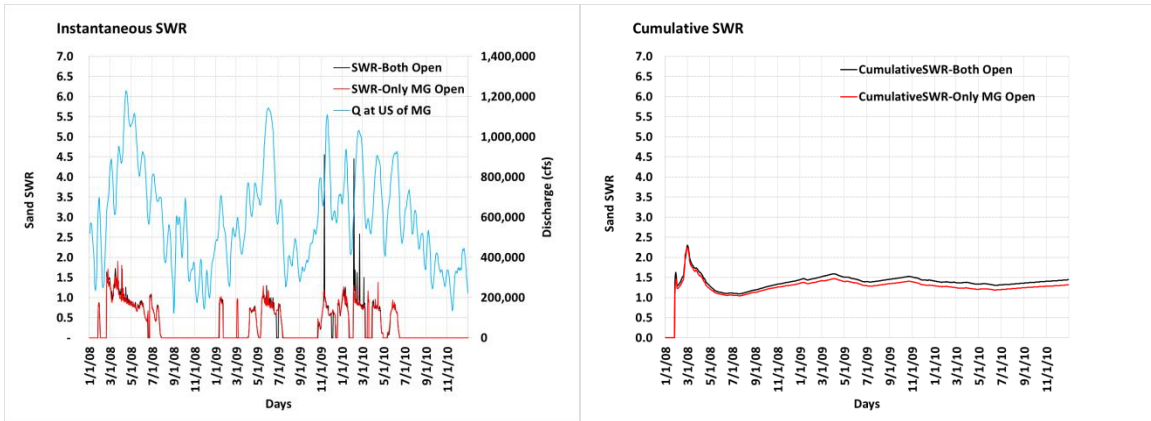
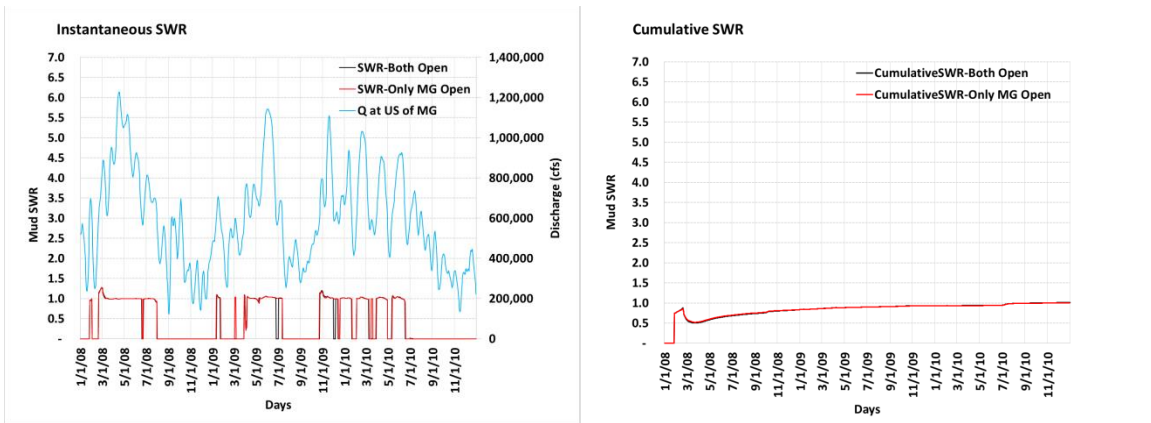


Figure 46. Mud Instantaneous and Cumulative SWR for MG.



## 4 Delft-3D Modeling – Upper Breton Sound

This chapter provides an overview of the Delft-3D modeling for the proposed sediment diversion at Upper Breton Sound (UBS) located near Caernarvon at river mile (RM) 81.5. The UBS model domain extends between RM 92.7 and RM 70. The list below summarizes the specific tasks performed in this study.

- Calibration and validation of the main stem hydrodynamics and sediment transport;
- Production runs with the complete model (main stem + diversion intake + outfall channel).

### 4.1 Calibration and Validation of Hydrodynamics and Sediment Transport

The calibration and validation of the Delft-3D model (Figure 47) includes the following:

- 2012 multibeam bathymetry provided by USACE;
- Setup in a three-dimensional format with 10 vertical sigma layers;
- The main calibration parameters were:
  - Hydrodynamics – bed roughness (Chézy coefficient);
  - Non-cohesive sediment Transport – Transport formula (van Rijn, 1984), suspended load and bed load factors, settling velocity and reference height;
  - Fine Sediment (Clay and Silt) – Critical Shear Stress, erosion parameter and settling velocity.

Based on the available hydrodynamic and sediment data, the following periods were selected for calibration and validation:

- Calibration: March 2013 to June 2013
- Validation: January 2008 to December 2010

The main stem model has a grid resolution ranging from 20m x 40m to 40m x 80m. A time-step of 0.10 min (6 s) was used in all calibration and validation simulations. The model was first calibrated and validated for hydrodynamics only. The following boundary conditions were used:

- US Boundary: flow at Belle Chasse USGS station ID: 07374525) near RM 76; gap for October 2008 filled with Baton Rouge USGS data;
- DS Boundary: calibrated between gauges at Belle Chasse (RM 76) and Algiers Lock (RM 88.3)

Hydrodynamic calibration was performed for stage, depth-averaged transect velocities and vertical velocity profiles. For the model calibration and validation, stage data were available from USACE stations at Algiers Lock (RM 88.3) and at Belle Chasse (RM 76). The depth averaged transect velocity and vertical velocity profile data were collected as part of this project by Mr. Thad Pratt (USACE – ERDC) and his team. The velocity data were available only during the calibration period.

Figure 47. Model domain, grid, and boundaries for UBS.

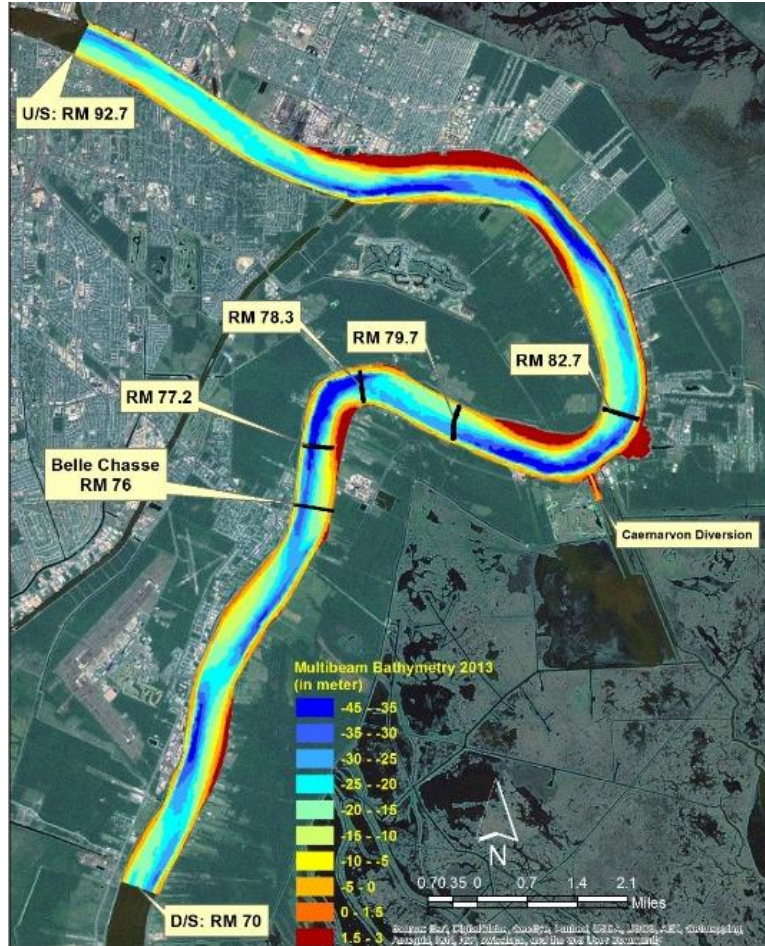


Figure 48 and Figure 49 display the stage calibration and validation performed at Algiers Lock (RM 88.3) and Belle Chasse (RM 76). The analysis shows that the model is able to reproduce the measured stages. The performance of the model is summarized through the statistical analysis provided in Table 25.

The calibration of depth-averaged velocity and vertical velocity profile are presented in Figure 50 and

Figure 51. There is good agreement between the model results and the measurements. The statistical analysis for the velocity is presented in Table 26. Some results shown in Table 26 are lower than the desired target, but are close to the acceptable target presented in Meselhe and



Rodrigue (2013). The combined root mean square error for vertical velocity profile was 61%, i.e. higher than the acceptable limit. This value was estimated based on the mean of the observed velocities in each vertical layer. The observed velocity in verticals were collected by boat based ADCP in a span of 15-20 minutes for each location.

Figure 51 shows that the observed velocities fluctuated around 5 ft/sec in 15-20 minutes in almost every location. The model was able to predict the velocity verticals within the variation observed, except at the left descending bank at RM 77. Additional validation of the model is warranted as more data become available; however, the model performance is reasonable for this effort.

Figure 48. Stage Calibration for UBS.

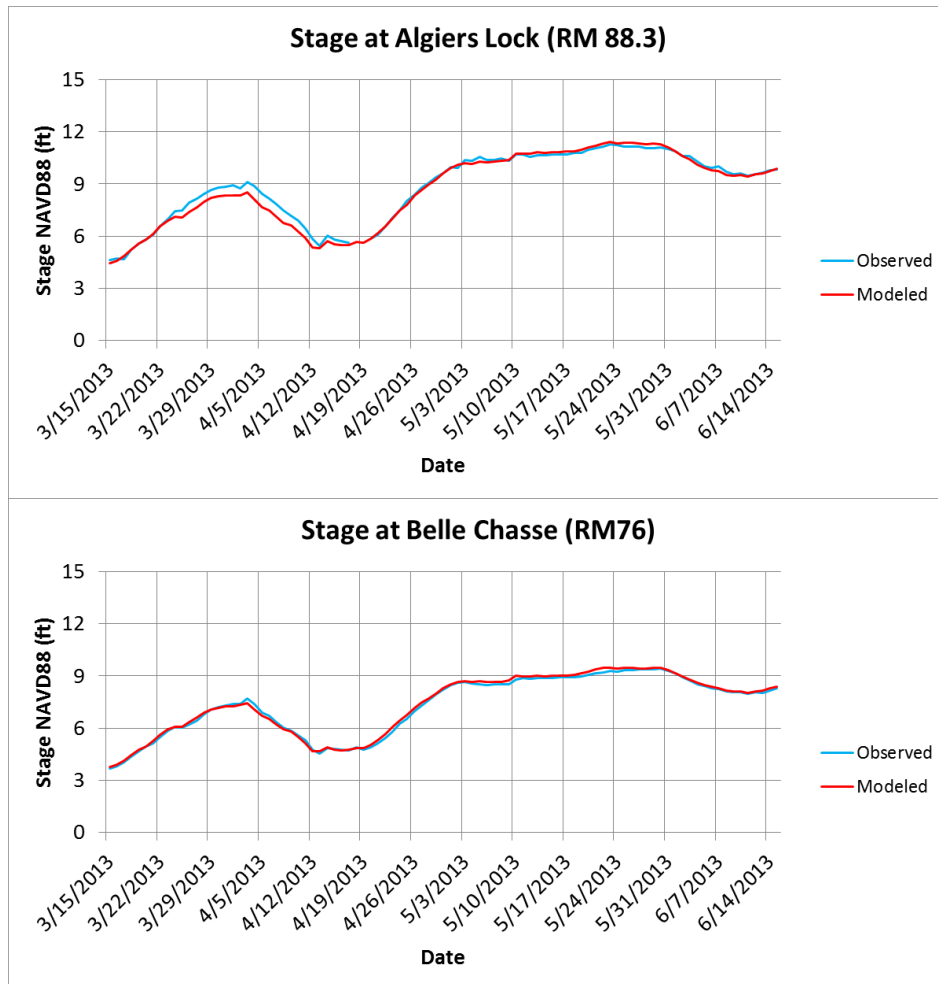


Figure 49. Stage Validation for UBS.

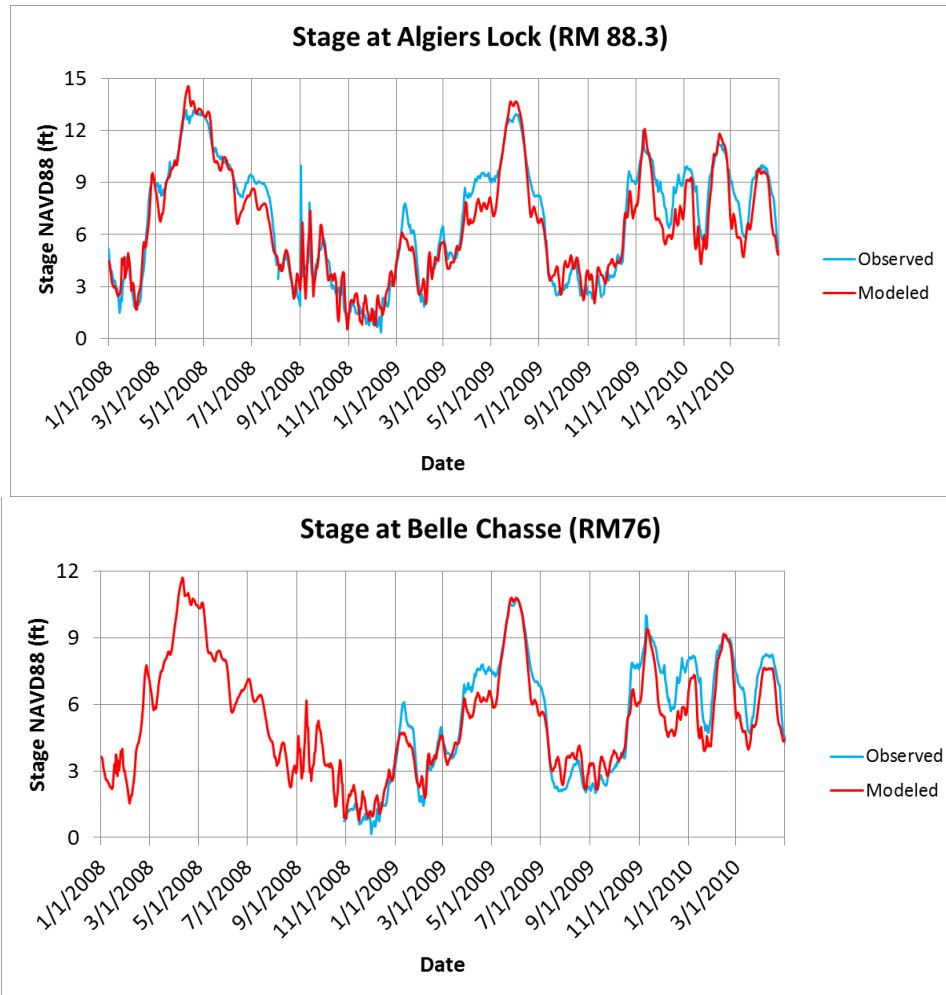


Table 25. Stage Calibration and Validation Statistical Analysis for UBS.

Modeled Period	Average Bias (ft)	Bias % of Range	RMSE%	Corr. Coef.
Calibration March- June 2013	-0.03	-0.38%	2.55%	1.00
Validation May 2010-Dec 2011	-0.22	-2%	21%	0.96
<b>Meselhe and Rodrigue (2013) Report</b>				
Target Desired	-	< 10% for all stations	< 15% for all stations	> 0.9 for all stations
Target Acceptable	-	< 10% for 80% of stations	< 15% for 80% of stations	> 0.9 for 80% of stations

Figure 50. Depth averaged velocity transect calibration for UBS.

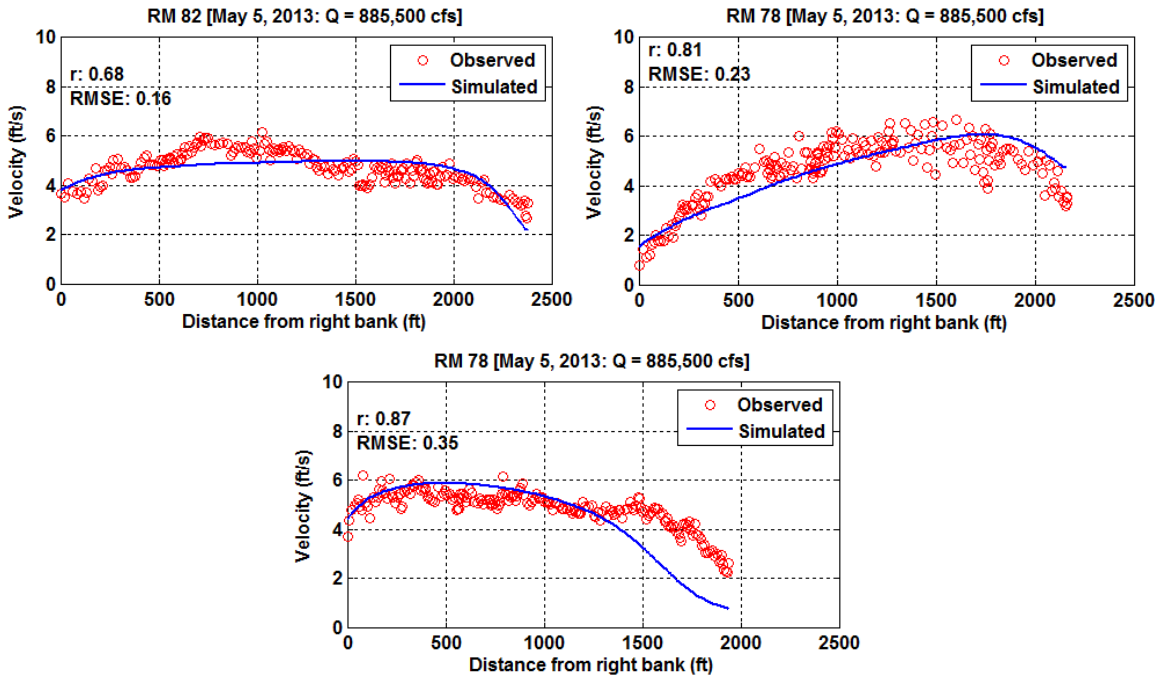
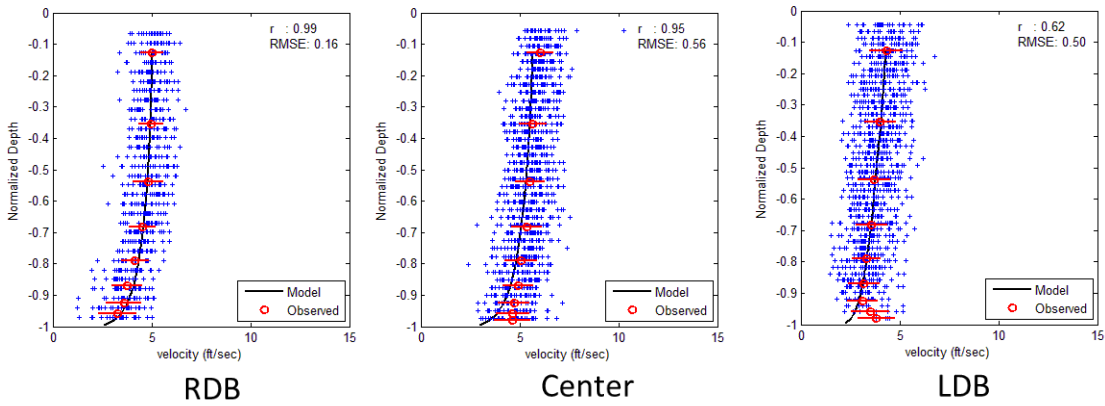
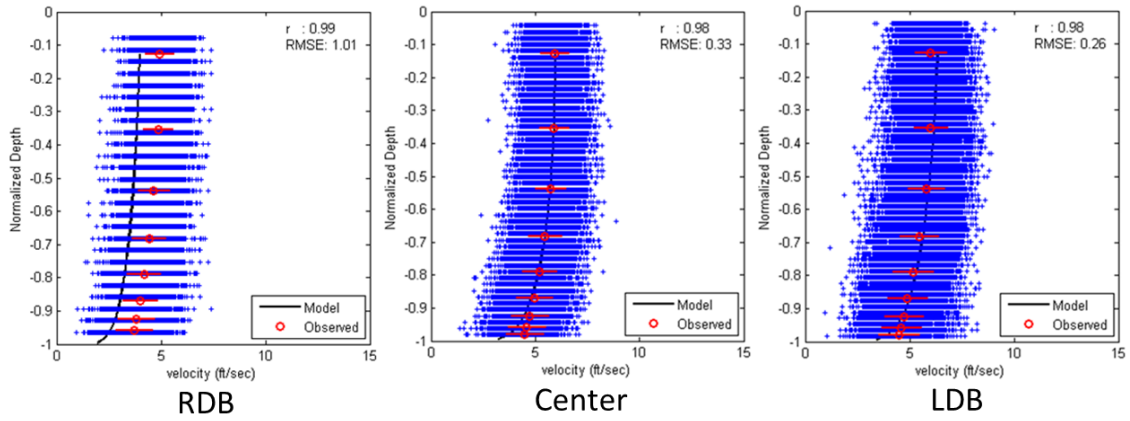


Figure 51. Velocity vertical profiles for UBS.

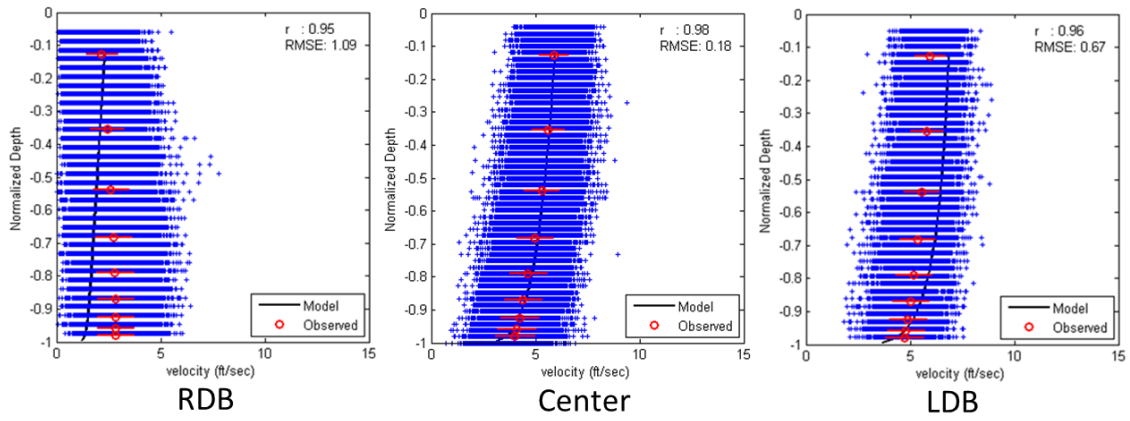
**Vertical Velocity Profile RM 82**



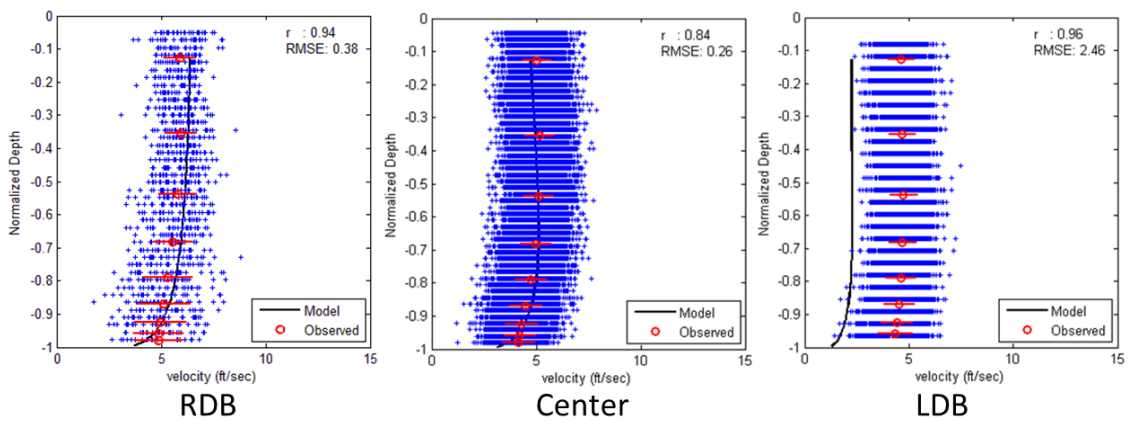
**Vertical Velocity Profile RM 79**



**Vertical Velocity Profile RM 78**



**Vertical Velocity Profile RM 77**



*RDB (right descending bank); LDB (left descending bank)*

Table 26. Velocity calibration statistical analysis for UBS.

Calibration Period - March to June 2013	RMSE%	Corr. Coef.
Velocity (transverse profile)	24%	0.80
Velocity (Vertical Profile)	61%	0.93
Meselhe and Rodrigue (2013) Report	RMSE%	Corr. Coef.
Target Desired	< 20% for all stations	> 0.75 for all stations
Target Acceptable	< 30% for 50% of stations	> 0.75 for 50% of stations

The calibration and validation of sediment transport followed the hydrodynamics validation. The boundary conditions prescribed were:

- US boundary: suspended sediment concentrations for the following size-classes:
- Non-cohesive Sediment: very fine sand ( $D_{50} = 83 \mu\text{m}$ ), fine sand ( $D_{50} = 167 \mu\text{m}$ ) and medium sand ( $D_{50} = 333 \mu\text{m}$ );
- Cohesive sediment: clay ( $D < 2 \mu\text{m}$ ) and silt ( $2 \mu\text{m} < D < 63 \mu\text{m}$ ).

Calibration and validation of sediment transport were performed for suspended load. The sediment data used for calibration were collected by Thad Pratt and his team as part of the MRHDMS study. The USGS measurements at Belle Chasse (RM 76) were also used for calibration and validation.

The suspended sediment concentrations were prescribed daily, based on rating curves developed by the Institute using USGS measurements at Belle Chasse (RM 74) for the period 2008-2012. The rating curves are presented in Chapter 1.

The multilayer bed composition and substrate thickness were defined the same as the Myrtle Grove-White Ditch model. **Error! Reference source not found.** and Figure 53 show the suspended fine load calibration and validation. The calibration was performed for five different transects where data were available: RM 82.3, RM 79.7, RM 78.3, RM 77.2, and Belle Chasse (RM 76). For the validation period, data were only available from Belle Chasse RM 76. Results of the statistical analysis indicate that the model is capable of capturing the order of magnitude and the signal of the suspended fine sediment transport. The statistical analysis results are presented in Table 27.

The calibration and validation of suspended sand load is shown in **Error! Reference source not found.** and Figure 55, while Table 28 shows the corresponding statistical analysis. The model performance is acceptable, except for the RMSE value in the validation period. However, the validation was performed based on only USGS Belle Chasse station. As such, additional validation of the model is recommended as more data become available.



Figure 56 and Figure 57 display the calibration and validation of total suspended load (suspended sand + suspended fines). The statistical analysis is presented in Table 29. The model performance is acceptable.

Figure 52. Suspended fine load calibration for UBS.

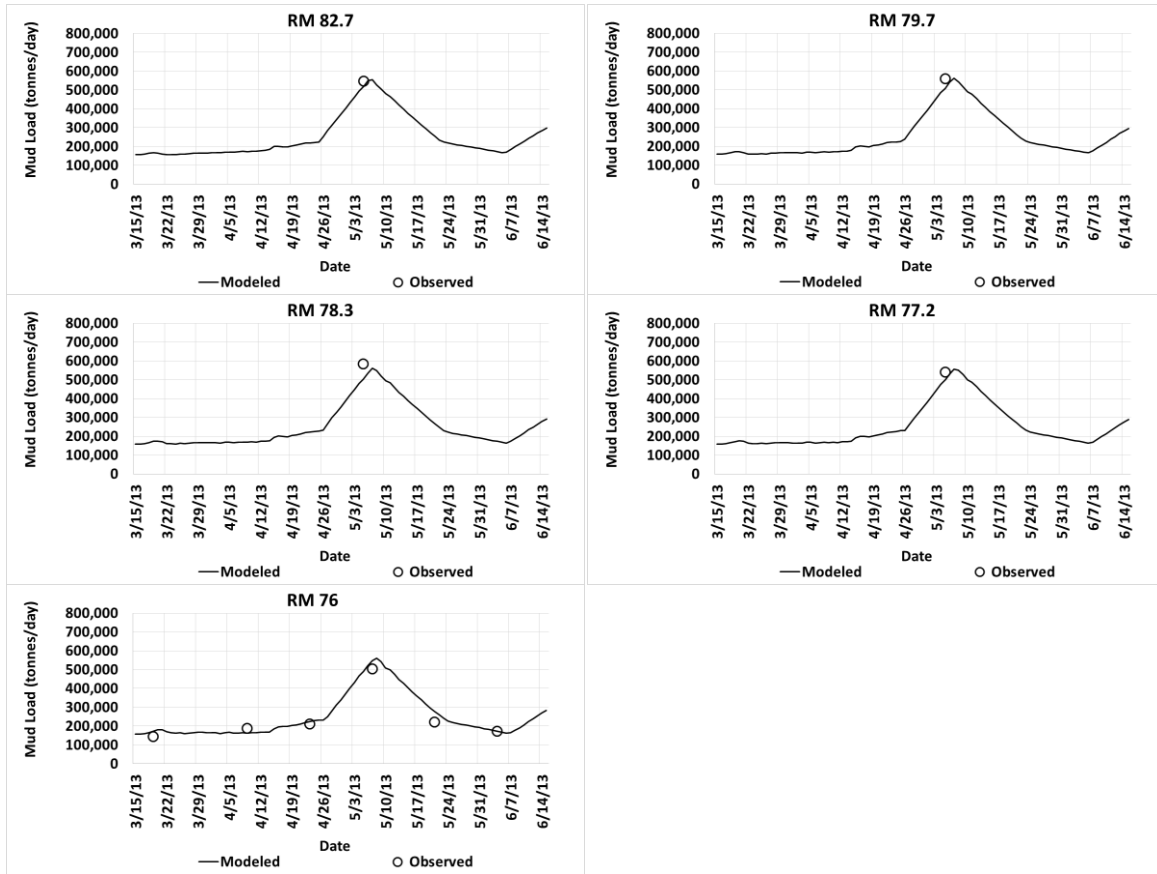


Figure 53. Suspended fine load validation for UBS.

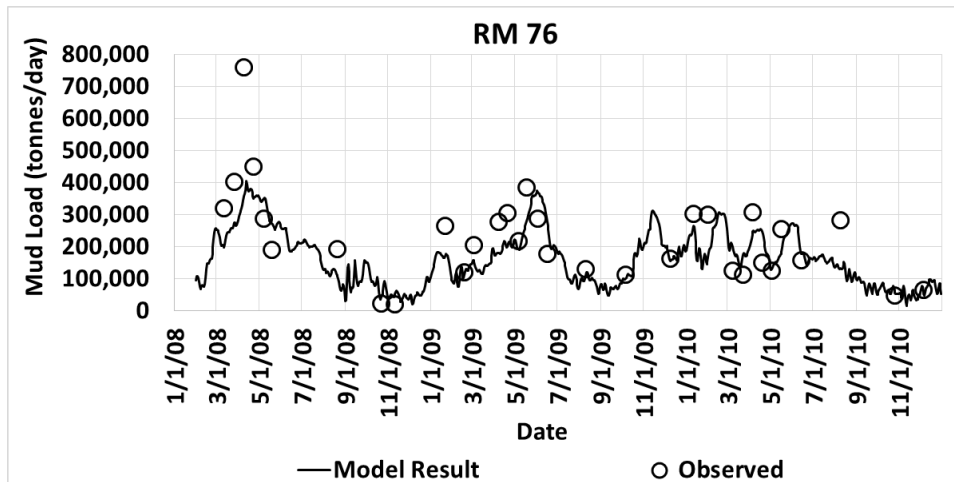


Table 27. Suspended fine load calibration and validation statistical analysis for UBS.

Modeled Period	Average Measured (tonnes/d)	Average Modeled (tonnes/d)	Average Bias (tonnes/d)	Bias (%)	RMSE%	Corr. Coef.
Calibration March to June 2013	367,223	358,454	-8769	-2%	N/A	N/A
Validation May 2010 to Dec 2011	227,099	191,308	-35,791	-16%	46%	0.74
Meselhe and Rodrigue (2013) Report	Average Measured (tonnes/d)	Average Modeled (tonnes/d)	Average Bias (tonnes/d)	Bias (%)	RMSE%	Corr. Coef.
Target Desired	-	-	-	< 20% for all stations	< 33% for all stations	> 0.5 for all stations
Target Acceptable	-	-	-	< 20% for all 50% of stations	< 50% for 50% of the stations	> 0.5 for 50% all stations

Figure 54. Suspended sand load calibration for UBS.

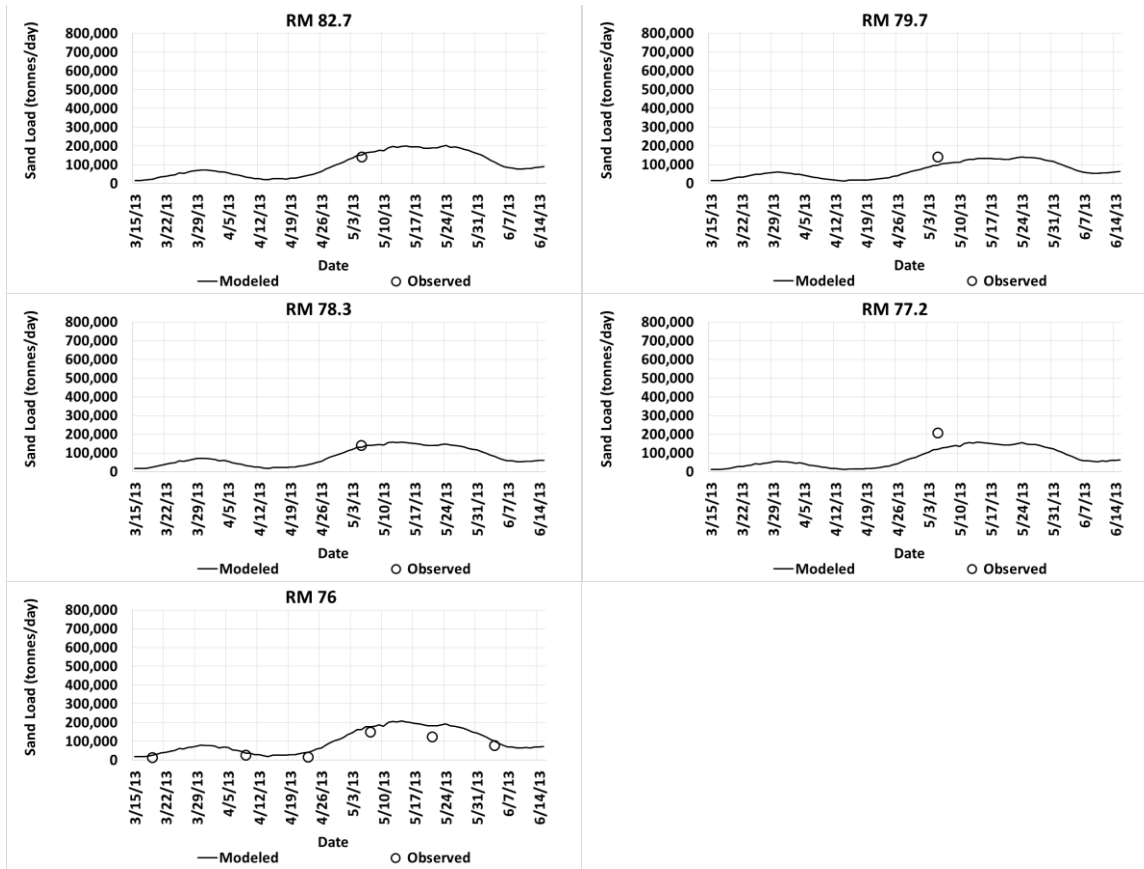




Figure 55. Suspended sand load validation for UBS.

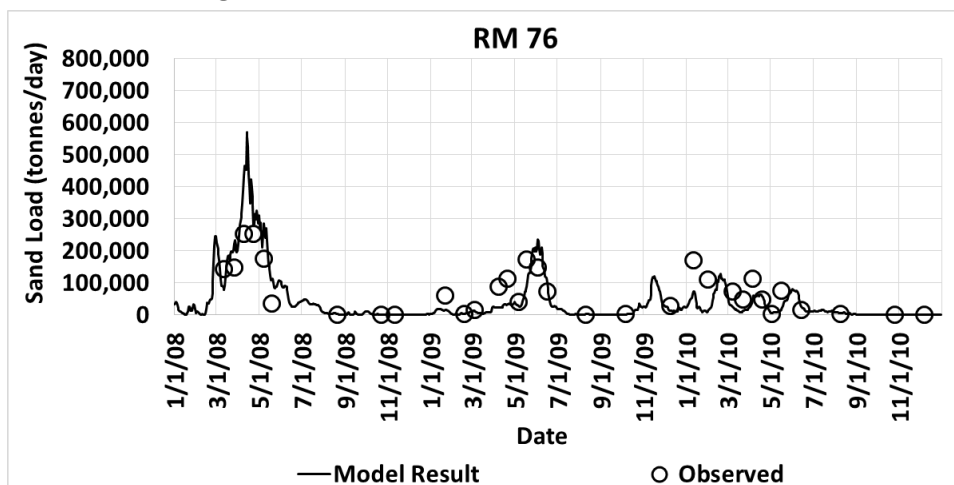


Table 28. Suspended sand load calibration and validation statistical analysis for UBS.

Modeled Period	Average Measured (tonnes/d)	Average Modeled (tonnes/d)	Average Bias (tonnes/d)	Bias (%)	RMSE%	Corr. Coef.
Calibration March- June 2013	103,308	106,718	3410	3%	N/A	N/A
Validation May 2010- Dec 2011	73318	68021	-5298	-7%	81%	0.82
<b>Meselhe and Rodrigue (2013) Report</b>	<b>Average Measured (tonnes/d)</b>	<b>Average Modeled (tonnes/d)</b>	<b>Average Bias (tonnes/d)</b>	<b>Bias (%)</b>	<b>RMSE%</b>	<b>Corr. Coef.</b>
Target Desired	-	-	-	< 20% for all stations	< 33% for all stations	> 0.5 for all stations
Target Acceptable	-	-	-	< 20% for 50% of stations	< 50% for 50% of the stations	> 0.5 for 50% of stations

Figure 56. Total suspended load calibration for UBS.

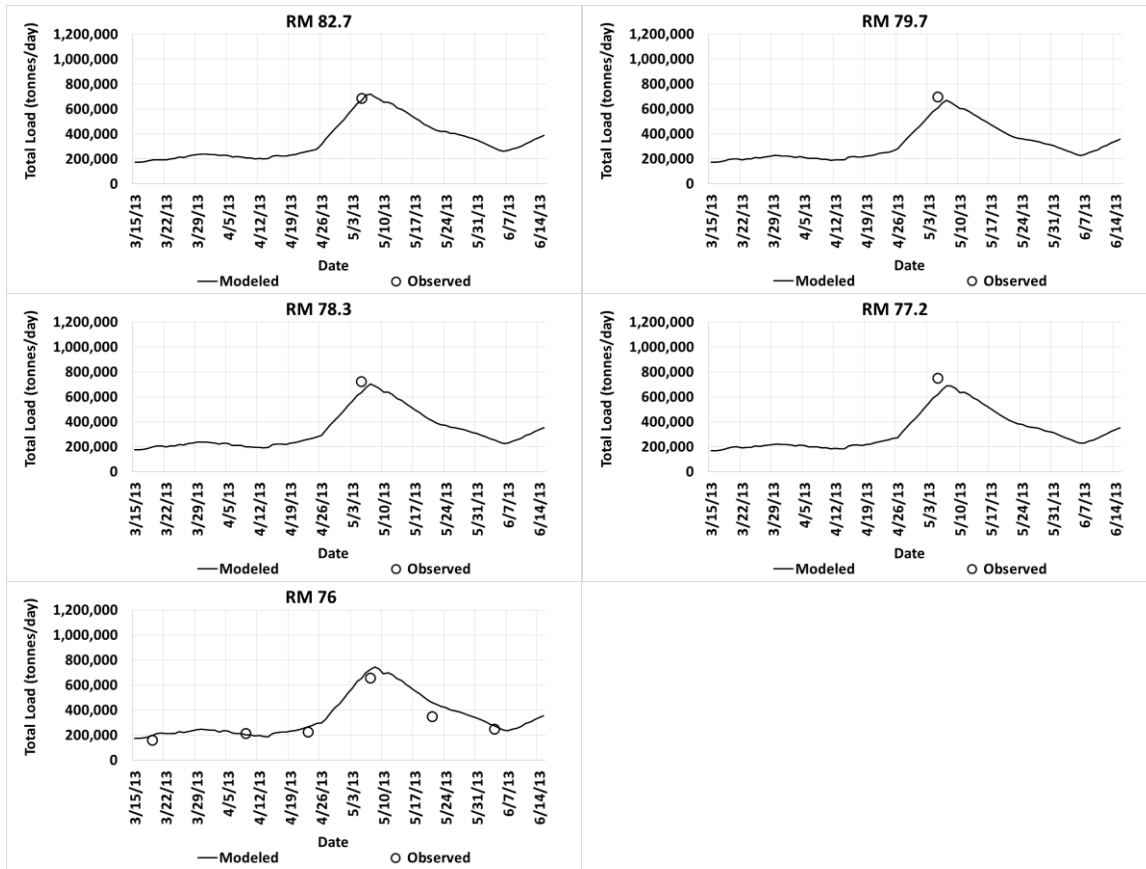


Figure 57. Total suspended load validation for UBS.

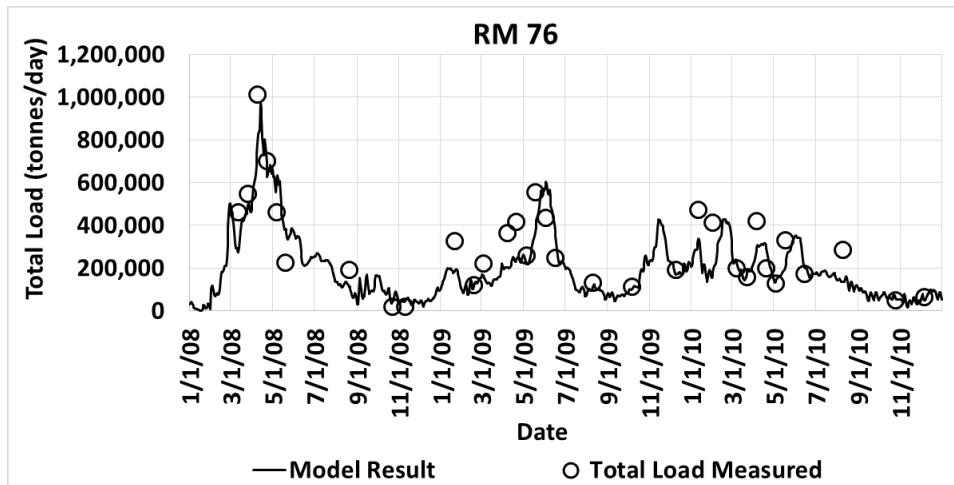


Table 29. Total suspended load calibration and validation statistical analysis for UBS.

Modeled Period	Average Measured (tonnes/d)	Average Modeled (tonnes/d)	Average Bias (tonnes/d)	Bias (%)	RMSE%	Corr. Coef.
Calibration March to June 2013	470,531	465,172	-5359	-1%	N/A	N/A
Validation May 2010 to Dec 2011	300,417	259329	-41088	-14%	39%	0.85
<b>Meselhe and Rodrigue (2013) Report</b>	<b>Average Measured (tonnes/d)</b>	<b>Average Modeled (tonnes/d)</b>	<b>Average Bias (tonnes/d)</b>	<b>Bias (%)</b>	<b>RMSE%</b>	<b>Corr. Coef.</b>
Target Desired	-	-	-	< 20% for all stations	< 33% for all stations	> 0.5 for all stations
Target Acceptable	-	-	-	< 20% for 50% of stations	< 50% for 50% of the stations	> 0.5 for 50% of stations

## 4.2 Model Application

The calibrated and validated UBS model was used to observe channel morphodynamic response to a large pulsed river diversion as well as the diversion efficiency with variable capacities. The following production runs (PR) were performed:

Table 30. Description of production runs for UBS model.

Production Run (PR) No.	Modeled Period	Diversion Location	Diversion capacity* (x10 <sup>3</sup> cfs)	Description
1	2008 - 2010	RM 77	250	Diversion was open with maintenance flow
2	2008 - 2010	RM 77	125	Diversion was open with maintenance flow
3	2008 - 2010	RM 77	75	Diversion was open with maintenance flow
4	2008 - 2010	RM 81.5	250	Diversion was placed at the location of existing Caernarvon diversion; Diversion was open with maintenance flow
5	2011 flood event June 2011 - June 2012	RM 77	250	Diversion was Open during the 2011 flood event assuming that Bonnet Carré spillway (BC) was closed. Diversion was closed similar to BC spillway following the 2011 flood

\*When river discharge = 1,000,000 cfs

The model setup includes the following:

- The bottom elevation of the intake is at -40ft NAVD88;
- The width of the intake is adjusted to the size of the diversion;
- Boundary Condition:
- US Boundary—flow at Belle Chasse USGS station ID: 07374525) near RM 76; gap for October 2008 filled with Baton Rouge USGS data;
- DS Boundary—calibrated between gauges at Belle Chasse (RM 76) and Algiers Lock (RM 88.3);
- Outfall Boundary - WD—Stage averaged between CRMS stations 0117 and 0115 and 0128;

Five sediment sizes were prescribed in the model as described in the calibration and validation effort.

The simulated discharge with the intake at RM 77 is shown in Figure 58 for three different sizes of the diversion. Figure 59 shows the calculated discharge for the location of the intake at RM 81.5. Data show that the flow passed through the diversion matches well to the design capacity of the intake and outfall channel for both locations discussed in this study.

Figure 58. Simulated discharge in the Mississippi River and UBS diversion at RM 77 in 2008 – 2010.

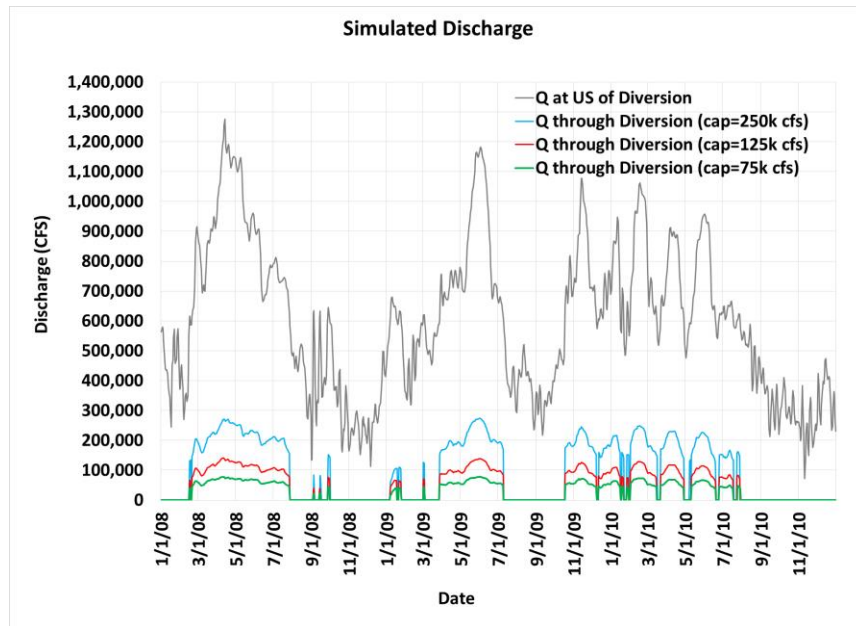
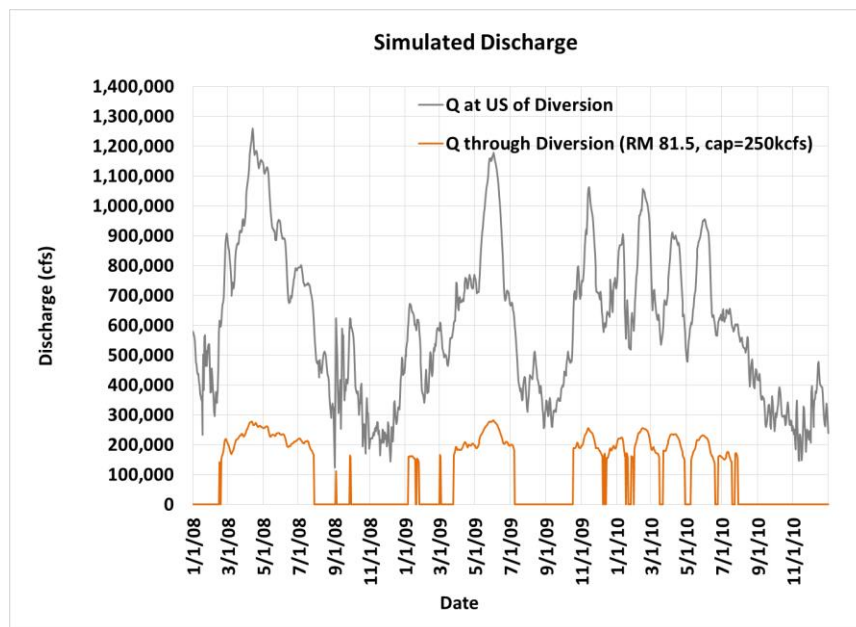


Figure 59. Simulated discharge in the Mississippi River and UBS diversion at RM 81.5 in 2008 – 2010.



Morphologic Response in the River Channel:

The change in erosion and accretion volume was calculated to quantify the morphological changes in response to the diversion. The change in erosion and accretion volume means the difference in volume occurred between “with” and “without” the project simulations for the same period. The river channel was divided into nine segments (polygons) to quantify the volume of the predicted accretion and erosion. The segments are labeled in Figure 60.

The erosion and accretion occurring in the river segments during the 2011 flood (PR5) is shown in Figure 61. Similar to the impact of Bonnet Carré spillway, the UBS diversion also showed that significant accretion occurred adjacent to, and downstream of, the diversion during the flood event and the deposited materials eroded in the subsequent year when the diversion was closed. SWR analysis showed that the UBS diversion was highly efficient in capturing both fine and coarse sediments (Mud SWR = 1, Sand SWR > 2) throughout the operation period in the 2011 flood. As such, the reduction of stream power in the river due to the reduction in discharge and water surface slope clearly caused the rapid aggradation downstream of the diversion.

Figure 62 shows the erosion and accretion volume change in the river segments for three different diversion sizes (PR1, PR2, and PR3). The model results showed that accretion occurring DS of the diversion decreased as the diversion size became smaller.

Figure 60. River segments considered to quantify morphologic changes for UBS model.



Figure 61. Erosion and accretion volume change in response to UBS diversion for the 2011 flood.

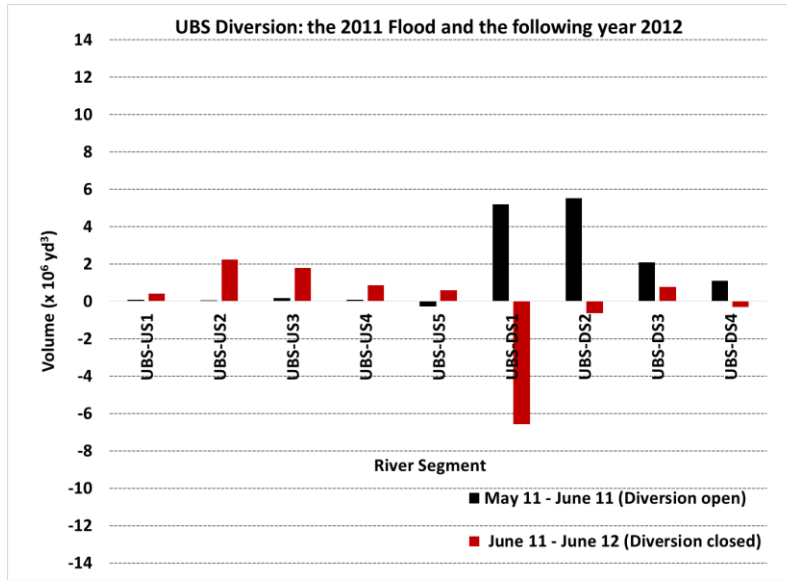
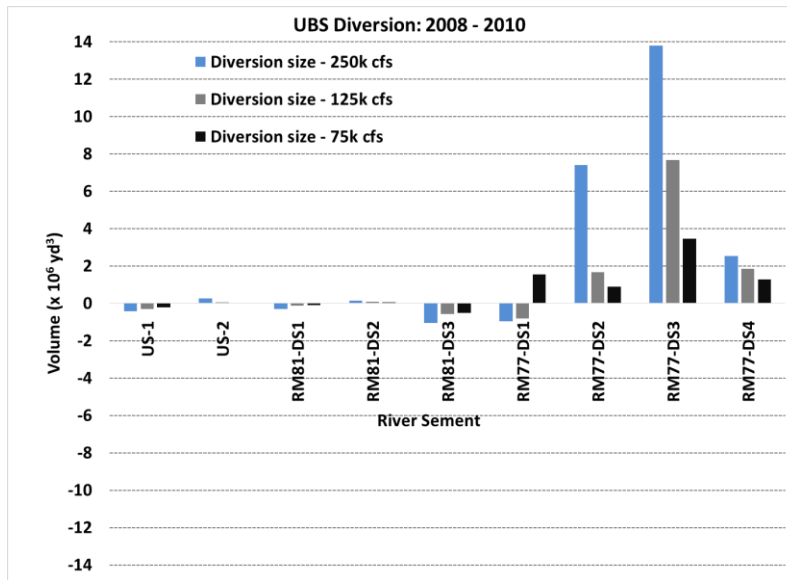


Figure 62. Erosion and accretion volume change in response to UBS diversion in 2008 - 2010.



The UBS model was later used to model the diversion at RM 81.5 to investigate the diversion performance and morphologic impact in the river. As shown in Figure 59, the diversion was able to capture the water according to the design capacity of 250,000 cfs. The erosion and accretion volumes in response to the diversion were compared between two locations: RM 81.5 and RM 77. The accretion resulted on the river bed due to the diversion at RM 81.5 was significantly higher than the volume for diversion at RM 77 (Figure 63). The sediment water ratio analysis at RM 81.5 (presented in the following section) has shown that the diversion at RM 81.5 had an average sediment water ratio of 0.5 during the three year of the production run. The large diversion carrying

disproportional amount of water and sediment caused substantial deposition downstream of the diversion. In addition to that, the sharp bend below English Turn at RM 77 also reinforced the depositional behavior shown in Figure 63. The temporal variation in mass quantities deposited in the river channel due to the diversion at RM 81.5 shows that the deposited materials moves downstream with time (Figure 64). Therefore, the river segments in further downstream of the domain have more deposition than the segments at the upstream.

Figure 63. Erosion and accretion volume change in response to UBS diversion at RM 77 and RM 81.5.

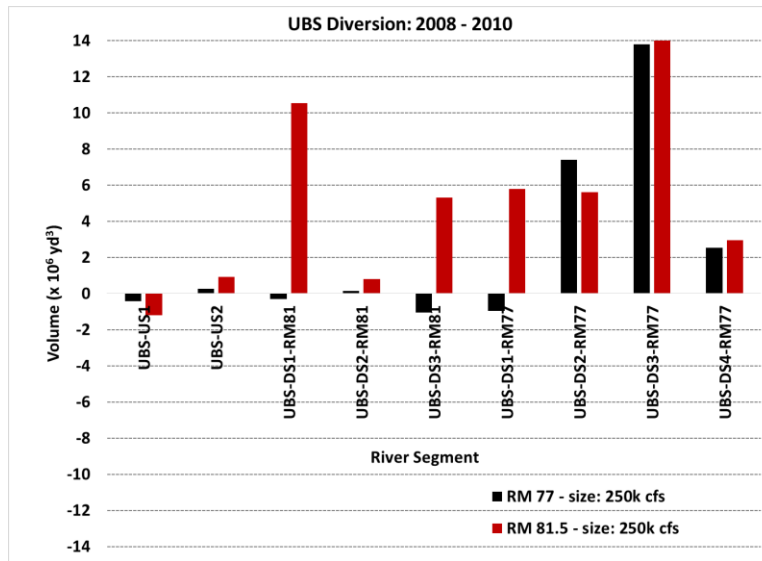
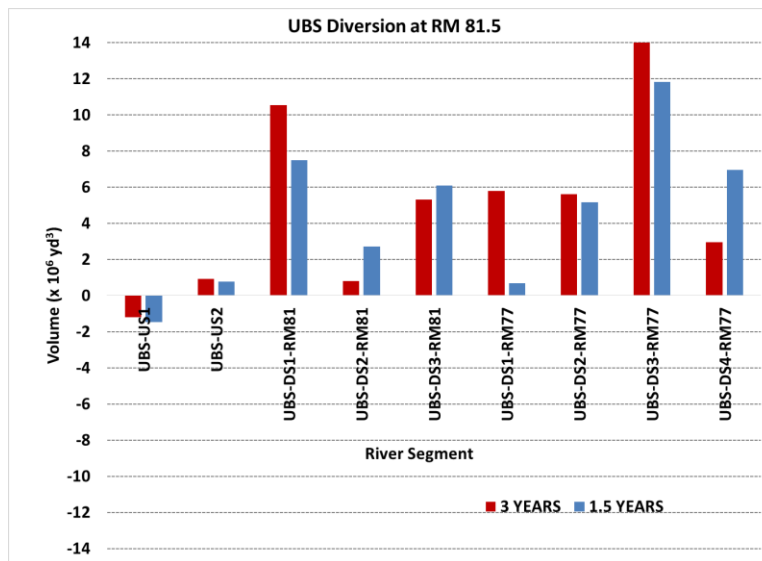


Figure 64. Erosion and accretion volume change in 1.5 and 3 years due to the UBS diversion at RM 81.5.



Sediment Budget:



Sediment budgets were developed for the production runs to provide additional insights into the morphologic response of the river to the diversion. The budgets were calculated for coarse and fine sediment separately and then added together for total sediment load. The sediment budgets are presented in Table 31 through Table 45. The sediment budget during the year 2008-2010 indicated that the diversion size impacts the deposited volume adjacent to, and DS of, the intake in response to the diversion. The sediment budget for the 250,000 cfs capacity of the diversion showed that around 30 million tonnes of sediment materials deposited on the river bed (over the three year period) and 60 million tonnes exited the outfall channel to the receiving basin (Table 33). A 50% reduction in diversion size, to 125,000 cfs, lowered the aggradation near the structure by 56%, while the total sediment diversion declined by 50% (Table 36). Further, the diversion size was reduced by 70% which also showed a 70% decrease in diversion volume, but 76% decrease in deposition volume on the river bed (Table 39). The sediment budget for the intake at RM 81.5 (design capacity =250,000 cfs) showed that approximately 152 million tonnes of sediment was deposited on the river bed due the diversion (Table 42) which was significantly more than the intake at RM 77. In addition, the amount of coarse sediment captured at the diversion decreased by 77% for placing the intake at RM 81.5 (Table 40). For reference, the total volume of water extracted through the 250,000 cfs diversion during the same 3-year period was 17% of the total water volume entering at the upstream end.

Sediment Budget for Production Run 1:

- Diversion size: 250,000 cfs
- Modeled period: 2008 – 2010
- Location: RM 77

Table 31. Sediment budget for sand load for PR 1: UBS model.

	Inflow at the U/S of the diversion	Outflow at the D/S	Deposited in the river	Deposited in the Outfall Channel	Diverted to the Receiving Basin
Total Mass (10 <sup>6</sup> tonnes)	48	3	22	0	24
Total Volume (10 <sup>6</sup> yd <sup>3</sup> )	55	4	25	0	27
% of U/S Inflow		7%	45%	~0%	48%

Table 32. Sediment budget for fine sediment for PR 1: UBS model.

	Inflow at the U/S of the diversion	Outflow at the D/S	Deposited in the river	Deposited in the Outfall Channel	Diverted to the Receiving Basin
Total Mass (10 <sup>6</sup> tonnes)	179	133	9	0	37
Total Volume (10 <sup>6</sup> yd <sup>3</sup> )	202	150	10	0	42
% of U/S Inflow		74%	5%	~0%	21%

Table 33. Sediment budget for total sediment load for PR 1: UBS model.

	Inflow at the U/S of the diversion	Outflow at the D/S	Deposited in the river	Deposited in the Outfall Channel	Diverted to the Receiving Basin
Total Mass (10 <sup>6</sup> tonnes)	228	136	31	0	60
Total Volume (10 <sup>6</sup> yd <sup>3</sup> )	257	154	35	0	68
% of U/S Inflow		60%	14%	~0%	27%

## Sediment Budget for Production Run 2:

- Diversion size: 125,000 cfs
- Modeled period: 2008 – 2010
- Location: RM 77

Table 34. Sediment budget for sand load for PR 2: UBS model.

	Inflow at the U/S of the diversion	Outflow at the D/S	Deposited in the river	Deposited in the Outfall Channel	Diverted to the Receiving Basin
Total Mass (10 <sup>6</sup> tonnes)	48	25	10	0	13
Total Volume (10 <sup>6</sup> yd <sup>3</sup> )	55	28	12	0	15
% of U/S Inflow		52%	21%	~0%	27%

Table 35. Sediment budget for fine sediment for PR 2: UBS model.

	Inflow at the U/S of the diversion	Outflow at the D/S	Deposited in the river	Deposited in the Outfall Channel	Diverted to the Receiving Basin
Total Mass (10 <sup>6</sup> tonnes)	179	158	3	0	17
Total Volume (10 <sup>6</sup> yd <sup>3</sup> )	202	179	4	0	19
% of U/S Inflow		89%	2%	~0%	10%

Table 36. Sediment budget for total sediment load for PR 2: UBS model.

	Inflow at the U/S of the diversion	Outflow at the D/S	Deposited in the river	Deposited in the Outfall Channel	Diverted to the Receiving Basin
Total Mass (10 <sup>6</sup> tonnes)	227	184	14	0	30
Total Volume (10 <sup>6</sup> yd <sup>3</sup> )	256	207	15	0	34
% of U/S Inflow		81%	6%	~0%	13%

Sediment Budget for Production Run 3:

- Diversion size: 75,000 cfs
- Modeled period: 2008 – 2010
- Location: RM 77

Table 37. Sediment budget for sand load for PR 3: UBS model.

	Inflow at the U/S of the diversion	Outflow at the D/S	Deposited in the river	Deposited in the Outfall Channel	Diverted to the Receiving Basin
Total Mass (10 <sup>6</sup> tonnes)	48	36	6	0	6
Total Volume (10 <sup>6</sup> yd <sup>3</sup> )	54	40	7	0	7
% of U/S Inflow		74%	13%	~0%	13%

Table 38. Sediment budget for fine sediment for PR 3: UBS model.

	Inflow at the U/S of the diversion	Outflow at the D/S	Deposited in the river	Deposited in the Outfall Channel	Diverted to the Receiving Basin
Total Mass (10 <sup>6</sup> tonnes)	179	164	3	0	11
Total Volume (10 <sup>6</sup> yd <sup>3</sup> )	202	186	4	0	13
% of U/S Inflow		92%	2%	~0%	6%

Table 39. Sediment budget for total sediment load for PR 3: UBS model.

	Inflow at the U/S of the diversion	Outflow at the D/S	Deposited in the river	Deposited in the Outfall Channel	Diverted to the Receiving Basin
Total Mass (10 <sup>6</sup> tonnes)	227	200	10	0	17
Total Volume (10 <sup>6</sup> yd <sup>3</sup> )	256	226	11	0	20
% of U/S Inflow		88%	4%	~0%	8%

Sediment Budget for Production Run 4:

- Diversion size: 250,000 cfs
- Modeled period: 2008 – 2010
- Location: RM 81.5

Table 40. Sediment budget for sand load for PR 4: UBS model.

	Inflow at the U/S of the diversion	Outflow at the D/S	Deposited in the river	Deposited in the Outfall Channel	Diverted to the Receiving Basin
Total Mass (10 <sup>6</sup> tonnes)	60	4	51	1	5
Total Volume (10 <sup>6</sup> yd <sup>3</sup> )	68	4	57	1	6
% of U/S Inflow		6%	84%	1%	9%

Table 41. Sediment budget for fine sediment for PR 4: UBS model.

	Inflow at the U/S of the diversion	Outflow at the D/S	Deposited in the river	Deposited in the Outfall Channel	Diverted to the Receiving Basin
Total Mass (10 <sup>6</sup> tonnes)	179	33	102	0	44
Total Volume (10 <sup>6</sup> yd <sup>3</sup> )	202	37	115	0	50
% of U/S Inflow		18%	57%	~0%	25%

Table 42. Sediment budget for total sediment load for PR 4: UBS model.

	Inflow at the U/S of the diversion	Outflow at the D/S	Deposited in the river	Deposited in the Outfall Channel	Diverted to the Receiving Basin
Total Mass (10 <sup>6</sup> tonnes)	239	37	152	0	50
Total Volume (10 <sup>6</sup> yd <sup>3</sup> )	270	41	172	1	56
% of U/S Inflow		15%	64%	~0%	21%

Sediment Budget for Production Run 5:

- Diversion size: 250,000 cfs
- Modeled period: 2011 flood event
- Location: RM 77

Table 43. Sediment budget for sand load for PR 5: UBS model.

	Inflow at the U/S of the diversion	Outflow at the D/S	Deposited in the river	Deposited in the Outfall Channel	Diverted to the Receiving Basin
Total Mass (10 <sup>6</sup> tonnes)	27	1	13	0	12
Total Volume (10 <sup>6</sup> yd <sup>3</sup> )	30	2	15	0	14
% of U/S Inflow		5%	49%	0%	46%

Table 44. Sediment budget for fine sediment for PR 5: UBS model.

	Inflow at the U/S of the diversion	Outflow at the D/S	Deposited in the river	Deposited in the Outfall Channel	Diverted to the Receiving Basin
Total Mass (10 <sup>6</sup> tonnes)	29	21	1	0	8
Total Volume (10 <sup>6</sup> yd <sup>3</sup> )	33	24	1	0	9
% of U/S Inflow		73%	3%	0%	24%

Table 45. Sediment budget for total sediment load for PR 5: UBS model.

	Inflow at the U/S of the diversion	Outflow at the D/S	Deposited in the river	Deposited in the Outfall Channel	Diverted to the Receiving Basin
Total Mass (10 <sup>6</sup> tonnes)	56	23	14	0	20
Total Volume (10 <sup>6</sup> yd <sup>3</sup> )	63	25	16	0	22
% of U/S Inflow		40%	25%	0%	35%

Sediment-Water Ratio:

The SWR was calculated to quantify the efficiency of the UBS diversion at different sizes and at two different locations. Similar to the MG-WD model, the SWR analysis presented herein was performed for MR flows over 600,000 cfs. The comparison of a cumulative SWR is presented in Figure 22 through Figure 25. Similar to the other two models, the UBS model also showed that the SWR of fine sediment was ~1.0 during the modeled period. The sand SWR of the UBS diversion was consistently over 2.0 for all three sizes at RM 77. The diversion is located on a sand bar and on the inside of a bend at RM 77. The adequately deep invert of the diversion on a sand bar and the secondary motion on the inside of the bend helped in capturing large amounts of coarse material from the river channel and augmented the sand SWR for the UBS diversion. Later, placement of the diversion at RM 81.5 evidently proved this point when the sand SWR of the same diversion reduced to 0.5 as the diversion intake was not located on a sand bar or on the inside of a bend (Figure 66).

Figure 65. Cumulative SWR comparison for different sizes of diversion at RM 77 in 2008 – 2010.

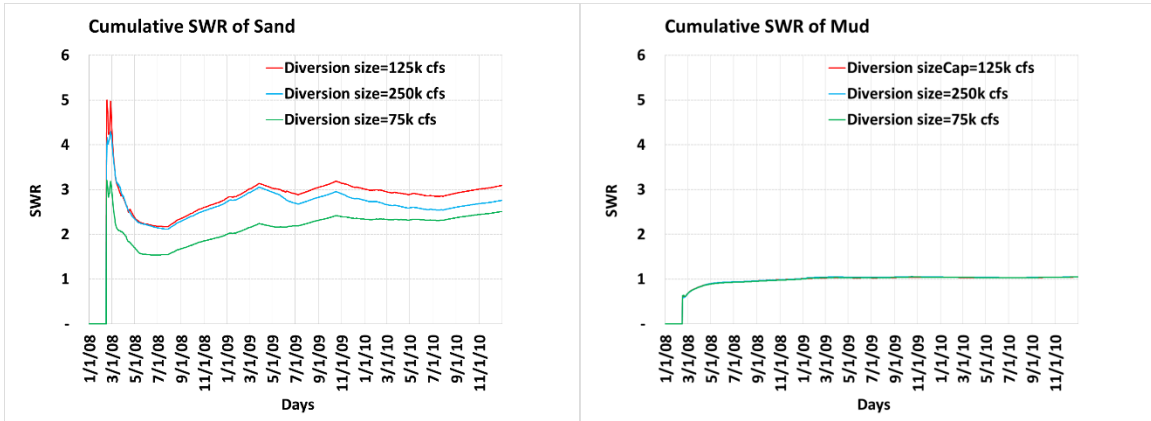
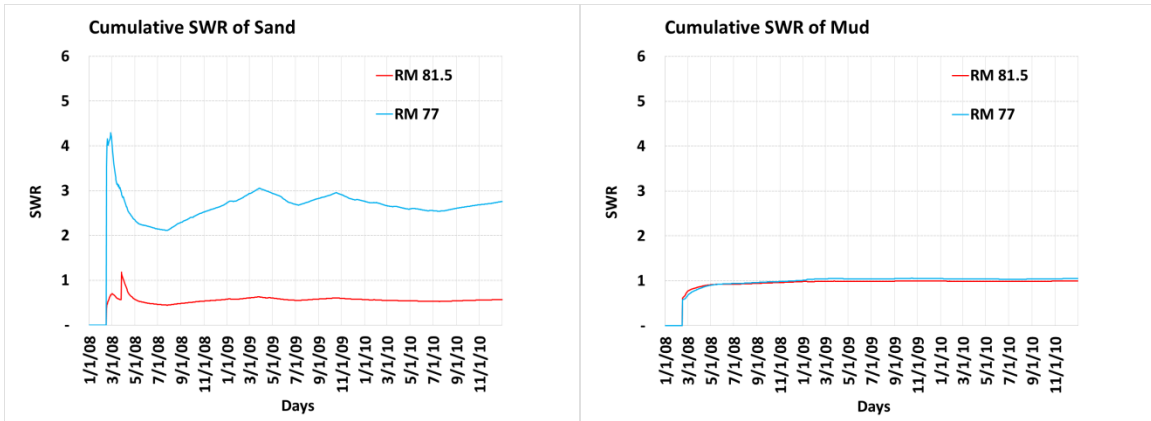


Figure 66. Cumulative SWR comparison for different locations at capacity 250k cfs in 2008 – 2010.



## 5 Conclusions and Closing Remarks

The Delft-3D near-field local models for the Bonnet Carré spillway and for the proposed diversions at Upper Breton Sound, White Ditch, and Myrtle Grove have been calibrated and validated for both hydrodynamics and sediment transport. The model results compare well against field measurements. The BC model has also been validated for the morphologic responses of the river to the spillway operation during the 2011 flood, based on the multibeam surveys available before and after the flood event, and in the subsequent year in June 2012. The Bonnet Carré analysis serves as a morphodynamic analogue and as such the model setup for morphology at BC was migrated to the UBS, MG, and WD models.

The Bonnet Carré model supported by detailed field observations was used to provide insights onto the potential morphologic response of a river to a large pulsed diversion. The analysis showed that the 56-day opening extracted nearly 20% of the flow and approximately 10% of the inflowing sand and 22% of fine sediment loads. Much of the sediment escaping the channel was deposited in the forebay area upstream of the diversion structure, while the remaining passed through the structure. The validated model was later used to reproduce the 1997 and 2008 flood and showed similar sediment distribution adjacent to, and the downstream of, the structure. The significant reduction in the stream power exacerbated by a disproportionate extraction of water and sediment resulted in massive deposition within the river channel immediately downstream of the diversion intake that amounted to nearly 30% of the inflowing total sand load. To further explain the morphological response of the river to this diversion event, SWR estimates and stream power loss were performed. The SWR is indicative of the efficiency of a diversion in capturing sediment from the river. A ratio of unity or higher would mean that the sediment concentration in the diverted water is similar or higher than the average sediment concentration in the main river. As such, to minimize sediment deposition in the river, an SWR higher than unity is desired. For the Bonnet Carré Spillway, the fine sediment SWR was 1.0, but the sand SWR was approximately 0.5.

The combined MG-WD model provided an opportunity to observe interactions between these two diversions while operating concurrently for a 3-year period. The operation of the MG diversion showed no influence on the WD diversion in capturing sediment from the river channel. In addition, the WD diversion actually enhanced the efficiency of the MG diversion. The deposition that occurred DS of the WD diversion provided more sediment upstream of MG that was entrained into the water column and captured by the MG diversion during flood events. As a result, the sediment water ratio for MG got slightly higher when both diversions were operated.



The UBS diversion is a proposed large diversion with the design capacity of 250,000 cfs. The sand SWR of the UBS diversion was around 3.0 during the operation period as opposed to the Bonnet Carré spillway. The intake of the diversion was well designed with a bottom elevation at -40ft NAVD88. The UBS model has confirmed that the outfall geometry including the invert elevation greatly enhanced the diversion efficiency. The UBS model was used to analyze the impact of the diversion at different design capacities. The analysis shows that a 70% reduction in the diversion size also reduces the sediment diversion by 70%, while the aggradation DS of the diversion was lowered by 76%. The size of the diversion affects the deposition DS of the intake due to the stream power loss through the diversion. The model was also used to test the diversion efficiency at RM 81.5. The sand SWR at RM 81.5 was around 0.5 during a 3-year period. The low SWR for the intake at RM 81.5 almost doubled the aggradation DS of the diversion compared the diversion location at RM 77. As such, the placement of the diversion is also important to minimize the impact on the river channel. A diversion located on a sand bar (RM 77) minimizes the potential aggradation on the river bed.

In general, accretion occurred adjacent to, and downstream of, the diversion due to the stream power loss regardless of its capture efficiency. The deposited material could provide an opportunity for dedicated dredging. There are little to no morphologic changes upstream of the diversion. This suggests that the diversion does not alter the morphology of the upstream sand bar, at least not during the short-term (three year) analysis provided by this modeling effort.

## 6 References

- Allison, M. A., & Meselhe, E. A. (2010). The use of large water and sediment diversions in the lower Mississippi River (Louisiana) for coastal restoration. *Journal of Hydrology*, 387, 346-360.
- Allison, M. A., Demas, C. R., Ebersole, B. A., Kleiss, B. A., Little, C. D., Meselhe, E. A., Powell, N. J., Pratt, T. C., & Vosburg, B. M. (2012). A water and sediment budget for the lower Mississippi–Atchafalaya River in flood years 2008–2010: Implications for sediment discharge to the oceans and coastal restoration in Louisiana. *Journal of Hydrology*, 432-433, 84-97.
- Allison, M.A., Vosburg, B.M., Ramirez, M.T., & Meselhe, E. A. (2013). Mississippi River Channel response to the Bonnet Carré Spillway opening in the 2011 flood and its implications for the design and operation of River Diversions. *Journal of Hydrology*, 477, 104-118. <http://dx.doi.org/10.1016/j.jhydrol.2012.11.011>.
- Bagnold, R. A. (1966). An approach to the sediment transport problem from general physics (Geological Survey professional paper). *U.S. Geological Survey*. U. S. Govt. Printing Office.
- Deltares (2011). Simulation of multidimensional hydrodynamic flows and transport phenomena, including sediments. *User Manual Delft-3D Flow*, <http://oss.deltares.nl/web/delft3d/manuals>.
- Meselhe, E.A., Georgiou, I., Allison, M.A., & McCorquodale, J.A. (2012). Numerical modeling of hydrodynamics and sediment transport in lower Mississippi at a proposed delta building diversion. *Journal of Hydrology*, 472–473, 340-354.
- Meselhe, E. A. & Rodrigue, M. D. (2013). Models Performance Assessment Metrics and Uncertainty Analysis. *Louisiana Coastal Area Program Mississippi River Hydrodynamics and Delta Management Study*. <http://www.lca.gov/Projects/22/Default.aspx>.
- Meselhe, E.A.; Pereira, J.F.; Jung, H., Khadka, A. & Kazi, S. (2014). *Mid-Barataria Sediment Diversion Report*. Prepared for HDR and CPRA. The Water Institute of the Gulf.
- Van Rijn, L. C. (1984a). Sediment transport, Part I: bed load transport. *Journal of Hydraulic Engineering*, 110(10), 1431-1456.

Van Rijn, L. C. (1984b). Sediment transport, Part II: suspended load transport. *Journal of Hydraulic Engineering*, 110(11), 1613 - 1640.

Yang, C. T. (1971a). Potential energy and stream morphology. *Water Resources Research*, V. 7(2): 311-322.